Reactivity of Polyphosphorus Complexes towards Nucleophiles

Dissertation

zur Erlangung des

DOKTORGRADES DER NATURWISSENSCHAFTEN

(Dr. rer. Nat.)

der Naturwissenschaftlichen Fakultät Chemie und Pharmazie

der Universität Regensburg

vorgelegt von

Felix Riedlberger

aus Tattenhausen

Regensburg 2020

Diese Arbeit wurde angeleitet von Prof. Dr. Manfred Scheer.

Das Promotionsgesuch wurde eingereicht am: 27.08.2020

Datum des wissenschaftlichen Kolloquiums: 25.09.2020

Prüfungskomission:

Vorsitzender: Prof. Dr. Arno Pfitzner

1. Gutachter: Prof. Dr. Manfred Scheer

2. Gutachter: Prof Dr. Henri Brunner

weitere Gutachter: Prof. Dr. Frank-Michael Matysik

Universität Regensburg

Affidavit

I hereby confirm that this thesis “Reactivity of Polyphosphorus Complexes towards Nucleophiles” is the result of my own work. I did not receive any help or support from third parties or commercial consultants. All sources and/or concepts applied directly or indirectly are listed and specified in the thesis stating the relevant literature.

Eidesstattliche Erklärung

Ich erkläre hiermit an Eides statt, dass ich die vorliegende Arbeit mit dem Titel „Reactivity of Polyphosphorus Complexes towards Nucleophiles” ohne unzulässige Hilfe Dritter und ohne Benutzung anderer als der angegebenen Hilfsmittel angefertigt habe; die aus anderen Quellen direkt oder indirekt übernommenen Daten und Konzepte sind unter Angabe des Literaturzitats gekennzeichnet.

_____

Felix Riedlberger

The practical work leading to this thesis has been conducted between **April 2015** and **August 2020** at the Department of Inorganic Chemistry at the University of Regensburg under the supervision of Prof. Dr. Manfred Scheer.

One chapter of this thesis is already published:

F. Riedlberger, S. Todisco, P. Mastrorilli, A. Y. Timoshkin, M. Seidl, M. Scheer, "NHCs as Neutral Donors towards Polyphosphorus Complexes", *Chem. Eur. J.* 10.1002/chem.202003393

And another chapter is close to being published:

F. Riedlberger, M. Seidl, M. Scheer, "The Reaction behavior of $[Cp_2Mo_2(CO)_4(\mu,\eta^{2:2}\text{-}P_2)]$ and $[Cp''Ta(CO)_2(\eta^4\text{-}P_4)]$ towards Hydroxide and tert-Butyl nucleophiles", *Chem. Commun.*

dedicated to Steffi and my parents

“Wenn ich groß bin, möchte ich groß sein“

Maxim Markow

Preface

Some of the herein reported results are already published (*vide supra*) or close to being published. Therefore, if possible, a license number is given at the beginning of a chapter. This thesis is structured in such a manner that every chapter stands as an own paper, ready for publishing and therefore the numbering for compounds, figures and tables start new.

Each chapter includes a list of authors. At the beginning of each chapter the individual contribution of each author is described. A general “Introduction” and the “Research Objectives” are given at the beginning of this thesis. In addition, a comprehensive “Conclusions” of this work is presented at the end of this thesis.

Table of Contents

1. Introduction

1.1 Phosphorus: Element of life and science

Phosphorus is an essential element for life. In the nature, it is found in phosphate rocks, which are used after modification as fertilizers to increase the harvest and are also part of bones and teeth. In the living organisms, phosphorus is also found in the DNA building the genetic code of every being on this earth. The RNA, which also bears phosphorus, is also very important to code, decode, regulate and express genes. Moreover, phosphorus is found in ATP (adenosine triphosphate) which is one of the most important energy providers used for many processes in living cells. Phosphorus has different modifications. White phosphorus is the most reactive modification of phosphorus and is self-igniting in air. However, white phosphorus has a bad repute in the general public, because it was used in firebombs during several wars, like the Second World War. Some of these bombs were duds and parts of it are still found nowadays in cities, other grounds and at the beach. This is extremely dangerous, because of the above-mentioned self-ignition in air. Some of the wet white phosphorus is found by tourists at the beaches. They believe it to be amber and put it into their pockets. After drying, the white phosphorus gets contact with air and set the clothes of the finder on fire. Although, the general public is wary towards phosphorus, this element gets considerable attention from the scientific community.[1]

White phosphorus was discovered by the German alchemist Henning Brand by accident on his quest to find the philosopher's stone.[2] He concentrated urine to dryness and handled the residue under exclusion of air. Phosphorus means "light-bearer" in Greek and is caused by the chemiluminescence that occurs when phosphorus reacts with air. White phosphorus is not the only modification of phosphorus. Red and black modifications are also known. The thermodynamic stability of these modification increases from white to red to black phosphorus at room temperature (vide infra).[3] All mentioned modifications vary in their molecular structure (Scheme 1).

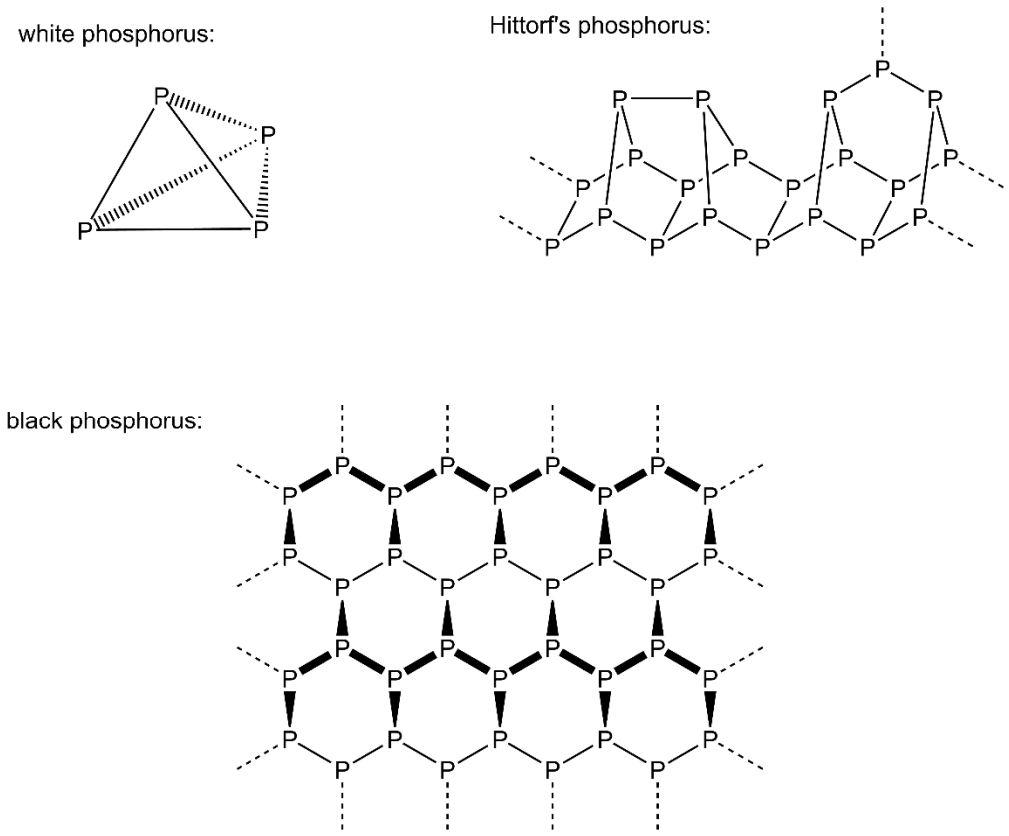

Scheme 1. Selected modifications of phosphorus.

White phosphorus consists of tetrahedral P_4 molecules.[4] This is the most reactive allotrope and has a melting point of 44.25°C and a boiling point of 280.5°C. The rate of transformation into other modifications is slow under normal conditions. Temperatures over 200°C, or irradiation are needed to obtain red phosphorus. This modification is divided in five different types. While violet and fibrous are crystalline, the other types are amorphous phases.[5] Fibrous phosphorus forms fine fibers when exposed to mechanical stress. The X-ray diffractions of fibrous phosphorus revealed infinite tubes where P_8 and P_9 moieties are linked by P_2 units in the solid state.[6] A pairwise parallel connection of two tubes result into double-tubes. Violet phosphorus was discovered by the German physicist Johann Wilhelm Hittorf in 1865.[7] The molecular structure of violet phosphorus was revealed more than 100 years later.[8] The Hittorf's phosphorus forms similar cages like the fibrous phosphorus, but two tubes are linked in a rectangular fashion.

Black phosphorus is the densest modification and thermodynamically stable. It is favored under high pressure and has been synthesized by heating white phosphorus to 200°C under 12000 bar. In the solid state, black phosphorus consists of condensed P_6 rings in chair conformation.[9]

1.2 Activation of white phosphorus and P_n ligand complexes

Substituent free polyphosphorus ligands, so called P_n ligands are known since 1971 when A. P. Ginsberg and W. E. Lindsell reported about the complex $[ClRh(PPh_3)(\eta^2\text{-}P_4)]$[10] (Figure 1). The P_4 unit in this complex coordinates side-on to a rhodium fragment. The second P_n ligand complex reported is $[Co_2(CO)_6(\mu,\eta^2\text{-}P_2)]$ (Figure 1) in which the two cobalt atoms and the two phosphorus atoms build a tetrahedron.[11]

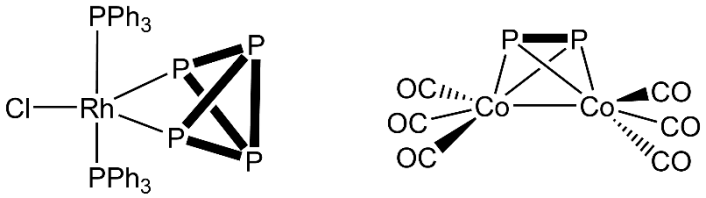

Figure 1. The two first published P_n ligand complexes. Left: $[ClRh(PPh_3)(\eta^2\text{-}P_4)]$ discovered by Ginsberg and Lindsell in 1971. Right: $[Co_2(CO)_6(\mu,\eta^2\text{-}P_2)]$ discovered by Markó *et al.* in 1973.

Since then, many other P_n ligand complexes and even E_n ligand complexes of heavier homologs of group 15 elements (E = As, Sb, Bi) were synthezised.[12] Photolysis or thermolysis of white phosphorus with suitable transition metal complexes are the most important synthetic routes. The new structural motifs of the polyphosphorus ligand in these complexes can be explained by several bond cleavages and bond formations starting from the P_4 tetrahedron. The formal successive degradation is shown in Scheme 2.

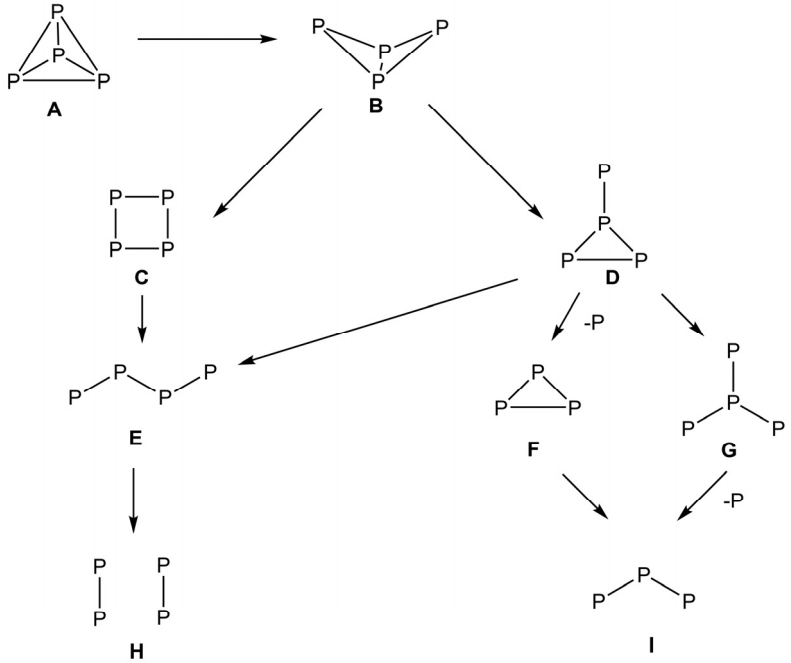

Scheme 2. Successive degradation of the P_4 tetrahedron via P-P bond cleavage. The resulting charges and lone pairs of electrons are not considered.

The structural motif **A** is quite rare and hence, only very few complexes containing an intact P_4 tetrahedron coordinated in an η^1 fashion to a metal fragment are known, such as $[(np_3)Ni(\eta^1\text{-}P_4)]$ (np_3 = $N\{CH_2CH_2PPh_2\}_3$) published by Sacconi *et al.*[13] By breaking of one phosphorus-phosphorus bonds, the structural motif **B** – the so called butterfly motif – can be obtained. This motif is found in mononuclear compounds such as $[Cp^*(CO)Co(\eta^2\text{-}P_4)]$[14] and binuclear compounds like $[\{Cp''(CO)_2Fe\}_2(\mu,\eta^1\text{:}\eta^1\text{-}P_4)]$.[15] A further P-P bond cleavage in this butterfly gives two possible products. The bond break between the two bridgehead P atoms result in a *cyclo*-P_4 unit (**C**) which can be degraded to two P_2 units (**H**) by two additional bond cleavages. The other resulting structural motif is a *cyclo*-P_3 ligand with an exocylic P atom (**D**) which can be degraded to a *cyclo*-P_3 ligand (**F**) and a single P_1 unit. Reactions between different structural motifs (**A**-**I**) are imaginable and an aggregation to P_n ligands with $n > 4$ is possible. Only some selected P_n ligand complexes will be presented in this work. However, P_n ligand complexes with up to 24 phosphorus atoms have already been published.[16]

P_1 ligands are quite versatile. They can coordinate in a bridging fashion to two, three and four metal fragments like in $[(Cp^*Mn(CO)_2)_2P][PF_6]$,[17] $[(CpMo(CO)_3)_3P]$[18] and $[(Fe_2(CO)_8)P(Fe_2(CO)_6Cl)]$,[19] respectively, or in a terminal fashion like in $[Mo(P)(NRAr)_3]$[20] (R = $C(CD_3)_2CH_3$, Ar = 3,5-C_6H_3Me) (Figure 2).

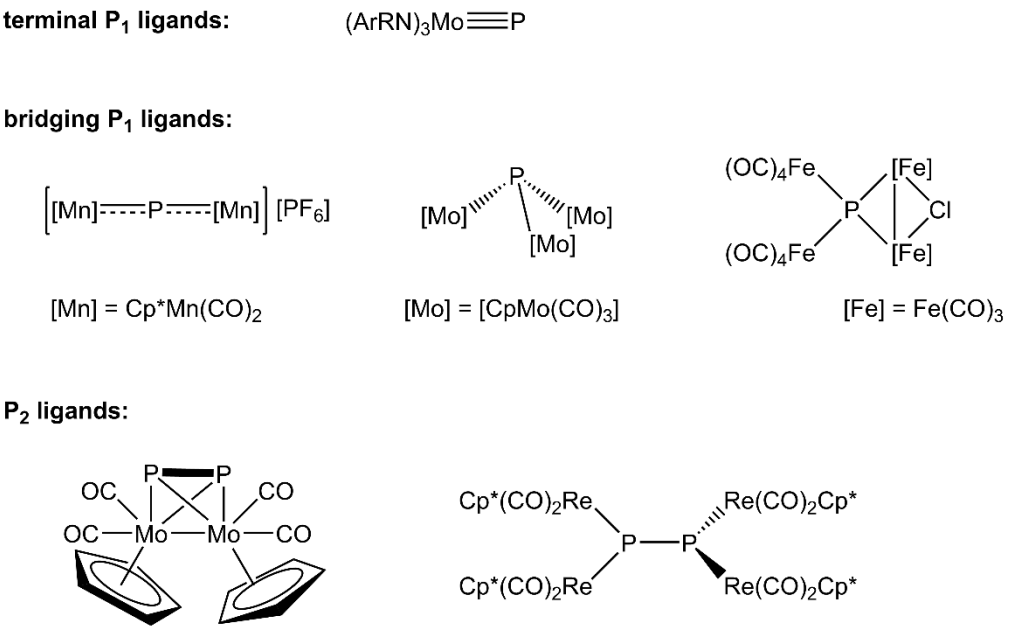

Figure 2. Selected examples for P_1 and P_2 ligand complexes.

P_2 ligands usually coordinate to two or four metal fragments, for example in the tetrahedral complex $[Cp_2Mo_2(CO)_4(\mu,\eta^{2:2}\text{-}P_2)]$.[21] Another example is the butterfly complex $[(Ni(PEt_3)_2)P_2]$,[22] where the two P atoms represent the bridgehead atoms and the Ni atoms the wing tip atoms. The coordination of the P_2 unit to four metal fragments is quite rare and appears for example in $[(Cp^*Re(CO)_2)_4(P_2)]$,[23] where every P atom is coordinated to two metal fragments. All mentioned P_2 ligand complexes are summarized in Figure 2. Most of the time, the P_3 ligand occurs as a *cyclo*-P_3 unit. It can coordinate to

one or two metal fragments like in [Cp*Ni(η^3-P_3)][24] or in [(Ni(triphos))$_2$(μ,$\eta^{3:3}$-P_3)][25] (triphos = 1,1,1-tris(diphenylphosphino-methyl)ethan), respectively (Figure 3).

The "naked" *cyclo*-P_4 ligand is much more rare than the *cyclo*-P_3 ligand. Naked means, that the cyclo-P_4 ligand coordinates in an end-on fashion to one metal fragment and no P atom is coordinating to another metal fragment. [Cp''Ta($CO)_2$(η^4-P_4)] published by Scherer is one example of those end-on coordinated *cyclo*-P_4 ligands (Figure 3).[26]

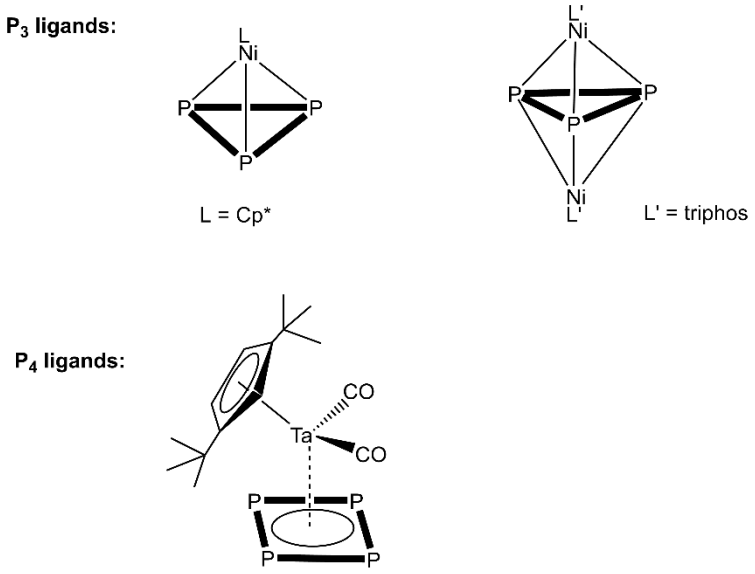

Figure 3. Selected P_3 and P_4 ligand complexes.

The P_5 and P_6 ligands often appear as cyclic ligands. Consequently, the *cyclo*-P_5 ligand is isoelectronic to the cyclopentadienyl ion ($C_5H_5^-$) and the *cyclo*-P_6 ligand is isoeletronic to benzene. The *cyclo*-P_5 ligand can coordinate as an end-on ligand to one metal fragment in [Cp*Fe(η^5-P_5)][27] or coordinate to two metal fragments in a triple decker complex like in [(Cp*Cr)$_2$(μ,$\eta^{5:5}$-P_5)][28] (Figure 4). The "hexaphosphabenzene" ligand can be found also in a triple decker complex like [(CpMo)$_2$(μ,$\eta^{6:6}$-P_6)][29] (Figure 4).

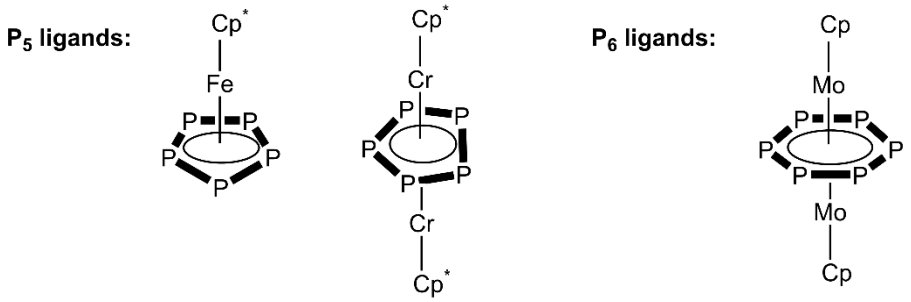

Figure 4. Selected P_5 and P_6 ligand complexes.

1.3 Pentaphosphaferrocene

Coordination chemistry

Pentaphosphaferrocene's big advantage over ferrocene is its potential to coordinate with five accesible lone pairs of the *cyclo*-P_5 unit to Lewis acids. A broad range of different coordination compounds is to be expected. Actually, reactivity studies of **1** towards the 16 valent electron transition metal fragments like $[Cr(CO)_5(thf)]$ and $[CpMn(CO)_2(thf)]$ were executed.[30] The chromium fragment is able to coordinate to two of the five phosphorus atoms and the manganese fragment, due to its less steric demand, to four P atoms. The planar structure of the P_5 ring remains intact in both cases. Ever since the coordination chemistry of **1** evolved considerably. The usage of the weakly coordinating anion $[Al\{OC(CF_3)_3\}_4]^-$ made it possible to synthesize a variety of soluble coordination polymers. Example are the corresponding Ag(I) salt[31] or the group 13 element compounds $M[Al\{OC(CF_3)_3\}_4]$ (M = Tl, In, Ga)[32] (Scheme 3).

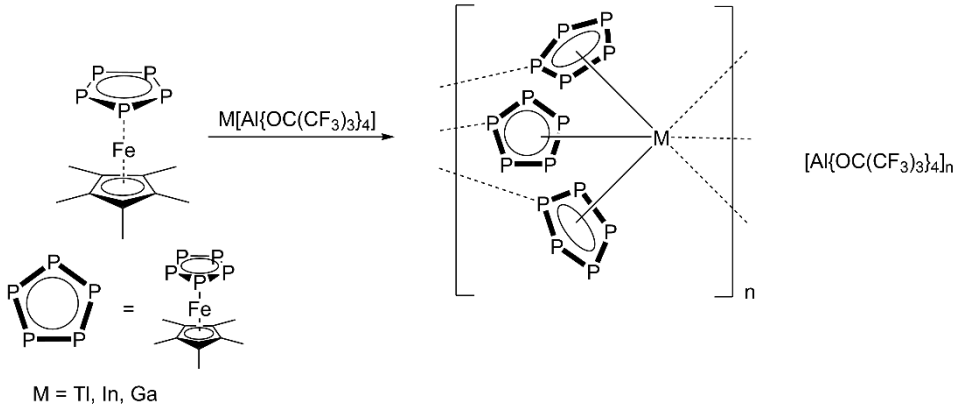

Scheme 3. Reaction of **1** with $M[Al\{OC(CF_3)_3\}_4]$ (M = Tl, In, Ga) and the resulting coordination polymers.

The stoichiometry of such coordination reactions with **1** is essential. Different structures of polymer chains can be obtained, when Cu(I) halides are used as reaction partner of **1** (Scheme 4).[33]

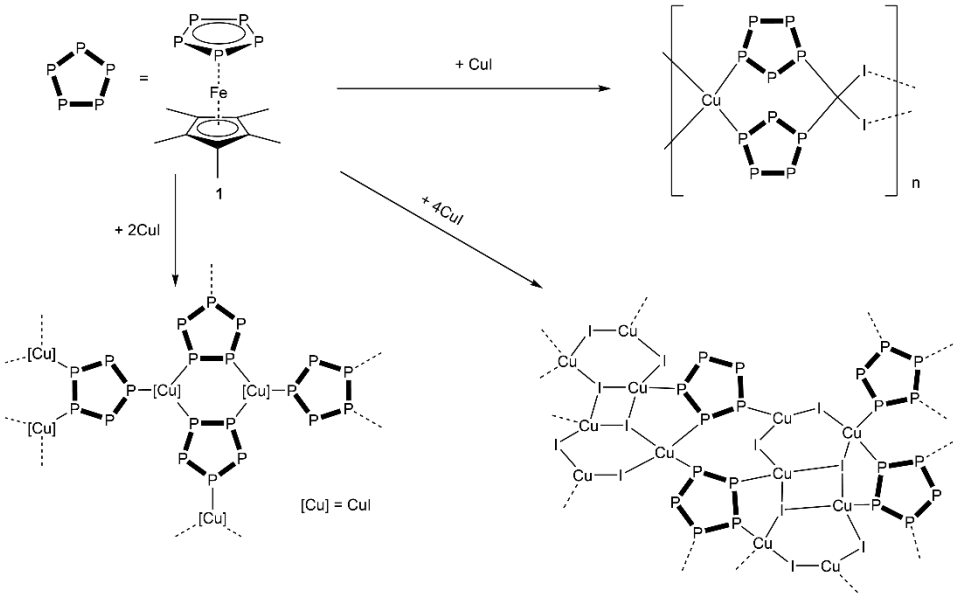

Scheme 4. Different coordination modes and polymers obtained by reacting **1** with different stoichiometries of CuI.

Redox chemistry

The first complex with an end-on coordinated η^5-P_5 ring was published by Scherer in 1987 and is the iron complex $[Cp^*Fe(\eta^5\text{-}P_5)]$[27] (**1**). Because it is isoelectronic and isostructural to ferrocene, it was named pentaphosphaferrocene. Ferrocene is often taken as internal standard in cyclovoltammetric (CV) studies, because it shows a reversible oxidation. The redox properties of pentaphosphaferrocene were studied comprehensively by CV from Winter and Geiger.[34] They observed an irreversible oxidation as well as an irreversible reduction. Furthermore, they predicted a subsequent dimerization of these oxidation and reduction products. Later, it was possible to isolate these species. The dication $[(Cp^*Fe)_2(\mu,\eta^{4:4}\text{-}P_{10})]^{2+}$ and the dianion $[(Cp^*Fe)_2(\mu,\eta^{4:4}\text{-}P_{10})]^{2-}$ (**2**) as well as the non-predicted dianion $[(Cp^*Fe(\eta^4\text{-}P_5)]^{2-}$ (**3**) were isolated and fully characterized.[35] While the *cyclo*-P_5 unit in the starting material **1** is planar, it adopts an envelope-like conformation in the resulting ionic complexes and coordinates in a η^4 fashion to the iron atom. The envelope-like moieties in the binuclear complexes are connected by a P-P single bond and form a P_{10} ligand (Scheme 5).

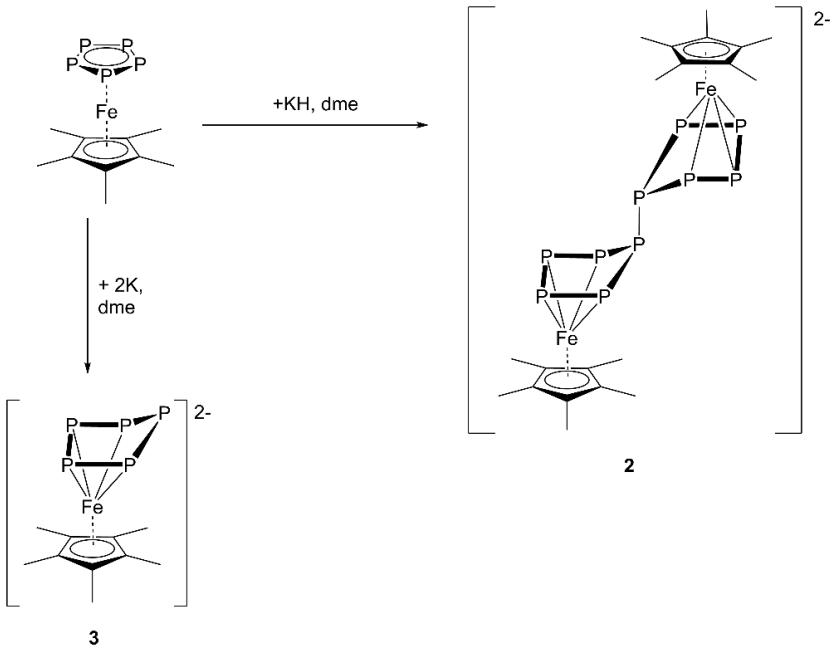

Scheme 5. Reduction of **1** with potassium and potassium hydride – synthesis of the mononuclear (**3**) and the binuclear dianion (**2**).

In prior studies, the in situ reduction of **1** with K/naphthalene and the subsequent reaction with [(Dipp$_2$pyr)SmI(thf)$_3$] (Dipp$_2$pyr = 2,5-bis{*N*-(2,6-diisopropylphenyl)iminomethyl}pyrrolyl) is reported.[36] The resulting 3d/4f element triple-decker complex consists of an envelope-like P_5 unit which is bonded via four phosphorus atoms to iron and via three phosphorus atoms to samarium (Scheme 6). The P_5 ring displays similarities to the uncoordinated reduced species **3**. The same P_{10} framework in **2** is obtained, when samarocene is added to **1**, as well as the coordination of two samarocene fragments.[37]

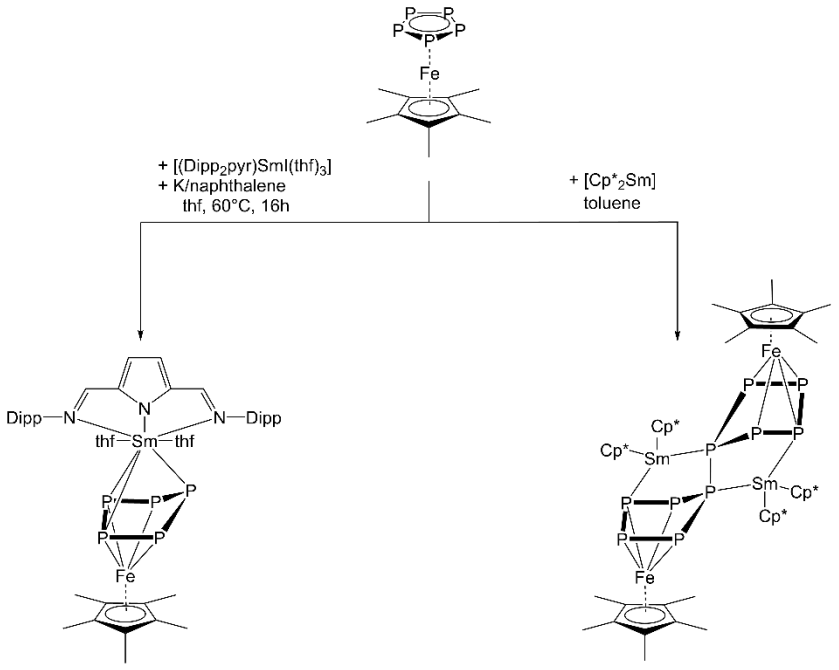

Scheme 6. Samarium containing complexes as reducing agents towards **1**.

Reactivity towards anionic main group element nucleophiles

Pentaphosphaferrocene was investigated by means of density functional theory calculations (DFT) which revealed, that the LUMO and LUMO+1 orbitals are mostly localized on the P atoms of the *cyclo*-P_5 ligand.[38] Hence, the attack of a nucleophile would be expected to occur at the phosphorus atoms. The reactivity of **1** towards nucleophiles was studied comprehensively[39] and different main group element centered nucleophiles were investigated. Reactions of **1** with and $LiCH_2SiMe_3$ or $LiNMe_2$ result in an immediate color change from green to dark brown. The resulting complexes $[Cp^*Fe(\eta^4\text{-}P_5R)]^-$ (R = CH_2SiMe_3, NMe_2) contain a *cyclo*-P_5 ligand in an envelope conformation and a newly formed P-C or P-N bond, respectively (Scheme 5). $NaNH_2$ can react as nucleophile, but is also a strong base. When $NaNH_2$ is reacted with **1**, a subsequent deprotonation of the resulting complex $[(Cp^*Fe(\eta^4\text{-}P_5NH_2)]^-$ with NH_2^- takes places. Therefore, it was neither possible to isolate the monoionic compound nor the dianionic complex $[\{Cp^*Fe(\eta^4\text{-}P_5)\}_2NH]^{2-}$ but the trianionic complex $[\{Cp^*Fe(\eta^4\text{-}P_5)\}_2N]^{3-}$ (**4**) (Scheme 5). Reaction of $LiPH_2$ with **1** results in the monoionic complex $[Cp^*Fe(\eta^4\text{-}P_5PH_2)]^-$ (**5**) and the dianionic complex $[\{Cp^*Fe(\eta^4\text{-}P_5)\}_2PH]^{2-}$ (Scheme 7). PH_2^- can act as a base like NH_2^-. The reason why $[\{Cp^*Fe(\eta^4\text{-}P_5)\}_2P]^{3-}$ is not obtained were explained by DFT calculations. All reactions of the iron complexes with NH_2^- are exothermic, which allows the isolation of **4**. The relative energy profile of the reaction of **1** with PH_2^- differs remarkably from the energy profile of the reaction of **1** and NH_2^-. The formation of the main product **5** is exothermic, while all subsequent reactions are endothermic.

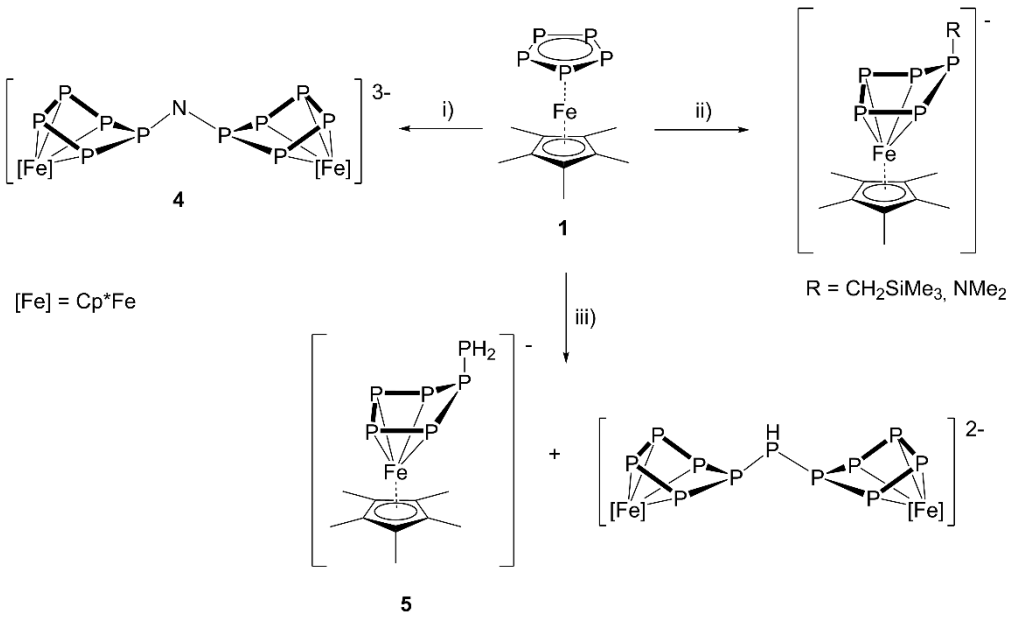

Scheme 7. Selected reactions of **1** with different main group element nucleophiles: i) $LiNH_2$, ii) $LiCH_2SiMe_3$ or $LiNMe_2$, iii) $LiPH_2$.

An electrophilic quenching of the anionic complexes $[Cp^*Fe(\eta^4\text{-}P_5CH_2SiMe_3)]^-$ and $[Cp^*Fe(\eta^4\text{-}P_5NMe_2)]^-$ is possible with $[(Cp'''MX)_2]$ (M = Cr (X = Cl), Fe (X = Br), Co (X = Cl), Ni (X = Br)) (Scheme 8).[40]

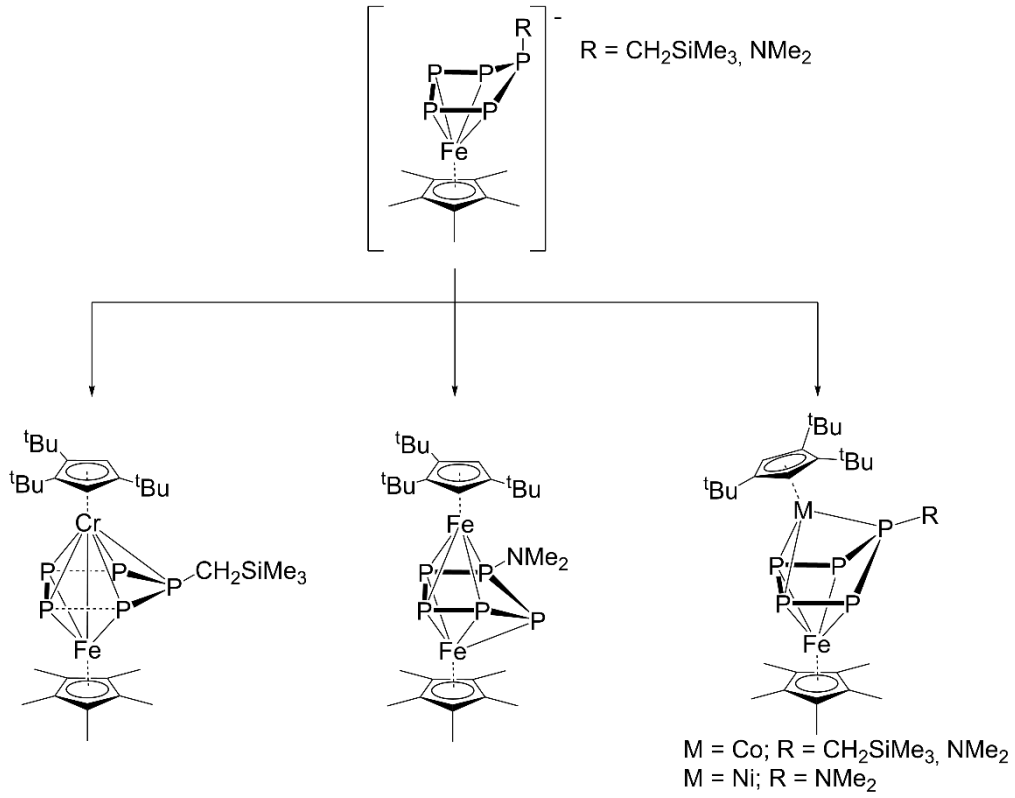

Scheme 8. Electrophilic quenching of $[Cp^*Fe(\eta^4\text{-}P_5R)]^-$ (R = CH_2SiMe_3, NMe_2) with cyclopentadienyl metal halide fragments.

References:

[1] J. R. Nitschke, *Nat Chem* **2011**, *3*, 90.
[2] F. Krafft, *Angew. Chem. Int. Ed.* **1969**, *8*, 660-671.
[3] A. F. Hollemann, N. Wiberg, E. Wiberg, *Lehrbuch der Anorganische Chemie, Vol. 102* **2007**, *Walter de Gruyter, Berlin*.
[4] a) H. Okudera, R. E. Dinnebier, A. Simon, *Z. Kristallogr.* **2005**, *220*, 259-264; b) A. Simon, H. Borrmann, H. Craubner, *Phosphorus, Sulfur Silicon Relat. Elem.* **1987**, *30*, 507-510.
[5] W. L. Roth, T. W. DeWitt, A. J. Smith, *J. Am. Chem. Soc.* **1947**, *69*, 2881-2885.
[6] M. Ruck, D. Hoppe, B. Wahl, P. Simon, Y. Wang, G. Seifert, *Angew. Chem. Int. Ed.* **2005**, *44*, 7616-7619.
[7] W. Hittorf, *Ann. Phys. Chem.* **1865**, *126*, 193.
[8] a) H. Thurn, H. Krebs, *Acta Crystallogr. Sect. B: Struct. Sci.* **1969**, *25*, 125-135; b) H. Thurn, H. Krebs, *Angew. Chem. Int. Ed.* **1966**, *5*, 1047-1048.
[9] P. W. Bridgman, *J. Am. Chem. Soc.* **1914**, *36*, 1344-1363.
[10] A. P. Ginsberg, W. E. Lindsell, *J. Am. Chem. Soc.* **1971**, *93*, 2082-2084.
[11] A. Vizi-Orosz, G. Pályi, L. Markó, *J. Organomet. Chem.* **1973**, *60*, C25-C26.
[12] a) M. Scheer, G. Balázs, A. Seitz, *Chem. Rev.* **2010**, *110*, 4236-4256; b) M. Caporali, L. Gonsalvi, A. Rossin, M. Peruzzini, *Chem. Rev.* **2010**, *110*, 4178-4235; c) O. J. Scherer, *Acc. Chem. Res.* **1999**, *32*, 751-762; d) O. J. Scherer, *Angew. Chem.* **1990**, *102*, 1137-1155.
[13] P. Dapporto, S. Midollini, L. Sacconi, *Angew. Chem. Int. Ed.* **1979**, *18*, 469-469.
[14] O. J. Scherer, M. Swarowsky, G. Wolmershaeuser, *Organometallics* **1989**, *8*, 841-842.
[15] O. J. Scherer, G. Schwarz, G. Wolmershäuser, *Z. Anorg. Allg. Chem.* **1996**, *622*, 951-957.
[16] F. Dielmann, M. Sierka, A. V. Virovets, M. Scheer, *Angew. Chem. Int. Ed.* **2010**, *49*, 6860-6864.
[17] A. Strube, J. Heuser, G. Huttner, H. Lang, *J. Organomet. Chem.* **1988**, *356*, C9-C11.
[18] V. Grossbruchhaus, D. Rehder, *Inorg. Chim. Acta* **1988**, *141*, 9-10.
[19] G. Huttner, G. Mohr, B. Pritzlaff, J. V. Seyerl, L. Zsolnai, *Chem. Ber.* **1982**, *115*, 2044-2049.
[20] C. E. Laplaza, W. M. Davis, C. C. Cummins, *Angew. Chem. Int. Ed.* **1995**, *34*, 2042-2044.
[21] O. J. Scherer, H. Sitzmann, G. Wolmershäuser, *J. Organomet. Chem.* **1984**, *268*, C9-C12.
[22] H. Schäufer, D. Binder, *Z. Anorg. Allg. Chem.* **1987**, *546*, 55-78.
[23] O. J. Scherer, M. Ehses, G. Wolmershäuser, *Angew. Chem. Int. Ed.* **1998**, *37*, 507-510.
[24] O. J. Scherer, J. Braun, G. Wolmershäuser, *Chem. Ber.* **1990**, *123*, 471-475.
[25] M. Di Vaira, S. Midollini, L. Sacconi, *J. Am. Chem. Soc.* **1979**, *101*, 1757-1763.
[26] O. J. Scherer, R. Winter, G. Wolmershäuser, *Z. Anorg. Allg. Chem.* **1993**, *619*, 827-835.
[27] O. J. Scherer, T. Brück, *Angew. Chem. Int. Ed.* **1987**, *26*, 59-59.
[28] O. J. Scherer, J. Schwalb, G. Wolmershäuser, W. Kaim, R. Gross, *Angew. Chem. Int. Ed.* **1986**, *25*, 363-364.
[29] M. Fleischmann, C. Heindl, M. Seidl, G. Balázs, A. V. Virovets, E. V. Peresypkina, M. Tsunoda, F. P. Gabbaï, M. Scheer, *Angew. Chem. Int. Ed.* **2012**, *51*, 9918-9921.
[30] O. J. Scherer, T. Brück, G. Wolmershäuser, *Chem. Ber.* **1989**, *122*, 2049-2054.
[31] M. Scheer, L. J. Gregoriades, A. V. Virovets, W. Kunz, R. Neueder, I. Krossing, *Angew. Chem. Int. Ed.* **2006**, *45*, 5689-5693.
[32] M. Fleischmann, S. Welsch, H. Krauss, M. Schmidt, M. Bodensteiner, E. V. Peresypkina, M. Sierka, C. Groger, M. Scheer, *Chem. Eur. J.* **2014**, *20*, 3759-3768.
[33] F. Dielmann, A. Schindler, S. Scheuermayer, J. Bai, R. Merkle, M. Zabel, A. V. Virovets, E. V. Peresypkina, G. Brunklaus, H. Eckert, M. Scheer, *Chem. Eur. J.* **2012**, *18*, 1168-1179.
[34] R. F. Winter, W. E. Geiger, *Organometallics* **1999**, *18*, 1827-1833.
[35] M. V. Butovskiy, G. Balázs, M. Bodensteiner, E. V. Peresypkina, A. V. Virovets, J. Sutter, M. Scheer, *Angew. Chem. Int. Ed.* **2013**, *52*, 2972-2976.
[36] T. Li, J. Wiecko, N. A. Pushkarevsky, M. T. Gamer, R. Köppe, S. N. Konchenko, M. Scheer, P. W. Roesky, *Angew. Chem. Int. Ed.* **2011**, *50*, 9491-9495.
[37] T. Li, M. T. Gamer, M. Scheer, S. N. Konchenko, P. W. Roesky, *Chem. Commun.* **2013**, *49*, 2183-2185.

[38] a) E. J. P. Malar, *Eur. J. Inorg. Chem.* **2004**, 2723-2732; b) H. Krauss, G. Balázs, M. Bodensteiner, M. Scheer, *Chem. Sci.* **2010**, *1*, 337-342.
[39] E. Mädl, M. V. Butovskii, G. Balázs, E. V. Peresypkina, A. V. Virovets, M. Seidl, M. Scheer, *Angew. Chem. Int. Ed.* **2014**, *53*, 7643-7646.
[40] E. Madl, E. Peresypkina, A. Y. Timoshkin, M. Scheer, *Chem. Commun.* **2016**, *52*, 12298-12301.

2. Research Objectives

The redox chemistry and reactivity of [Cp*Fe(η^5-P_5)] towards main group nucleophiles and subsequent electrophilic quenching was studied in our group. Many different nucleophiles and electrophilic metal fragments were used but no neutral nucleophiles have been reacted with [Cp*Fe(η^5-P_5)]. Accordingly, the first research objectives of this work are:

- Investigation of the reactivity of [Cp*Fe(η^5-P_5)] towards neutral nucleophiles
- Investigation of the reactivity of [Cp*Fe(η^5-P_5)] towards anionic nucleophiles and of the quenching reactions of the obtained anionic complexes with organic electrophiles

The manifold reactivity of [Cp'''Co(η^4-P_4)] towards reduction agents and main group nucleophiles was investigated in our group. This is another example for the interesting and versatile functionalization of polyphosphorus ligands. The *cyclo*-P_4 ligand ban be rearranged, fragmentated and aggregated. Although, there are numerous of P_n ligand complexes known, only a few have been studied with respect to their behavior towards main group nucleophiles. Therefore, the objectives of the second part of this thesis can be summarized as follows:

- Investigation of the reactivity of [$Cp_2Mo_2(CO)_4$(μ,$\eta^{2:2}$-P_2)] towards nucleophiles
- Investigation of the reactivity of [Cp''Ta$(CO)_2$(η^4-P_4)] towards nucleophiles

3. NHCs as Neutral Donors towards Polyphosphorus Complexes

Felix Riedlberger, Stefano Todisco, Piero Mastrorilli, Alexey Y. Timoshkin, Michael Seidl and Manfred Scheer

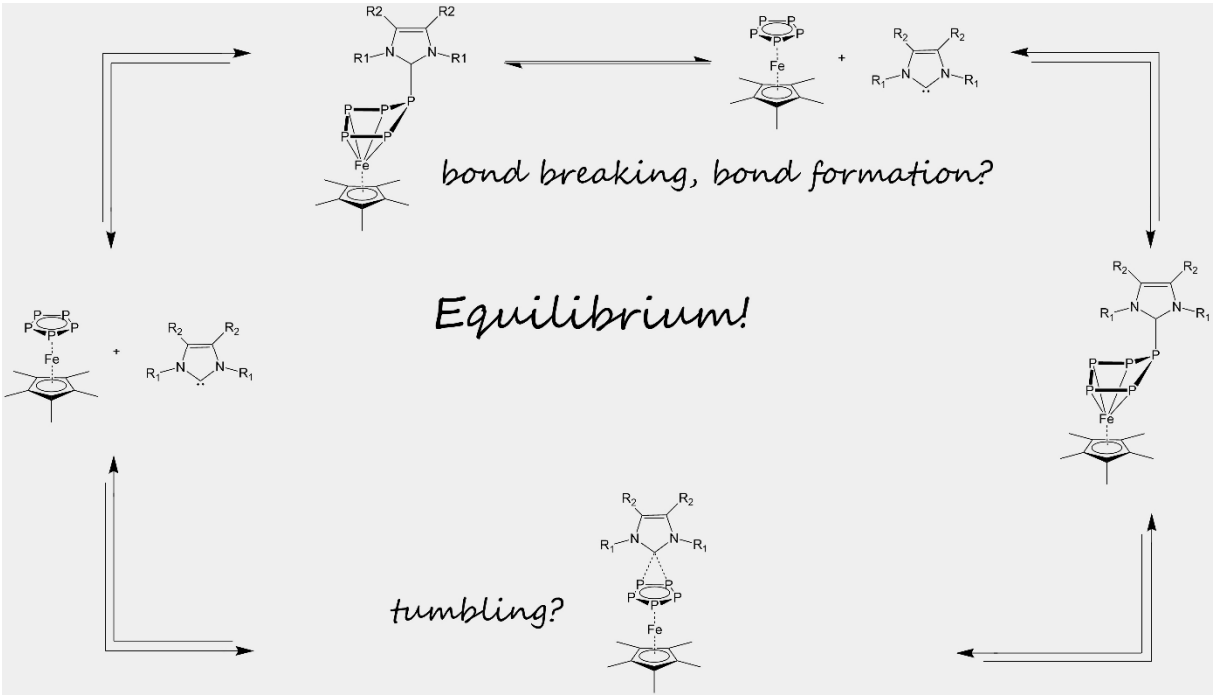

- All compounds were synthesized by Felix Riedlberger.
- The manuscript was written by Felix Riedlberger, except for parts regarding DFT calculations, which were written by Alexey Y. Timoshkin and some parts of the NMR discussion, which were written by Piero Mastrorilli.
- Figures were made by Felix Riedlberger, except figures regarding any calculations, which were made by Alexey Y. Timoshkin and figures regarding X-ray structure determinations in the supporting information were made by Michael Seidl.
- X-ray structure analyses and refinements were performed by Felix Riedlberger and finally checked by Michael Seidl.

3.1 Introduction

Abstract: *The first adducts of NHCs (= N-heterocyclic carbenes) with aromatic polyphosphorus complexes are reported. The reactions of [Cp*Fe(η^5-P_5)] (**1**) (Cp* = pentamethyl-cyclopentadienyl) with IMe (= 1,3,4,5-tetramethylimidazolin-2-ylidene), IMes (= 1,3-bis(2,4,6-trimethylphenyl)-imidazolin-2-ylidene) and IDipp (= 1,3-bis(2,6-diisopropylphenyl)-imidazolin-2-ylidene) led to the corresponding neutral adducts which can be isolated in the solid state. However, in solution, they quickly undergo a dissociative equilibrium between the adduct and **1** including the corresponding NHC. The equilibrium is influenced by the bulkiness of the NHC. [Cp''Ta(CO)$_2$(η^4-P_4)] (Cp'' = 1,3-di-tert-butylcyclopentadienyl) reacts with IMe under P atom abstraction to give an unprecedented cyclo-P_3-containing anionic tantalum complex. DFT calculations shed light onto the energetics of the reaction pathways.*

Pentaphosphaferrocene [Cp*Fe(η^5-P_5)] (**1**) (Cp* = pentamethyl-cyclopentadienyl) was first synthesized by Scherer *et al*.[1] and its reactivity was intensively investigated. It was shown that **1** can coordinate to transition-metal carbonyl species as the *cyclo*-P_5 unit acts as a nucleophile. As a result, triple-decker complexes and other organometallic compounds containing distorted P_5 units were obtained.[2] In the reaction with Cu(I) halides, 1D and 2D polymers result,[3] as well as fullerene-like superballs.[4] Furthermore, Winter and Geiger studied the redox properties of **1** by cyclovoltammetry and predicted a dimerization of the resulting monoionic species.[5] Later, it was possible to isolate and fully characterize these species, *i.e.* the dication $[(Cp^*Fe)_2(\mu,\eta^{4:4}\text{-}P_{10})]^{2+}$ and the dianion $[(Cp^*Fe)_2(\mu,\eta^{4:4}\text{-}P_{10})]^{2-}$ as well as the monomeric dianion $[(Cp^*Fe(\eta^4\text{-}P_5)]^{2-}$.[6] Compared to the starting material **1**, the *cyclo*-P_5 unit in these ionic complexes loses its planarity and adopts an envelope-like structure. This structural motif is also observed when **1** reacts with charged main group element nucleophiles that bind to one phosphorus atom.[7] For this type of reactions, only anionic nucleophiles have been used so far, which give strong adducts since ionic products are formed. However, the reactivity of **1** towards neutral nucleophiles was not yet investigated and, in case of success, neutral and thus moderately stable products are expected to form. One such neutral nucleophile could be the NHCs (= N-heterocyclic carbenes). After the discovery of the first stable NHCs,[8] many others were synthesized and characterized.[9] In fact, NHCs are strong σ donors,[10] which is why they are used as ligands for transition metals,[11] in homogenous catalysis[12] and for stabilizing small molecules.[13] Our first use of NHCs in their reactions towards polyphosphorus complexes containing *cyclo*-P_4 and *cyclo*-P_6 ligands as end- and as middle deck, respectively, showed that P atom elimination reactions occur leading to ring contractions in which the NHCs act as strong nucleophiles and not as simple donor molecules.[14] Therefore, the question arises whether a ring contraction would occur also towards the *cyclo*-P_5 ring in **1** resulting in an anionic *cyclo*-P_4 ligand complex of Fe for which a precedent was recently reported ($[Cp^{Ar}Fe(\eta^4\text{-}P_4)]^-$[15]), or whether unprecedented metastable neutral adducts would result, representing a novel class of compounds, which, for the first time, might reveal no static structures in solution. This question is of general interest, since

NHCs are known to react in deprotonation and dehydrocoupling reactions, respectively, E-H bond activation or ring opening towards main-group element compounds, depending on both the nature of the NHC and the feature (as for instance acidity) of the corresponding compound.[16] Reports on the reactivity of NHCs towards homoatomic aromates in general are unknown, because they act as nucleophiles. In this respect the behavior of NHCs towards non-carbon containing aromates bound in the coordination sphere of transition metals is of general interest, paving the way for our understanding of bonding and interactions. Herein, we report on the reactivity of NHCs towards the polyphosphorus ligand complexes [Cp*Fe(η^5-P_5)] (**1**) and [Cp"Ta(CO)$_2$(η^4-P_4)] (**2**) (Cp" = 1,3-di-*tert*-butylcyclopentadienyl) in which the first neutral adducts of **1** could be isolated.

3.2 Results and Discussion

Depending on the bulkiness and the nucleophilicity of the NHC, adducts of different stability were isolated whose dynamic behavior in solution was elucidated by VT NMR and EXSY experiments. Moreover, in comparison, the behavior of a *cyclo*-P_4 complex of tantalum towards NHC was investigated, showing a reaction pattern in which a novel contracted ring product was formed.

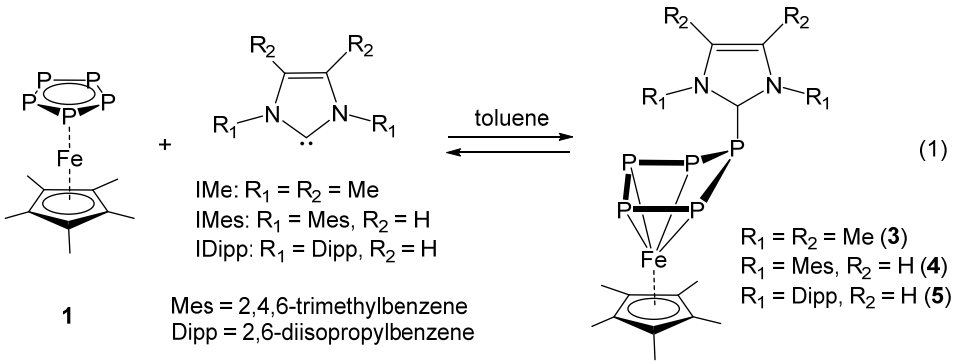

An equimolar mixture of **1** with each of these three different NHCs: IMe (= 1,3,4,5-tetramethylimidazolin-2-ylidene), IMes (= 1,3-bis(2,4,6-trimethylphenyl)-imidazolin-2-ylidene) and IDipp (= 1,3-bis(2,6-diisopropylphenyl)-imidazolin-2-ylidene) in toluene was stirred for 1 h at room temperature. After removing the volatiles, each reaction residue was dissolved in thf and layered with *n*-hexane. Dark green crystals of [Cp*Fe(η^4-P_5IMe)] (**3**), [Cp*Fe(η^4-P_5IMes)] (**4**) and [Cp*Fe(η^4-P_5IDipp)] (**5**) formed in moderate to good yields at 4 °C for **3**, -30 °C for **4** and -78 °C for **5**, respectively (Equation 1). The central structure motif of these neutral complexes in the solid state is a P_5 ring, which loses its planarity and adopts an envelope-like conformation with the NHC being bonded to one phosphorus atom (Figure 1). These structures are reminiscent of products of **1** with anionic nucleophiles,[7] with the difference that, for the first time, neutral adducts (**3**, **4** and **5**) are now accessible. While in ionic derivatives coulomb forces contribute decisively to their stability, there are no such additional forces in the present case of neutral compounds. In comparison to [Cp*Fe(η^4-$P_5CH_2SiMe_3$)]$^-$ (**1a**), the P-P bond lengths (2.1342(11) - 2.1535(9) Å) in **3** and **4** are similar (**3**: 2.1302(8) - 2.1572(7) Å, and **4**: 2.063(3) - 2.184(5) Å). This indicates the multiple-bond character for all P-P bonds. The P-C

bonds of **3** and **4 (**1.860(2) and 1.849(2) Å, respectively) are slightly longer than in **1a** (1.843(3) Å), indicating a weaker bonding in the case of the NHCs as nucleophiles. Despite numerous efforts, the obtained single crystals of **5** were of limited quality and therefore the bond features are not discussed in detail.[17]

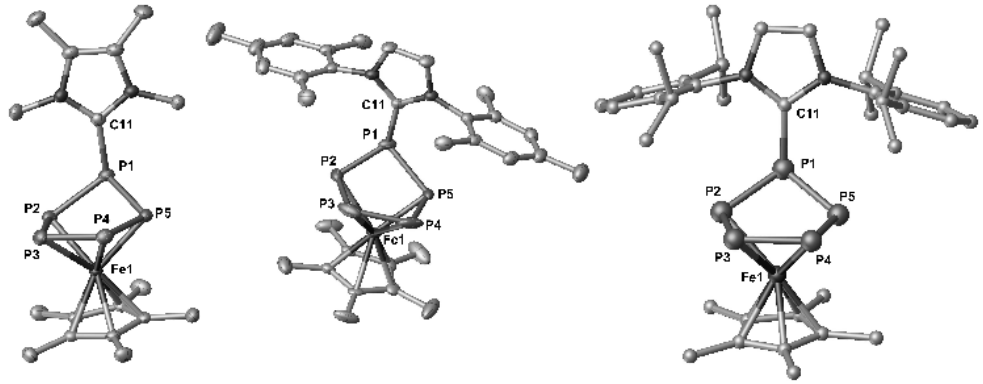

Figure 1. Molecular structure of 3 (left), 4 (middle) and 5 (right) in the solid state. H atoms are omitted for clarity. Selected distances [Å] and angles [°]: for 3: P1-P2 2.1572(7), P1-P5 2.1621(7), P2-P3 2.1552(8), P3-P4 2.1302(8), P4-P5 2.1575(7), P1-C11 1.860(2), Fe1-P2 2.2979(6), Fe1-P3 2.3415(6), Fe1-P4 2.3422(6), Fe1-P5 2.3077(5); P5-P1-P2 95.03(3), P3-P2-P1 107.62(3), P4-P3-P2 104.18(3), P3-P4-P5 104.19(3), P4-P5-P1 107.86(3). For 4: P1-P2 2.063(3), P1-P5 2.184(5), P2-P3 2.143(3), P3-P4 2.115(3), P4-P5 2.138(5), P1-C11 1.849(2), Fe1-P2 2.339(3), Fe1-P3 2.3531(19), Fe1-P4 2.303(2), Fe1-P5 2.263(5); P5-P1-P2 96.04(14), P3-P2-P1 107.57(11), P4-P3-P2 104.12(12), P3-P4-P5 104.08(16), P4-P5-P1 105.7(2). For 5: The figure is drawn as a balls and sticks model (cf.: Supporting Information).

The $^{31}P\{^{1}H\}$ NMR spectra of a 1:1 mixture of **1** and IMe, IMes or IDipp (the same as if crystals of **3** or **4** were dissolved at low temperatures) showed broad signals over a wide range of temperatures, indicating a dynamic behavior of the adducts of **1** with these NHCs. Furthermore, the $^{31}P\{^{1}H\}$ NMR spectra of the 1:1 mixture of **1** and another NHC (I^{t}Bu = 1,3-di-*tert*-butyl-imidazolin-2-ylidene) or an NHO (= N-heterocyclic olefins), IDipp=CH_2 (= $(HCNDipp)_2C=CH_2$, Dipp = 2,6-di-isopropylphenyl) were also recorded at room temperature, because of the pronounced donor ability of I^{t}Bu and IDipp=CH_2.[18] However, no broad signals or a broadening for **1** were detected in these $^{31}P\{^{1}H\}$ NMR spectra, not even at -80°C.

To shed light onto this behavior, DFT calculations at the B3LYP/6-31G* level of theory were performed for adducts of **1** with IMe, IMes and IDipp as well as with I^{t}Bu and IDipp=CH_2 (Table 1). The complexation reactions with IMe, IMes and IDipp are exothermic, and therefore the interactions with **1** are energetically favorable. However, in the case of I^{t}Bu and IDipp=CH_2, gas phase reactions with **1** are predicted to be energetically unfavorable. But, the absolute values of the standard enthalpies are small, and considering that the reaction is accompanied by a lowering of the entropy, the Gibbs energies for

all gaseous reactions are positive (the complex formation is endergonic). Since, experimentally, the reaction proceeds in toluene solution, this indifferent solvent will only slightly affect the enthalpy of the reaction, but the entropy loss will be much less than in the gas phase. The estimation of the reaction entropy in solution according to the literature[19] leads to the values of the equilibrium constants at room temperature of $1.82 \cdot 10^3$, 0.37, and $1.1 \cdot 10^{-4}$ for reactions of **1** with IMe, IMes and IDipp, respectively (see Table 1).

Table 1. Standard enthalpies of complex formation between [Cp*Fe(η^5-P_5)] (**1**) and NHCs/NHO (further abbreviation as LB): **1 + LB** = **1·LB**. Reaction energies $\Delta E°_0$, standard enthalpies $\Delta H°_{298}$, Gibbs energies $\Delta G°_{298}$ (kJ · mol^{-1}) and standard entropies $\Delta S°_{298}$ (J · mol^{-1} · K^{-1}) for the considered gas phase processes. B3LYP/6-31G* level of theory.

LB	$\Delta E°_0$	$\Delta H°_{298}$	$\Delta S°_{298}$(g)	$\Delta G°_{298}$(g)	$\Delta S°_{298}$(soln)	$\Delta G°_{298}$(soln)	K_{298}(soln)	$T_{(K=1)}$,K
IMe	-47.0	-38.6	-157.2	8.2	-67.2	-18.6	$1.82 \cdot 10^3$	575
IMes	-32.2	-28.1	-192.6	29.3	-102.6	2.5	0.37	274
IDipp	-16.4	-9.8	-198.7	49.4	-108.7	22.6	$1.1 \cdot 10^{-4}$	90
I^{t}Bu	41.6	46.8	-185.2	102.0	-95.2	75.2	$6.6 \cdot 10^{-14}$	-
IDipp=CH_2	10.4	18.9	-179.8	72.6	-89.8	45.7	$9.8 \cdot 10^{-9}$	-

The exothermic reactions are thermodynamically favorable at low temperatures. The estimated temperatures at which the equilibrium constant equals 1.0, are 575, 274, and 90 K for IMe, IMes and IDipp, respectively. Therefore, the reaction of **1** with IDipp is expected to occur at much lower temperatures than reactions with IMe and IMes. This reflects the preparative accessibility of the products as seen by the required crystallisation temperature of the adducts. In contrast, in the case of I^{t}Bu and IDipp=CH_2, reactions with **1** both in the gas phase and in solution are predicted to be highly endergonic and thermodynamically prohibited at any temperature.

To gain insights into the dynamic behavior of **1** and IMe in solution, $^{31}P\{^1H\}$ NMR spectra of a 1:1 mixture of **1** and IMe at variable temperatures were recorded (Figure 2). Two very broad signals were observed at room temperature, centered at δ 40 and δ -50. By lowering the temperature, the signals sharpen and a new signal at δ 150.2 appears which can be assigned to free **1**. However, at 193 K, besides the signal for free **1**, three signals at δ 34.7, δ 31.6 and δ -49.1 in an integral ratio of 2:1:2 were detected. This NMR spectrum indicates the formation of a compound containing an envelope-like P_5 ring at low temperatures according to the molecular structure of **3**. Additionally, these spectroscopic investigations show the occurrence of a highly dynamic system in solution. To explain this dynamic process between **1** and IMe, two mechanisms are conceivable: either a tumbling process where the IMe migrates around

the P_5 ring and interacts with more than one P atom at the same time or a P–C bond formation and breaking (dissociative/associative) process.

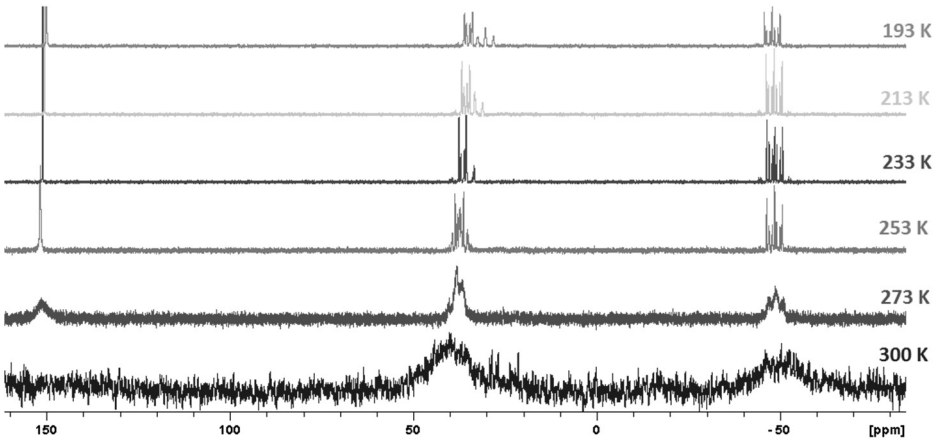

Figure 2. $^{31}P\{^1H\}$ NMR spectra of 1 and IMe in toluene-d_8 in the range of 300 to 193 K.

To clarify which of the two mechanisms does take place, a ^1H EXSY spectrum of a toluene-d_8 solution containing **1** and IMe at 263 K was recorded (Figure 3) which showed two cross peaks: one between the signals at δ 1.5 and δ 0.6 and one between the signals at δ 3.5 and δ 2.8 ppm. The signals at δ 1.5 and δ 3.5 are assigned to the C-CH_3 and N-CH_3 methyl groups of free IMe, respectively, whereas the signals at δ 0.6 and δ 2.8 are assigned to the C-CH_3 and N-CH_3 methyl groups in the adduct [Cp*Fe(η^4-P_5IMe)] (**3**). Thus, the ^1H EXSY spectrum of **1** plus IMe revealed a strong exchange between free and P-bonded IMe at 263 K, which is compatible with the dissociative/associative process.

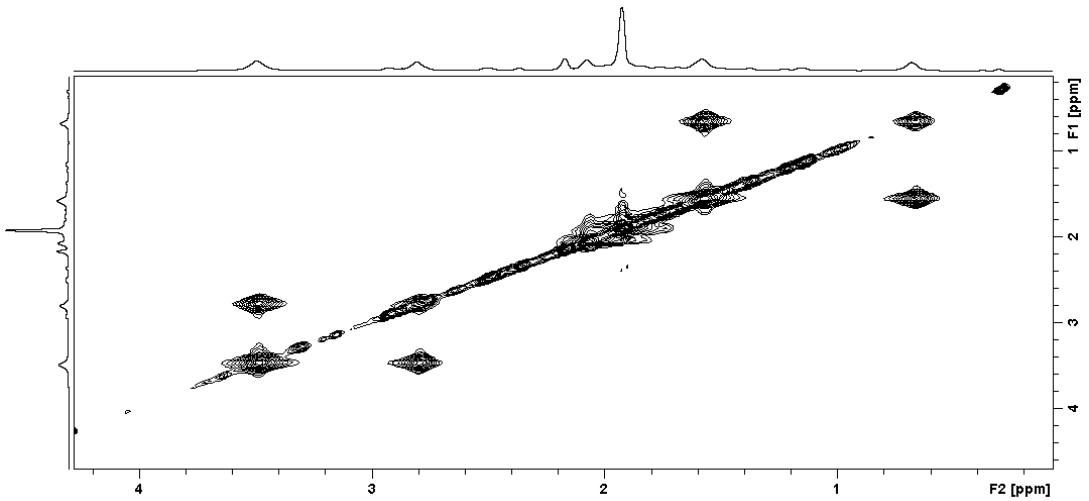

Figure 3. ^1H EXSY spectrum of **1** and IMe in toluene-d_8 at 263 K.

The definite proof that the dynamic process occurring for **1** and IMe in solution is the P–C bond formation and breaking process was derived from the $^{31}P\{^1H\}$ EXSY spectrum of a solution of **1** and

IMe in toluene-d_8 at 263 K (Figure 4). This spectrum showed cross peaks between each of the ^{31}P signals of the diagonal (at δ 150.2 for **1** and at δ 37 and δ -48.7 for **3**) and both other signals, indicating that the ^{31}P nucleus of **1** interchanges with each of the ^{31}P nuclei of **3** (and that the ^{31}P nuclei of **3** exchange each other). Considering exclusively a tumbling process of **3** in solution, there would not be a cross peak between the signals for **1** and **3**. Consequentially, the dynamic behavior of IMe and **1** at 263 K can be explained by a bond formation and bond breaking process.

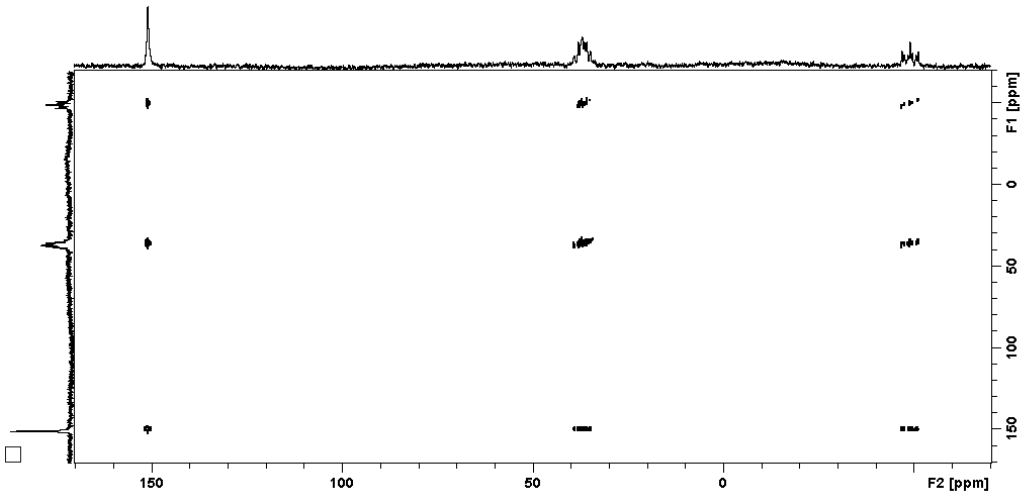

Figure 4. $^{31}P\{^1H\}$ EXSY spectrum of **1** and IMe in toluene-d_8 at 263 K.

In addition to the NMR investigations in solution, a study of the solid-state behavior by recording the ^{31}P MAS NMR exemplified for **3** was executed (Figure 5). Two measurements with spinning frequencies of 14.5 kHz and 12.5 kHz were carried out in order to determine the isotropic chemical shift of the ^{31}P nuclei which were found at δ 123, δ 70, δ 50, δ -27 and δ -46 ppm, indicating that the five ^{31}P nuclei in **3** are inequivalent, as expected on the basis of the X-ray structure.

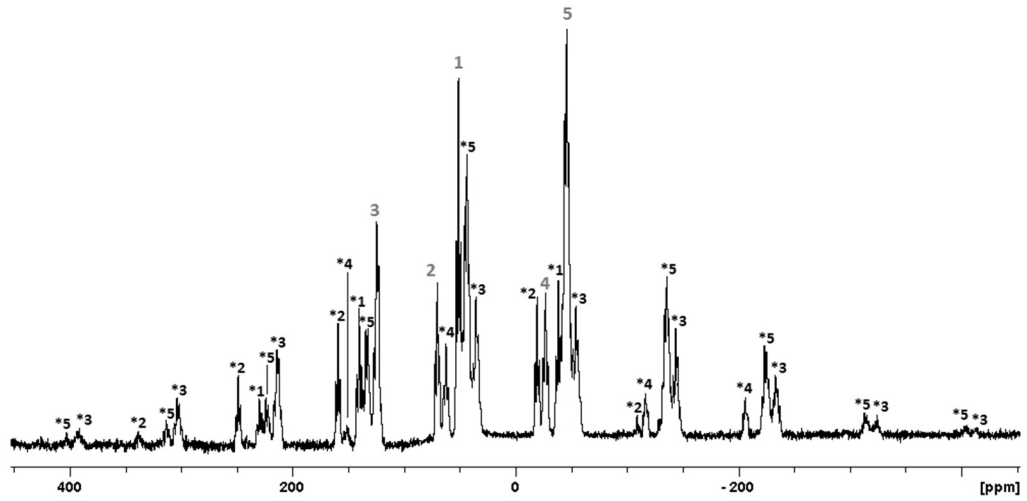

Figure 5. ^{31}P MAS NMR spectrum of **3** obtained at 298 K at a spinning rate of 14.5 kHz. The green numbers without asterisk denote the isotropic ^{31}P chemical shifts.

The $^{31}P\{^{1}H\}$ NMR spectrum of a 1:1 mixture of **1** and IMes at room temperature showed a very broad signal at δ 49 which, upon cooling, shows coalescence at 273 K and, upon further cooling, decoalesces giving rise, below 253 K, to three signals at δ 44.0, δ 33.0 and δ -66.0 with an integral ratio of 1:2:2 that can be assigned to **4**, plus a singlet at δ 150.2, ascribable to **1** (Figure S 3). This behavior is interpreted assuming that complex **4** is more labile in solution than **3** and that at room temperature only an averaged signal for the ^{31}P nuclei of **1** and **4** (in fast equilibrium, see eq. 1) is detectable. The higher lability of **4** as opposed to **3** is in accordance with the DFT calculations (vide supra), which predict a minimum stability for the adduct **5** with respect to **4** and **3**. And, in fact, a distinct interaction between **1** and IDipp was detected at much lower temperatures than with IMe or IMes. The $^{31}P\{^{1}H\}$ NMR spectrum of the 1:1 mixture of **1** and IDipp showed clear signals for **5** (δ 40.5, δ 35.7 and δ -62.1 with an integral ratio of 1:2:2), along with **1**, only at a temperature as low as 193 K (Figure S 5). From 233 K upwards, the averaged signal for the ^{31}P nuclei of **1** and **5** is detected with chemical shifts that move towards that of **1** when the temperature is raised. At room temperature, only the singlet at δ 150.2 assigned to **1** could be detected, indicating that at room temperature a negligible interaction between **1** and IDipp occurs. Isolated crystals of **5** are extremely temperature-sensitive and can only be handled at temperatures below 195 K.

Once having ascertained that the *cyclo*-P_5 ring does form neutral adducts with NHCs, the question arises if such neutral adduct formation can be transferred also to *cyclo*-P_4 rings. To answer this question, we reacted [Cp"Ta(CO)$_2$(η^4-P$_4$)] (**2**)[20] with IMe in toluene, obtaining, to our surprise, the unprecedented *cyclo*-P_3 complex [(IMe)$_2$P][Cp"Ta(CO)$_2$(η^3-P$_3$)] (**6**) in good yields (Equation 2).

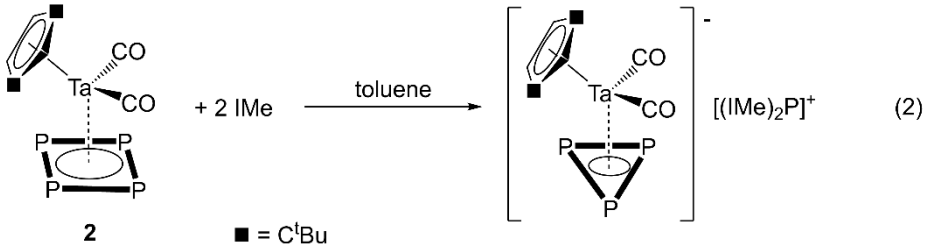

(2)

If less than two equivalents of IMe are used, the conversion is not complete and the $^{31}P\{^{1}H\}$ NMR spectrum shows unreacted **2** and **6**. Thus, the tantalum species **2** loses one phosphorus atom to form an anionic complex with an η^3-P_3 ring and the eliminated phosphorus atom is coordinated by two NHC molecules forming the $[(IMe)_2P]^+$ cation. The $^{31}P\{^{1}H\}$ NMR spectrum of **6** showed a singlet at δ -113.1 for the $[(IMe)_2P]^+$ cation and a singlet at δ -421.9 for the $[(Cp"Ta(CO)_2(\eta^3\text{-}P_3)]^-$ anion in a 1:3 integral ratio. Red crystals of **6** were obtained in a saturated acetonitrile solution, which were submitted to XRD analysis. In the solid state, the anion of **6** shows an unprecedented cyclic P_3 unit coordinated to the tantalum atom carrying additionally two carbonyl and the Cp" ligands (Figure 6). The distances between the tantalum and the phosphorus atoms differ. Two shorter bonds (2.563(2) and 2.568(2) Å) and one slightly elongated bond (2.614(2) Å) are found.

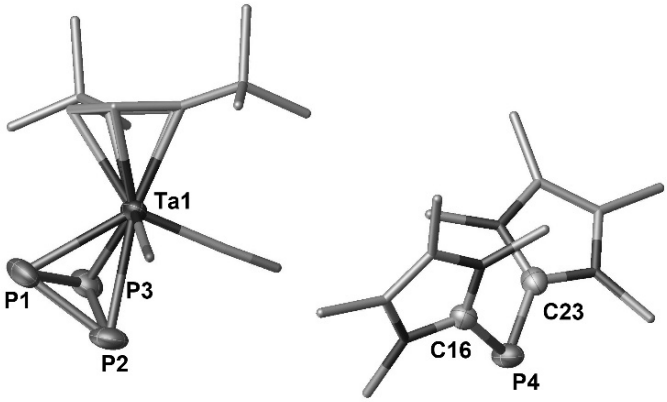

Figure 6. Molecular structure of 6 in the solid state. H atoms are omitted for clarity. Selected distances [Å] and angles [°]: P1-P2 2.169(4), P1-P3 2.186(3), P2-P3 2.184(3), P4-C16 1.797(8), P4-C23 1.796(8), Ta1-P1 2.568(2), Ta1-P2 2.614(2), Ta1-P3 2.563(2); P1-P2-P3 60.26(12), P2-P3-P1 59.53(13), P3-P1-P2 60.21(12), C16-P4-C23 97.9(3).

The calculated Wiberg bond indexes (WBIs) using the experimental solid-state geometry of the anion at the B3LYP/def2-SVPD level of theory (see Supporting Information) reveal for the shorter Ta-P distances values of 0.85 and 0.87. The WBI for the elongated Ta-P distance is 0.76. The P-P bond lengths within the P_3 ring are 2.184(4), 2.186(3) and 2.169(4) Å with WBIs of 1.00, 1.00 and 1.01. The P-C distances of the cation are 1.797(8) and 1.796(8) Å and are therefore characteristic of P-C single bonds. The angle between the two NHC carbon atoms and the phosphorus atom (C23-P4-C16) in the cation is close to right (97.9(3)°).

3.3 Conclusion and References

In summary, we reported the synthesis of the first neutral iron complexes [Cp*Fe(η^4-P_5NHC)] (NHC = IMe: **3**, NHC = IMes: **4**, NHC = IDipp: **5**) in which the NHCs act as neutral donors and the *cyclo*-P_5 unit adopts an envelope-like structure. VT NMR experiments elucidated their dynamic behavior in solution, consisting in C–P bond breaking and reformation. The stability of the adducts **3**-**5** decreases in the order **3**>**4**>**5**, as indicated by DFT calculations and dynamic NMR studies. In contrast to the reaction of the NHCs with the *cyclo*-P_5 ring of **1**, the *cyclo*-P_4 ring of [Cp"Ta$(CO)_2$(η^4-P_4)] reacts with IMe with a phosphorus atom being abstracted to form an unprecedented anionic tantalum complex with a *cyclo*-P_3 unit and a cationic phosphorus atom stabilized by two NHC units. These results exhibit the high potential of NHCs in the chemistry of heteroaromates revealing adduct formations or elimination reactions, a topic which will further investigated in a broader scope.

References:

[1] O. J. Scherer, T. Brück, *Angew. Chem. Int. Ed.* **1987**, *26*, 59-59.

[2] a) M. Detzel, T. Mohr, O. J. Scherer, G. Wolmershäuser, *Angew. Chem. Int. Ed.* **1994**, *33*, 1142-1144; b) O. J. Scherer, *Acc. Chem. Res.* **1999**, *32*, 751-762.

[3] a) M. Scheer, L. J. Gregoriades, A. V. Virovets, W. Kunz, R. Neueder, I. Krossing, *Angew. Chem. Int. Ed. Engl.* **2006**, *45*, 5689-5693; b) J. Bai, A. V. Virovets, M. Scheer, *Angew. Chem. Int. Ed.* **2002**, *41*, 1737-1740.

[4] a) S. Welsch, C. Groger, M. Sierka, M. Scheer, *Angew. Chem. Int. Ed. Engl.* **2011**, *50*, 1435-1438; b) T. Li, J. Wiecko, N. A. Pushkarevsky, M. T. Gamer, R. Köppe, S. N. Konchenko, M. Scheer, P. W. Roesky, *Angew. Chem. Int. Ed.* **2011**, *50*, 9491-9495; c) M. Scheer, A. Schindler, J. Bai, B. P. Johnson, R. Merkle, R. Winter, A. V. Virovets, E. V. Peresypkina, V. A. Blatov, M. Sierka, H. Eckert, *Chem. Eur. J.* **2010**, *16*, 2092-2107; d) M. Scheer, A. Schindler, C. Groger, A. V. Virovets, E. V. Peresypkina, *Angew. Chem. Int. Ed. Engl.* **2009**, *48*, 5046-5049; e) M. Scheer, A. Schindler, R. Merkle, B. P. Johnson, M. Linseis, R. Winter, C. E. Anson, A. V. Virovets, *J. Am. Chem. Soc.* **2007**, *129*, 13386-13387; f) M. Scheer, J. Bai, B. P. Johnson, R. Merkle, A. V. Virovets, C. E. Anson, *Eur. J. Inorg. Chem.* **2005**, *2005*, 4023-4026; g) J. Bai, A. V. Virovets, M. Scheer, *Science* **2003**, *300*, 781-783.

[5] R. F. Winter, W. E. Geiger, *Organometallics* **1999**, *18*, 1827-1833.

[6] M. V. Butovskiy, G. Balázs, M. Bodensteiner, E. V. Peresypkina, A. V. Virovets, J. Sutter, M. Scheer, *Angew. Chem. Int. Ed.* **2013**, *52*, 2972-2976.

[7] E. Mädl, M. V. Butovskii, G. Balázs, E. V. Peresypkina, A. V. Virovets, M. Seidl, M. Scheer, *Angew. Chem. Int. Ed.* **2014**, *53*, 7643-7646.

[8] A. J. Arduengo III, R. L. Harlow, M. Kline, *J. Am. Chem. Soc.* **1991**, *113*, 361-363.

[9] a) D. Martin, M. Melaimi, M. Soleilhavoup, G. Bertrand, *Organometallics* **2011**, *30*, 5304-5313; b) M. Melaimi, M. Soleilhavoup, G. Bertrand, *Angew. Chem. Int. Ed. Engl.* **2010**, *49*, 8810-8849; c) J. Vignolle, X. Cattoën, D. Bourissou, *Chem. Rev.* **2009**, *109*, 3333-3384; d) O. Schuster, L. Yang, H. G. Raubenheimer, M. Albrecht, *Chem. Rev.* **2009**, *109*, 3445-3478; e) F. E. Hahn, M. C. Jahnke, *Angew. Chem. Int. Ed. Engl.* **2008**, *47*, 3122-3172.

[10] O. Back, M. Henry-Ellinger, C. D. Martin, D. Martin, G. Bertrand, *Angew. Chem. Int. Ed.* **2013**, *52*, 2939-2943.

[11] W. A. Herrmann, *Angew. Chem. Int. Ed.* **2002**, *41*, 1290-1309.

[12] a) E. S. Díez-González), R. S. o. C. Publishing, Cambridge, **2011**; b) G. C. Vougioukalakis, R. H. Grubbs, *Chem. Rev.* **2010**, *110*, 1746-1787; c) S. Díez-González, N. Marion, S. P. Nolan, *Chem. Rev.* **2009**, *109*, 3612-3676.

[13] a) O. Back, B. Donnadieu, P. Parameswaran, G. Frenking, G. Bertrand, *Nat. Chem.* **2010**, *2*, 369-373; b) Y. Wang, Y. Xie, P. Wei, R. B. King, H. F. Schaefer III, P. von Schleyer, G. H. Robinson, *Science* **2008**, *321*, 1069-1071.

[14] M. Piesch, S. Reichl, M. Seidl, G. Balázs, M. Scheer, *Angew. Chem. Int. Ed.* **2019**, *58*, 16563-16568.

[15] U. Chakraborty, J. Leitl, B. Mühldorf, M. Bodensteiner, S. Pelties, R. Wolf, *Dalton Trans* **2018**, *47*, 3693-3697.

[16] S. Wurtemberger-Pietsch, H. Schneider, T. B. Marder, U. Radius, *Chem. Eur. J.* **2016**, *22*, 13032-13036.

[17] Due to the limited quality of single crystals of **5** and their extreme sensibility (they can only be handled at temperatures < -70°C, also in the solid state), the best X-ray structure analysis only gave a confident atom connectivity (for details cf. Supporting Informations).

[18] M. M. D. Roy, E. Rivard, *Acc. Chem. Res.* **2017**, *50*, 2017-2025.

[19] A. S. Lisovenko, A. Y. Timoshkin, *Inorg. Chem.* **2010**, *49*, 10357-10369.

[20] O. J. Scherer, R. Winter, G. Wolmershäuser, *Z. Anorg. Allg. Chem.* **1993**, *619*, 827-835.

3.4 Supporting Information

Experimental details: complex syntheses and characterization

General Procedures: All manipulations were performed with rigorous exclusion of oxygen and moisture in Schlenk-type glassware on a dual manifold Schlenk line in Argon atmosphere or in Argon filled glove box with a high-capacity recirculator (<0.1 ppm O_2). THF, toluene, *n*-hexanes and acetonitrile were dried using conventional techniques, degassed and saturated with Argon. Deuterated solvents were degassed, dried and distilled prior to use. The complexes [Cp*Fe(η^5-P_5)][1] (1) and [Cp''Ta$(CO)_2$(η^4-P_4)][2] (2) as well as the NHCs (IMe,[3] IMes,[4] IDipp,[5] I^{t}Bu,[6] IDipp=CH_2[7]) were prepared according to published procedure. NMR spectra were recorded on a Bruker Avance 300 MHz and Bruker Avance 400 MHz spectrometers. Chemical shifts are given in ppm; they are referenced to TMS for ^{1}H, and external 85% H_3PO_4 for ^{31}P. Elemental analyses (CHN) were determined using in-house facility. NMR spectrum simulations were performed with the simulation module "daisy", embedded in the software *Bruker Topspin (V. 3.6.1)*. Solid-state ^{31}P NMR: ^{1}H–^{31}P CP/MAS NMR experiments were performed on a Bruker Avance I 400 spectrometer using a 4.0 mm HX MAS probe at 298 K. The sample was packed in a zirconia rotor. A two-pulse phase modulation (TPPM) decoupling scheme was used for ^{1}H decoupling. The spectra were recorded using 3.25 μs proton π/2 pulse length, a ν_{CP} of 55.0 kHz, a contact time of 5.0 ms, a ν_{dec} of 76.9 kHz and a recycle delay of 6 s.

Due to the dynamic behavior of [Cp*Fe(η^4-P_5IMe)] (3), [Cp*Fe(η^4-P_5IMes)] (4) and [Cp*Fe(η^4-P_5IDipp)] (5) in solutions it was impossible to receive meaningful mass spectra. Due to the low solubility of 1 and NHCs at low temperatures and the dynamic behavior in solutions no ^{13}C{^{1}H} NMR spectra of reasonable quality could be recorded.

Synthesis of 3, [Cp*Fe(η^4-P_5IMe)]:

A solution of 100 mg (0.289 mmol) [Cp*Fe(η^5-P_5)] and 35 mg (0.281 mmol) IMe in 10 mL toluene was stirred for 1 hour. The solvent was removed in vacuum and the green precipitate dissolved in 3 mL thf, layered with 6 mL *n*-hexanes and stored at 4 °C to give green crystals overnight.

Crystalline yield: 60 mg, 0,123 mmol, 44%.

^{1}H NMR (toluene-d_8, 213 K): δ [ppm] = 2.29 (s, 6H, N(1,3)-*Me*), 1.91 (s, 15H, *Cp**), 0.38 (s, 6H, C(4,5)-*Me*).

$^{31}P\{^{1}H\}$ NMR (toluene-d_8, 213 K): δ [ppm] = 34.7 (m, $P_M/P_{M'}$), 31.6 (P_A), -49.1 (m, $P_X/P_{X'}$). For coupling constants see Table S 1.

EA calculated for $C_{17}H_{27}FeN_2P_5$ (470,12 g·mol^{-1}): C: 43.43, H 5.79, N 5.96; found [%]: C: 43.50, H 5.74, N 5.81.

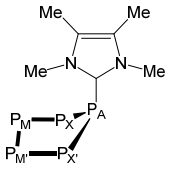

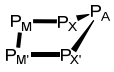

= [Cp*Fe(η^4-P_5)]

Synthesis of 4, [Cp*Fe(η^4-P_5IMes)]:

A solution of 100 mg (0.289 mmol) [Cp*Fe(η^5-P_5)] and 88 mg (0.289 mmol) IMes in 10 mL toluene was stirred for 1 hour. The solvent was removed in vacuum and the green precipitate dissolved in 5 mL thf, layered with 10 mL *n*-hexanes and stored at -30 °C to give green crystals within 48 h.

Crystalline yield: 93 mg, 0.143 mmol, 49%.

^{1}H NMR (toluene-d_8, 213 K): δ [ppm] = 6.74 (s, 4H, Ar-*H*), 4.82 (s, 2H, NC*H*), 2.19 (s, 6H, 4-*Me*), 1.99 (s, 12H, 2,6-*Me*), 1.67 (s, 15H, *Cp**).

$^{31}P\{^{1}H\}$ NMR (toluene-d_8, 213 K): δ [ppm] = 44.0 (m, P_A), 33.0 (m, $P_M/P_{M'}$), -66.0 (m, $P_X/P_{X'}$). For coupling constants see Table S 2.

EA calculated for $C_{31}H_{39}FeN_2P_5$ (650.37 g·mol^{-1}): C: 57.25, H 6.04, N 4.31; found [%]: C: 57.97, H 6.26, N 4.07.

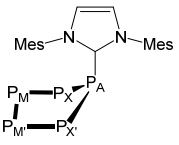

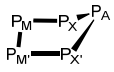

= [Cp*Fe(η^4-P_5)]

Synthesis of 5, [Cp*Fe(η^4-P_5IDipp)]:

A solution of 100 mg (0.289 mmol) [Cp*Fe(η^5-P_5)] and 110 mg (0.289 mmol) IDipp in 10 mL toluene was stirred for 1 hour. All volatiles were removed in vacuum, the green precipitate dissolved in 4 mL thf, layered with 20 mL *n*-hexane and stored at -80 °C to give green crystals overnight.

Crystalline yield: 112 mg, 139 mmol, 48%.

^{1}H NMR (toluene-d_8, 213 K): δ [ppm] = 6.74 (s, 4H, Ar-*H*), 4.82 (s, 2H, NC*H*), 2.19 (s, 6H, 4-*Me*), 1.99 (s, 12H, 2,6-*Me*), 1.67 (s, 15H, *Cp**).

^{31}P{^{1}H} NMR (toluene-d_8, 213 K): δ [ppm] = 44.0 (m, P_A), 33.0 (m, P_M/$P_{M'}$), -66.0 (m, P_X/$P_{X'}$). For coupling constants see Table S 2.

EA calculated for $C_{41}H_{59}FeN_2OP_5$ (806.63 g·mol^{-1}): C: 61.05, H 7.37, N 3.47; found [%]: C: 61.15, H 7.42, N 3.58.

Synthesis of 6, [(IMe)$_2$P][Cp''Ta(CO)$_2$(η^3-P_3)]:

100 mg (0.186 mmol) [Cp''Ta(CO)$_2$(η^4-P_4)] and 100 mg (4.33 eq, 0.805 mmol) IMe were dissolved in 10 mL toluene. The light brownish red solution was stirred for an hour before the solvent was removed. The red precipitate was washed with *n*-hexanes to remove the excess of IMe and then dissolved in 5 mL MeCN. After storage at -30 °C for ten days, red crystals were formed which were suitable for X-ray investigations.

Crystalline yield: 88 mg, 0.112 mmol, 60%.

^{1}H NMR (MeCN-d_3, 300 K): δ [ppm] = 5.11 (t, $^4J_{HH}$ = 2.2 Hz, 1H), 4.91 (d, $^4J_{HH}$ = 2.2 Hz, 2H), 3.53 (s, 12H, N(1,3)-*Me*), 2.16 (s, 12H, C(4,5)-*Me*), 1.18 (s, 18H, ^{t}Bu).

^{31}P{^{1}H} NMR (MeCN-d_3, 300 K): δ [ppm] = -113.1 (s, 1P, IMe-P-IMe), -421.9 (s, 3P, *cyclo*-P_3).

ESI-MS (acetonitrile): anion mode: *m/z* = 507.02 (100%, [Cp''Ta(CO)$_2$(η^3-P_3)]$^-$), cation mode: *m/z* = 279.18 (100%, [(IMe)$_2$P]$^+$).

EA calculated for $C_{29}H_{45}N_4O_2P_4Ta$ (786.54 g·mol^{-1}): C: 44.28, H: 5.77, N: 7.12; found [%]: C: 44.73, H: 5.77, N: 7.19.

Experimental and simulated NMR spectra

Variable temperature $^{31}P\{^{1}H\}$ NMR spectra of **3** in the temperature range of 300 K to 193 K:

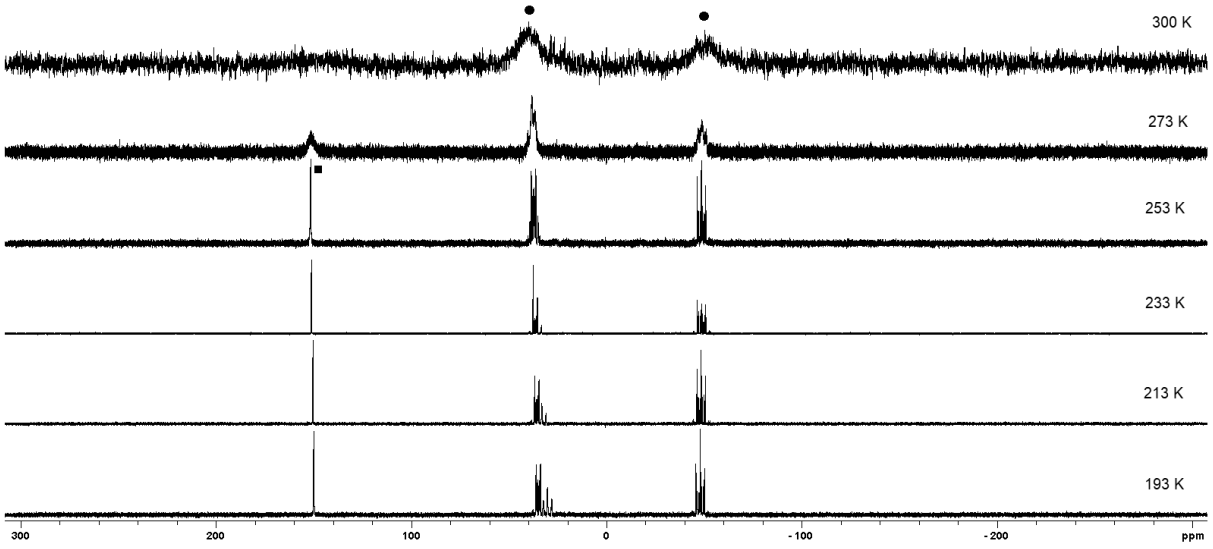

Figure S 1. $^{31}P\{^{1}H\}$ NMR spectra of freshly prepared solution of **1** and IMe in toluene-d_8 in temperature range of 193 K to 300 K. The signal marked with ■ is assigned to **1**. At 300 K first interactions can be detected and is marked with ●. These signals are getting clearer when cooling down and are assigned to compound **3**.

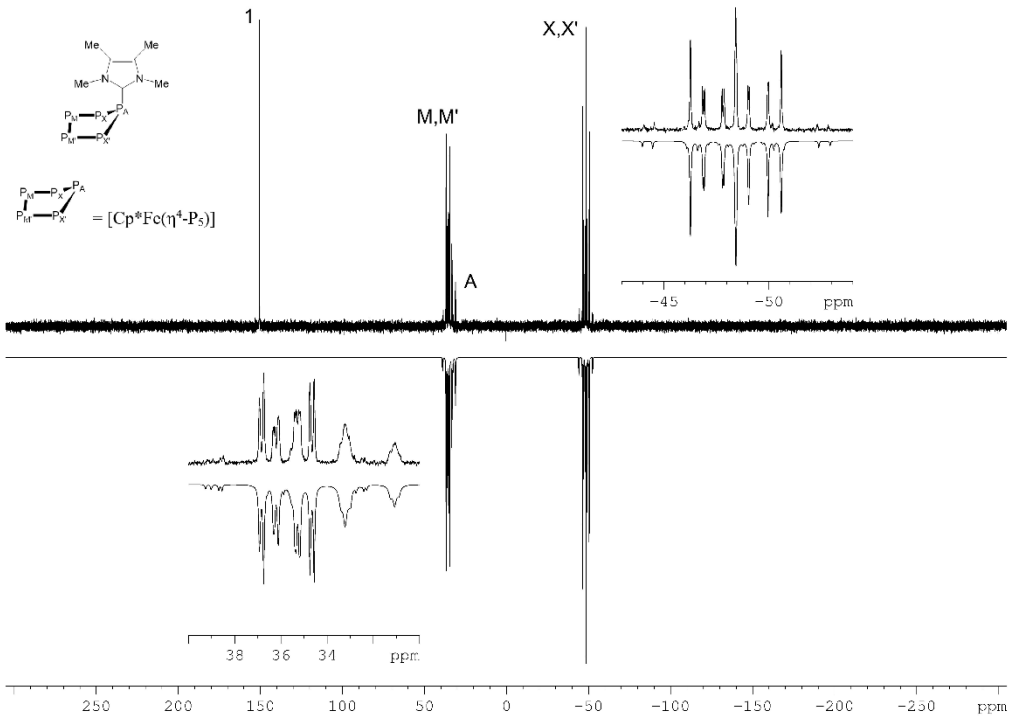

Figure S 2. Experimental (top) and simulated (bottom) $^{31}P\{^{1}H\}$ NMR (162 MHz, toluene-d_8) spectrum of **3** at 213 K.

Table S 1. Chemical shifts and coupling constants obtained from the simulation of the $^{31}P\{^{1}H\}$ NMR spectrum of **3** at 213 K.

***J* (Hz)**				***δ* (ppm)**	
$^{2}J_{P_A,P_M}$	-32.0	$^{1}J_{P_M,P_X}$	365.0	P_A	31.6
$^{2}J_{P_A,P_{M'}}$	-32.0	$^{2}J_{P_M,P_{X'}}$	-8.0	P_M	34.7
$^{1}J_{P_A,P_X}$	355.0	$^{1}J_{P_{M'},P_{X'}}$	365.0	$P_{M'}$	34.7
$^{1}J_{P_A,P_{X'}}$	355.0	$^{2}J_{P_{M'},P_X}$	-8.0	P_X	-49.1
$^{1}J_{P_M,P_{M'}}$	430.0	$^{2}J_{P_X,P_{X'}}$	-50.0	$P_{X'}$	-49.1

Variable temperature $^{31}P\{^{1}H\}$ NMR spectra of 4 in the temperature range of 300 K to 193 K:

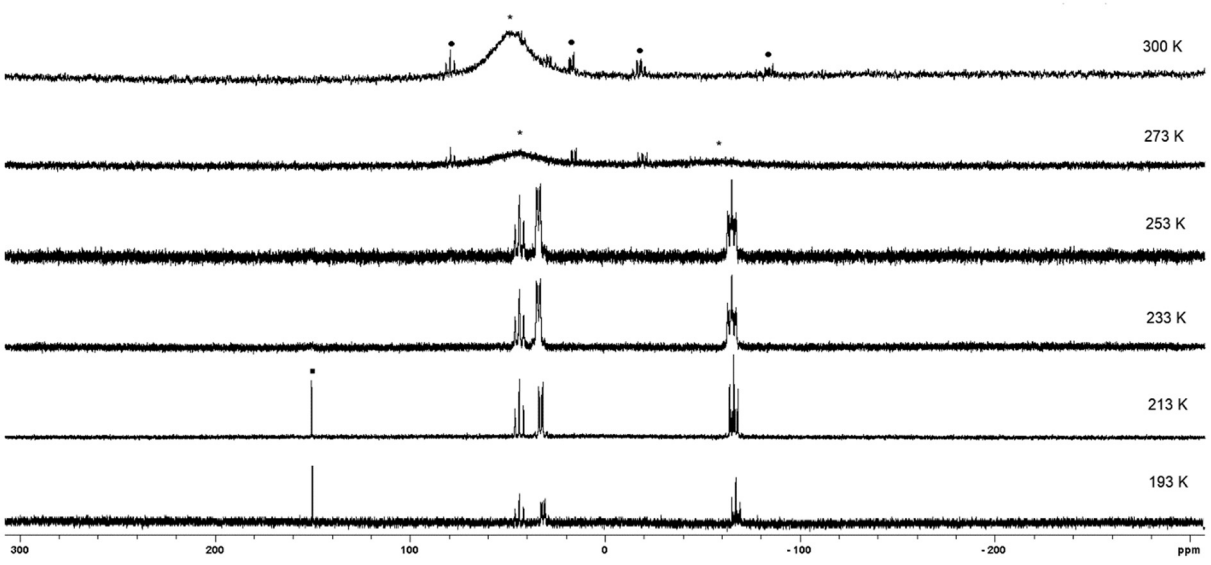

Figure S 3. $^{31}P\{^{1}H\}$ NMR spectra of freshly prepared solution of **1** and IMes in toluene-d_8 in temperature range of 193 K to 300 K. The signals marked with ■ and ● are assigned to **1** and impurities, respectively.

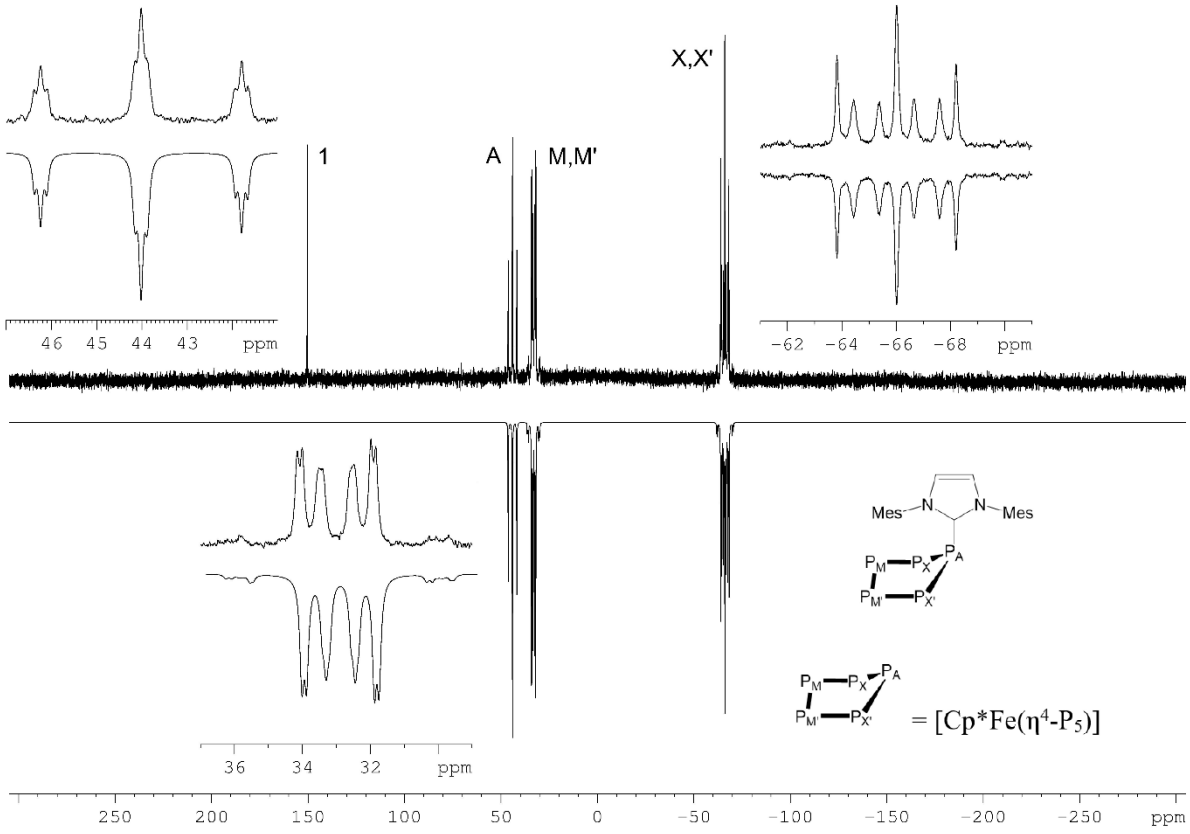

Figure S 4. Experimental (top) and simulated (bottom) $^{31}P\{^{1}H\}$ NMR (162 MHz, toluene-d_8) spectrum of **4** at 213 K.

Table S 2. Chemical shifts and coupling constants obtained from the simulation of the $^{31}P\{^{1}H\}$ NMR spectrum of **4** at 213 K.

***J* (Hz)**				***δ* (ppm)**	
$^{2}J_{P_A,P_M}$	-23.0	$^{1}J_{P_M,P_X}$	354.0	P_A	44.0
$^{2}J_{P_A,P_{M'}}$	-23.0	$^{2}J_{P_M,P_{X'}}$	-8.0	P_M	33.0
$^{1}J_{P_A,P_X}$	354.7	$^{1}J_{P_{M'},P_{X'}}$	354.0	$P_{M'}$	33.0
$^{1}J_{P_A,P_{X'}}$	354.7	$^{2}J_{P_{M'},P_X}$	-8.0	P_X	-66.0
$^{1}J_{P_M,P_{M'}}$	410.0	$^{2}J_{P_X,P_{X'}}$	-55.0	$P_{X'}$	-66.0

Variable temperature $^{31}P\{^{1}H\}$ NMR spectra of **5** in the temperature range of 300 K to 193 K:

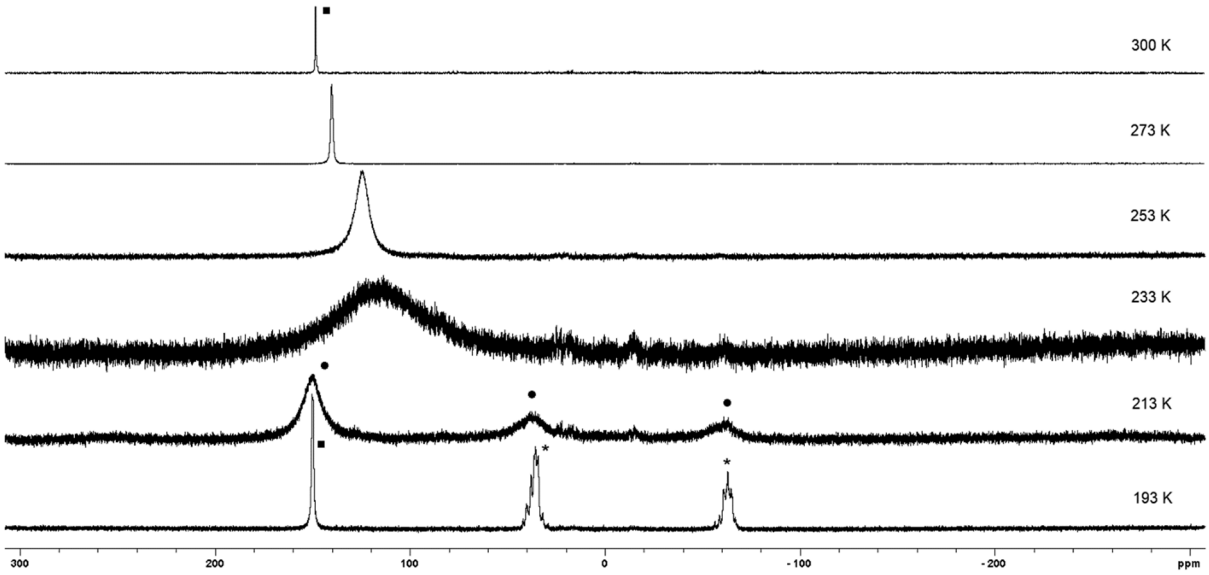

Figure S 5. $^{31}P\{^{1}H\}$ NMR spectra of freshly prepared solution of **1** and IDipp in toluene-d_8 in temperature range of 193 K to 300 K.

Variable temperature $^{31}P\{^{1}H\}$ NMR spectra of **1** and I^{t}Bu in the temperature range of 300 K to 193 K:

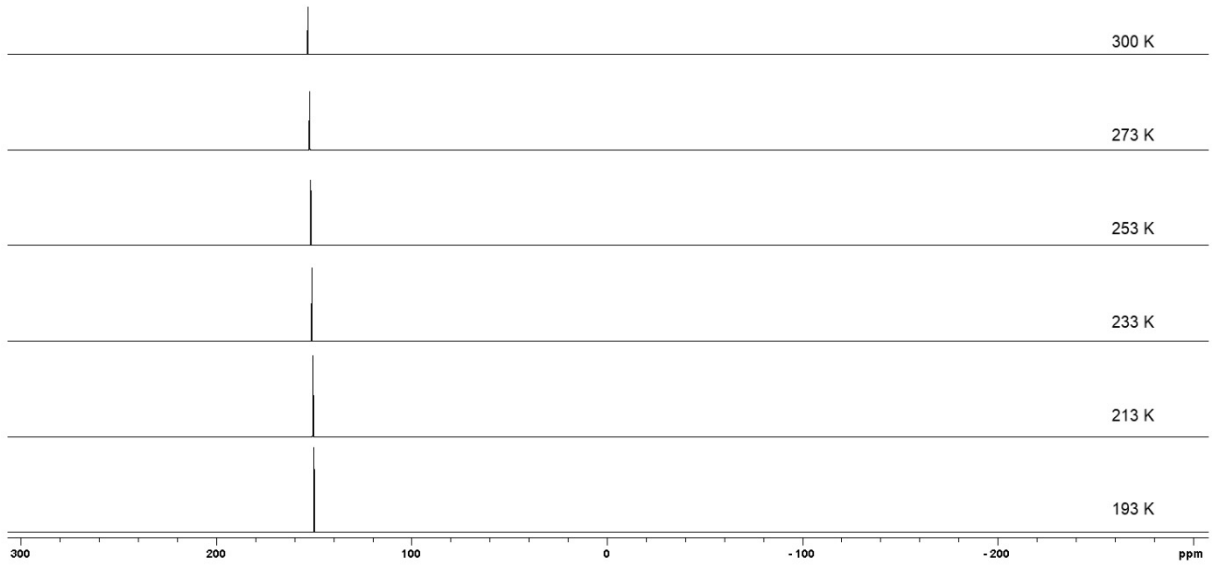

Figure S 6. $^{31}P\{^{1}H\}$ NMR spectra of freshly prepared solution of **1** and I^{t}Bu in toluene-d_8 in temperature range of 193 K to 300 K. Only the signal for **1** is detected.

Variable temperature $^{31}P\{^{1}H\}$ NMR spectra of **1** and IDipp=CH_2 in the temperature range of 300 K to 193 K:

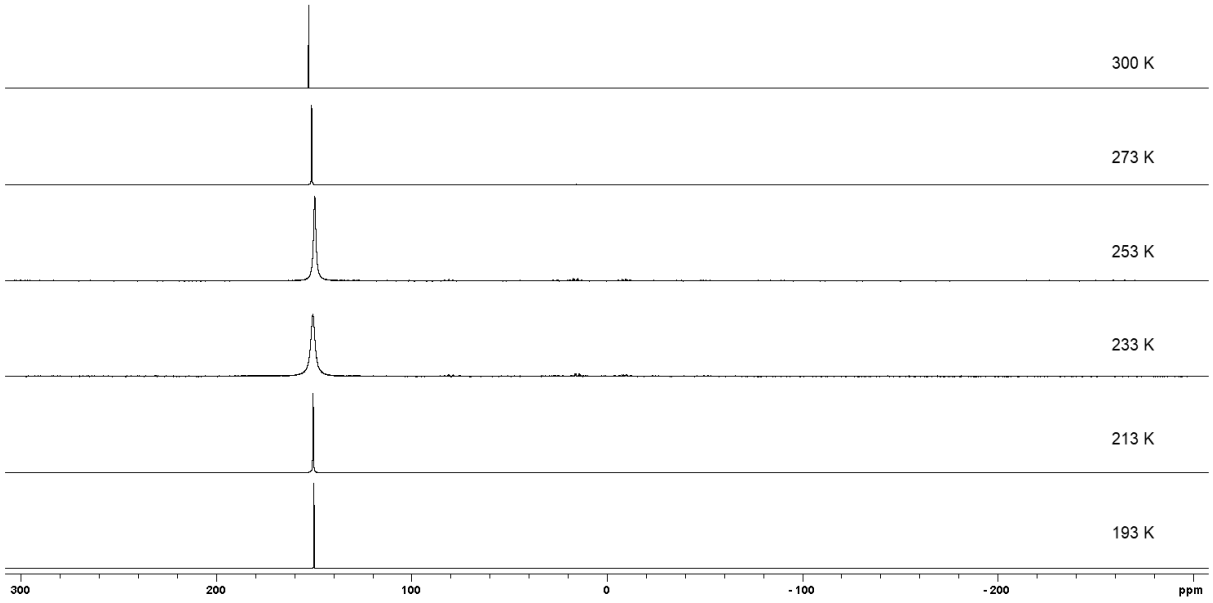

Figure S 7. $^{31}P\{^{1}H\}$ NMR spectra of freshly prepared solution of **1** and IDipp=CH_2 in toluene-d_8 in temperature range of 193 K to 300 K. Only the signal for **1** is detected.

$^{31}P\{^{1}H\}$ NMR spectrum of **6**:

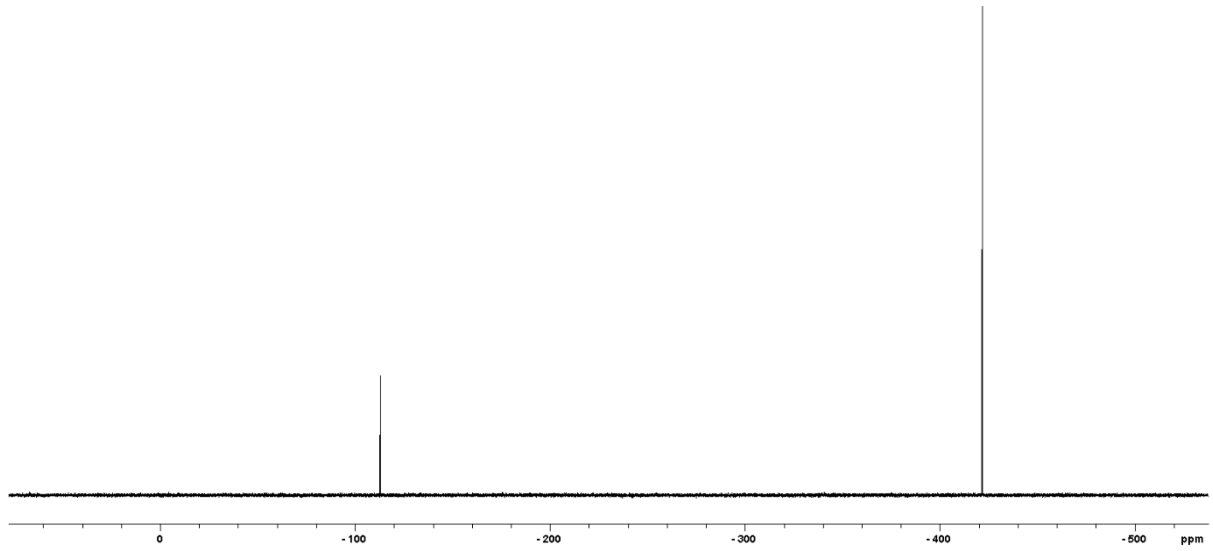

Figure S 8. $^{31}P\{^{1}H\}$ NMR spectrum of compound **6** at 300 K in MeCN-d_3. The singlet at -113.1 ppm is assigned to the cation $[(IMe)_2P]^+$ and the signal at -421.9 ppm is assigned to the anionic complex $[Cp''Ta(CO)_2(\eta^3\text{-}P_3)]^-$.

Crystallographic Details

The crystals were selected and mounted on a GV50 diffractometer equipped with a TitanS2 detector. All crystals were kept at T = 123(1) K during data collection. Data collection and reduction were performed with **CrysAlisPro** version 1.171.40.14a.[8] For compound (**3**) an analytical numeric absorption correction using a multifaceted crystal model based on expressions derived by R.C. Clark & J.S. Reid.(Clark, R. C. & Reid, J. S. (1995). Acta Cryst. A51, 887-897) was applied. For the compounds (**4**, **5**, **6**) a numerical absorption correction based on gaussian integration over a multifaceted crystal model and an empirical absorption correction using spherical harmonics, implemented in SCALE3 ABSPACK scaling algorithm was applied. Using **Olex2**,[9] all structures were solved by **ShelXT**[10] and a least-square refinement on F^2 was carried out with **ShelXL**.[11] All non-hydrogen atoms were refined anisotropically. Hydrogen atoms at the carbon atoms were located in idealized positions and refined isotropically according to the riding model. The images showing the compounds **3**-**6** were generated using **Olex2**.[9]

CCDC-2015543 (**3**), CCDC-2015544 (**4**), CCDC-2015545 (**5**) and CCDC-2015546 (**6**), contain the supplementary crystallographic data for this paper. These data can be obtained free of charge at www.ccdc.cam.ac.uk/contents/retrieving.html (or from the Cambridge Crystallographic Data Centre, 12 Union Road, Cambridge CB2 1EZ, UK; Fax: +44-1223-336-033; e-mail: deposit@ccdc.com.ac.uk).

Compound 3: There is one single molecule of **3** in the asymmetric unit

Compound 4: The asymmetric unit contains one molecule of **4** and two thf solvent molecules. One of these thf molecules was heavily disordered. Therefore, a solvent mask was calculated and 152 electrons were found in a volume of 520 Å^3 in one void per unit cell. This is consistent with the presence of one thf molecule per asymmetric unit, which account for 160 electrons per unit cell. Further, the second thf molecule showed a disorder over two positions (67:33). Additionally, both the P_5 and the Cp* ligand are disordered over two position with a distribution of 58:42 and 62:38, respectively. The restraints SADI and SIMU were applied to describe these disorders.

Compound 5: Crystals of compound **5** were very sensitive and could only be handled at low temperatures (-70°C). Further, the quality of the crystals was very low, despite several attempts of recrystallization. Additionally, the crystals were weakly diffracting, which is the reason that no reflections above a resolution of 0.89, with an I/σ higher than 3, could be detected. Although, the data quality does not allow the discussion of bond length or angles, the atom connectivity in compound **5** could still be determined unambiguously.

The asymmetric unit contains one molecule of **5** and 4.3 thf solvent molecules. Two of these thf solvent molecules were heavily disordered. Therefore, a solvent mask was calculated and 368 electrons were found in a volume of 1418 Å^3 in one void per unit cell. This is consistent with the presence of 2.3 thf molecules per asymmetric unit, which account for 368 electrons per unit cell. Additionally the P_5 ligand

shows a disorder over two positions (82:18). To describe this disorder the SADI and SIMU restraint was applied.

The asymmetric unit contains one molecule of **5** and 4.3 thf solvent molecules. Two of these thf solvent molecules were heavily disordered. Therefore, a solvent mask was calculated and 368 electrons were found in a volume of 1418 $Å^3$ in one void per unit cell. This is consistent with the presence of 2.3 thf molecules per asymmetric unit, which account for 368 electrons per unit cell. Additionally the P_5 ligand shows a disorder over two positions (82:18). To describe this disorder the SADI and SIMU restraint was applied.

Compound 6: The asymmetric unit contains the cation $[(IMe)_2P]^+$ and the anion $[Cp''Ta(CO)_2(\eta^3\text{-}P_3)]^-$.

Table S 3. Crystallographic data and details of the compounds **3**, **4**, **5** and **6**.

Compound	**3**	**4 • 2 thf**	**5 • 4.3 thf**	**6**
File Name	FR155	FR162	FR313	FR264
CCDC	2015543	2015544	2015545	2015546
Formula	$C_{17}H_{27}FeN_2P_5$	$C_{39}FeH_{55}N_2O_2P_5$	$C_{54.2}FeH_{85.4}N_2O_{4.3}P_5$	$C_{29}H_{45}N_4O_2P_4Ta$
$D_{calc.}$/ g cm^{-3}	1.478	1.305	1.211	1.542
□/mm^{-1}	9.334	5.132	3.767	8.023
Formula Weight	470.10	794.55	1044.54	786.52
Colour	dark green	dark green	green	red
Shape	block	block	plate	plate
Max size/mm	0.37	0.50	0.28	0.25
Mid size/mm	0.15	0.30	0.15	0.16
Min size/mm	0.09	0.24	0.04	0.06
T/K	122.99(16)	123.00(10)	122.96(11)	123.0(2)
Crystal System	monoclinic	monoclinic	monoclinic	monoclinic
Space Group	*I*2/*a*	$P2_1/n$	P21/c	$P2_1/c$
a/Å	13.9605(2)	14.6421(5)	13.6902(11)	13.3561(8)
b/Å	12.4727(2)	18.3526(6)	19.6372(9)	10.5354(6)
c/Å	24.9230(5)	15.9403(6)	22.1012(16)	24.9298(16)
α/°	90	90	90	90
β/°	103.223(2)	109.217(4)	105.284(8)	105.029(6)
γ/°	90	90	90	90
V/Å^3	4224.66(13)	4044.8(3)	5731.5(7)	3387.9(4)
Z	8	4	4	4
Z'	1	1	1	1
Q_{min}/°	3.644	3.558	3.347	3.426
Q_{max}/°	74.344	74.685	60.002	74.851
Measured Reflexes	18138	38670	20741	17862
Independent Reflexes	4225	8099	8371	6595
Reflections with I > 2(I)	4129	7434	5639	5529
R_{int}	0.0363	0.0810	0.1108	0.0753
Parameters	235	558	555	375
Restraints	0	166	16	0
Largest Peak	0.524	0.665	1.182	4.492
Deepest Hole	-0.661	-0.552	-0.519	-3.513
GooF	1.061	1.031	1.015	1.039
wR2 (all data)	0.0911	0.1197	0.2740	0.1996
wR2	0.0904	0.1163	0.2416	0.1869
R1 (all data)	0.0340	0.0461	0.1169	0.0811
R1	0.0334	0.0431	0.0911	0.0704

Compound 3:

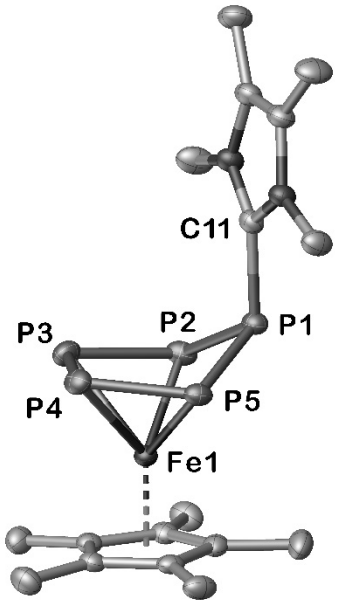

Selected Bond Lengths in Å		Selected Bond Angles in °	
P1–C11	1.860(2)	**C11–P1–P2**	114.99(7)
P1–P2	2.1572(7)	**C11–P1–P5**	111.43(6)
P2–P3	2.1552(8)	**P1–P2–P3**	107.62(3)
P3–P4	2.1302(8)	**P2–P3–P4**	104.18(3)
P4–P5	2.1491(7)	**P3–P4–P5**	104.19(3)
P5–P1	2.1621(7)	**P4–P5–P1**	107.86(3)
Fe1–P2	2.2979(6)	**P5–P1–P2**	95.03(3)
Fe1–P3	2.3415(6)		
Fe1–P4	2.3422(6)		
Fe1–P5	2.3077(5)		

Compound 4:

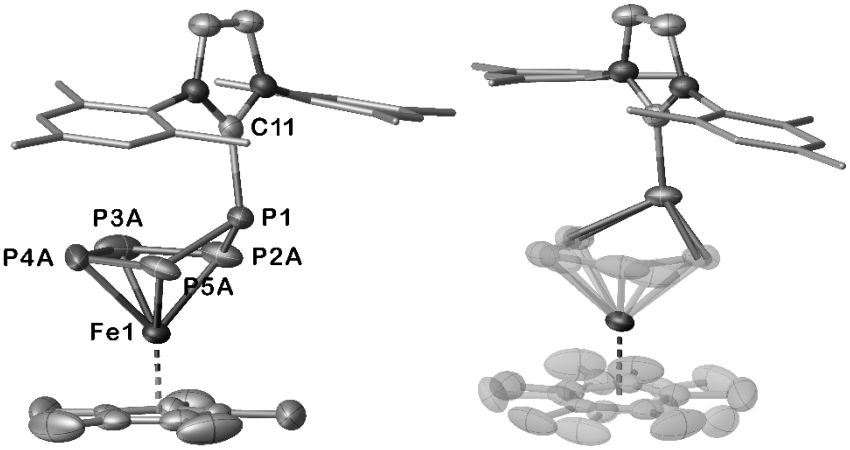

Selected Bond Lengths in Å		Selected Bond Angles in °	
P1–C11	1.849(2)	**C11–P1–P2A**	112.21(9)
P1–P2A	2.063(3)	**C11–P1–P5A**	112.21(15)
P2A–P3A	2.143(3)	**P1–P2A–P3A**	107.57(11)
P3A–P4A	2.115(3)	**P2A–P3A–P4A**	104.12(12)
P4A–P5A	2.138(5)	**P3A–P4A–P5A**	104.08(16)
P5A–P1	2.184(5)	**P4A–P5A–P1**	105.7(2)
Fe1–P2A	2.339(3)	**P5A–P1–P2A**	96.04(14)
Fe1–P3A	2.353(2)		
Fe1–P4A	2.303(2)		
Fe1–P5A	2.263(5)		

Compound 5:

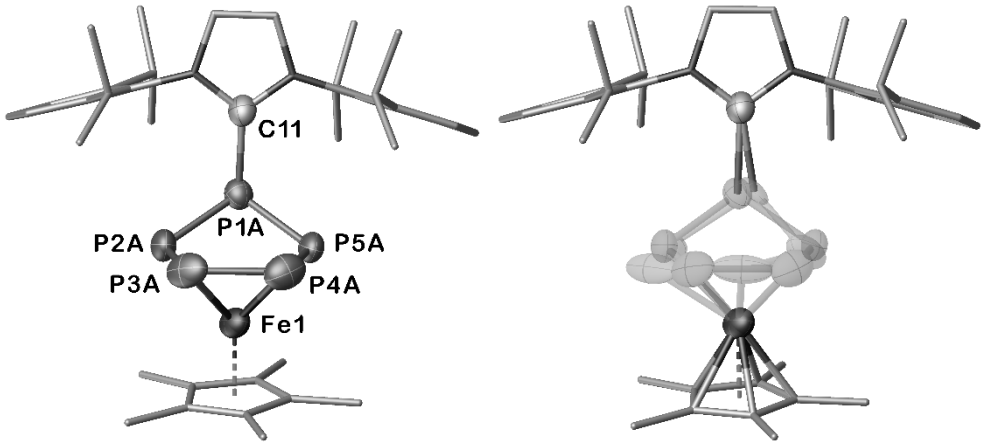

In the subsequent Table selected bond length and angles of compound **5** are listed. However, it should be kept in mind, that the data quality of the measurement was low. Therefore, the listed bond length and angles are only given to get a rough insight in the connectivity of **5**.

Selected Bond Lengths in Å		Selected Bond Angles in °	
P1A–C11	1.900(7)	**C11–P1A–P2A**	113.8(3)
P1A–P2A	2.146(4)	**C11–P1A–P5A**	110.4(3)
P2A–P3A	2.144(5)	**P1A–P2A–P3A**	109.00(19)
P3A–P4A	2.113(5)	**P2A–P3A–P4A**	105.19(14)
P4A–P5A	2.151(5)	**P3A–P4A–P5A**	104.11(18)
P5A–P1A	2.155(4)	**P4A–P5A–P1A**	109.2(2)
Fe1–P2A	2.295(3)	**P5A–P1A–P2A**	96.1(2)
Fe1–P3A	2.343(2)		
Fe1–P4A	2.387(3)		
Fe1–P5A	2.338(4)		

Compound 6:

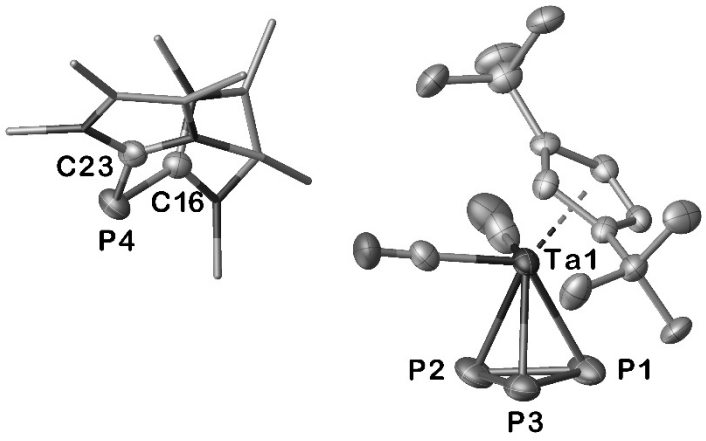

Selected Bond Lengths in Å		Selected Bond Angles in °	
P1–P2	2.184(4)	**P1–P2–P3**	60.26(12)
P1–P2	2.186(3)	**P2–P3–P1**	59.53(13)
P1–P2	2.169(4)	**P3–P1–P2**	60.21(12)
P4–C16	1.797(8)	**C16–P4–C23**	97.9(3)
P4–C23	1.796(8)	**P1–Ta1–P2**	49.49(9)
Ta1–P1	2.568(2)	**P2–Ta1–P3**	49.91(9)
Ta1–P2	2.614(2)	**P3–Ta1–P1**	50.43(8)
Ta1–P3	2.563(2)		

Details on DFT Calculations

The geometries of the compounds have been fully optimized with gradient-corrected density functional theory (DFT) in form of Becke's three-parameter hybrid method B3LYP[12] with all electron 6-31G* basis set as implemented in Gaussian 09 program package.[13] All structures correspond to minima on their respective potential energy surfaces as verified by the subsequent vibrational analysis.

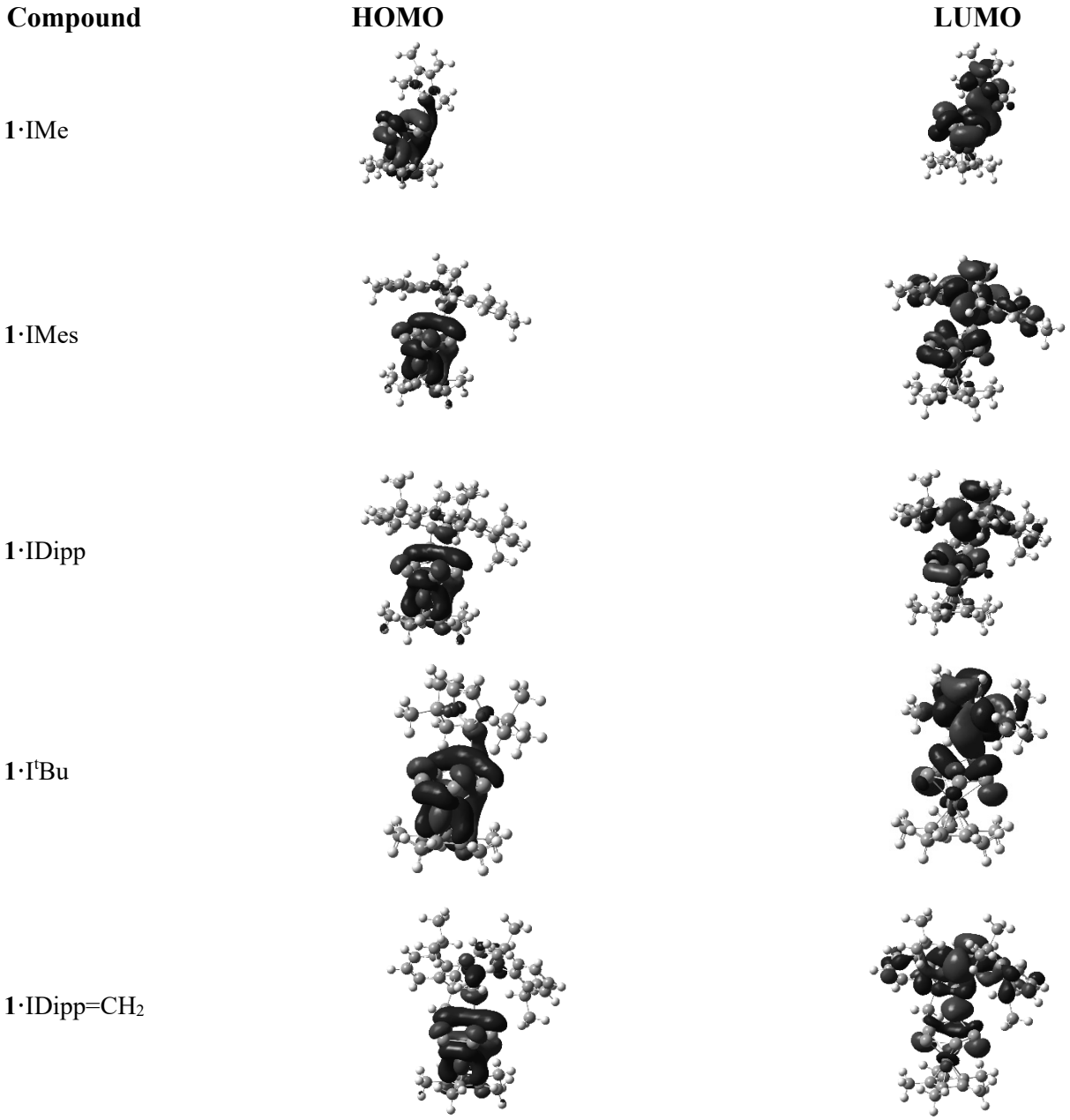

Figure S 9. HOMO and LUMO of the compounds **1·LB**.

Table S 4. Total energies E^o_0, sum of electronic and thermal enthalpies H^o_{298} (Hartree) and standard entropies S^o_{298} (cal $mol^{-1}K^{-1}$). B3LYP/6-31G* level of theory.

Compound	E^o_0	H^o_{298}	S^o_{298}
1	-3360.581389	-3360.32536	141.236
IMe	-383.4330252	-383.238585	94.543
IMes	-924.1712522	-923.748456	170.758
IDipp	-1160.035165	-1159.431988	201.557
I^{t}Bu	-540.6829029	-540.370817	117.416
IDipp=CH_2	-1199.35876	-1198.726726	206.183
1·IMe	-3744.032328	-3743.578663	198.213
1·IMes	-4284.764922	-4284.084528	259.300
1·IDipp	-4520.622797	-4519.76108	295.303
1·I^{t}Bu	-3901.248443	-3900.678339	208.290
1·IDipp=CH_2	-4559.936175	-4559.044872	304.439

Table S 5. Optimized geometries of theoretically studied compounds. xyz coordinates in angstroms. B3LYP/6-31G* level of theory.

[Cp*Fe(η^5-P_5)] (1)			
26	-0.075360000	0.000085000	0.000031000
15	-1.654218000	1.311178000	-1.258387000
15	-1.653967000	-0.792072000	-1.634911000
15	-1.654322000	-1.799677000	0.248956000
15	-1.651109000	1.603476000	0.858073000
15	-1.654404000	-0.319304000	1.789495000
6	1.623539000	0.216888000	-1.200334000
6	1.623440000	-1.074291000	-0.578033000
6	1.624473000	1.207397000	-0.164594000
6	1.623648000	-0.881921000	0.841844000
6	1.625751000	0.528285000	1.097435000
6	1.711293000	1.179464000	2.447225000
1	1.227445000	2.159900000	2.455420000
1	2.762003000	1.321882000	2.733561000
1	1.234936000	0.571703000	3.220971000
6	1.704000000	-1.965763000	1.877111000
1	1.233057000	-1.663910000	2.816378000
1	2.753255000	-2.209159000	2.091426000
1	1.210114000	-2.882183000	1.542548000
6	1.708089000	-2.394470000	-1.287313000
1	1.221526000	-3.192525000	-0.719243000
1	2.758922000	-2.679740000	-1.431862000
1	1.234302000	-2.356000000	-2.272216000
6	1.708147000	2.692550000	-0.365785000

1	1.236934000	3.000342000	-1.303473000
1	2.758664000	3.011817000	-0.397841000
1	1.217464000	3.240171000	0.444187000
6	1.703711000	0.484536000	-2.674421000
1	1.209782000	-0.299450000	-3.254408000
1	2.752954000	0.530005000	-2.995385000
1	1.231756000	1.434887000	-2.938080000

IMe

7	-1.060606000	-0.708576000	0.000002000
7	1.060607000	-0.708576000	-0.000002000
6	0.000000000	-1.576803000	-0.000001000
6	0.681925000	0.640154000	-0.000001000
6	-0.681926000	0.640154000	0.000003000
6	-2.434708000	-1.175017000	0.000002000
1	-2.402209000	-2.264931000	-0.000001000
1	-2.974117000	-0.829040000	0.889953000
1	-2.974119000	-0.829036000	-0.889948000
6	-1.662602000	1.766908000	-0.000004000
1	-2.314925000	1.745845000	-0.883278000
1	-2.314949000	1.745838000	0.883251000
1	-1.142686000	2.729490000	0.000007000
6	2.434709000	-1.175015000	-0.000001000
1	2.402211000	-2.264930000	0.000015000
1	2.974115000	-0.829049000	-0.889960000
1	2.974122000	-0.829022000	0.889941000
6	1.662601000	1.766908000	0.000003000
1	2.314937000	1.745837000	0.883267000
1	2.314936000	1.745846000	-0.883262000
1	1.142684000	2.729490000	0.000009000

IMes

7	0.000000000	1.064136000	-0.589575000
7	0.000000000	-1.064136000	-0.589575000
6	-0.000301000	2.435003000	-0.156715000
6	1.191450000	3.174723000	-0.221164000
6	0.000301000	-2.435003000	-0.156715000
6	0.000000000	0.000000000	0.280758000
6	-1.191858000	3.001056000	0.324685000
6	2.481348000	2.541941000	-0.687438000
1	2.683987000	1.615340000	-0.138983000
1	3.323541000	3.223573000	-0.535546000
1	2.451634000	2.279365000	-1.751938000
6	-1.191450000	-3.174723000	-0.221164000
6	1.191858000	-3.001056000	0.324685000
6	0.001144000	-0.677030000	-1.933047000
1	0.007062000	-1.388179000	-2.745420000
6	-0.007670000	5.114980000	0.658439000
6	1.162232000	4.511736000	0.187960000
1	2.082172000	5.091651000	0.147283000
6	-1.169403000	4.339925000	0.726829000
1	-2.086155000	4.787138000	1.105944000
6	-1.162232000	-4.511736000	0.187960000
1	-2.082172000	-5.091651000	0.147283000
6	-0.001144000	0.677030000	-1.933047000
1	-0.007062000	1.388179000	-2.745420000
6	-2.457593000	2.184890000	0.425123000

1	-2.770246000	1.805377000	-0.555613000
1	-3.276167000	2.785436000	0.833072000
1	-2.303995000	1.312685000	1.069289000
6	2.457593000	-2.184890000	0.425123000
1	2.770246000	-1.805377000	-0.555613000
1	3.276167000	-2.785436000	0.833072000
1	2.303995000	-1.312685000	1.069289000
6	0.007670000	-5.114980000	0.658439000
6	-2.481348000	-2.541941000	-0.687438000
1	-2.683987000	-1.615340000	-0.138983000
1	-3.323541000	-3.223573000	-0.535546000
1	-2.451634000	-2.279365000	-1.751938000
6	1.169403000	-4.339925000	0.726829000
1	2.086155000	-4.787138000	1.105944000
6	-0.020219000	6.569980000	1.066665000
1	0.953518000	6.885558000	1.456450000
1	-0.772735000	6.763251000	1.838527000
1	-0.254765000	7.221079000	0.213658000
6	0.020219000	-6.569980000	1.066665000
1	0.772735000	-6.763251000	1.838527000
1	0.254765000	-7.221079000	0.213658000
1	-0.953518000	-6.885558000	1.456450000

IDipp

7	-1.031417000	0.000004000	0.515457000
7	1.098225000	-0.000006000	0.543259000
6	0.693076000	-0.000011000	1.880610000
1	1.394718000	-0.000018000	2.701147000
6	-0.661378000	-0.000005000	1.862568000
1	-1.383590000	-0.000005000	2.665023000
6	3.135487000	1.234505000	-0.047440000
6	-3.057890000	1.232616000	-0.118468000
6	-2.404444000	0.000009000	0.079514000
6	0.044791000	0.000004000	-0.341149000
6	4.482446000	1.206577000	-0.428773000
1	5.014651000	2.139781000	-0.584374000
6	-2.351132000	2.571332000	0.065873000
1	-1.317309000	2.368063000	0.357248000
6	2.482239000	-0.000010000	0.139371000
6	-3.057905000	-1.232593000	-0.118450000
6	3.135471000	-1.234530000	-0.047468000
6	2.388367000	2.557805000	0.088170000
1	1.540101000	2.393154000	0.761386000
6	-2.994938000	3.405054000	1.190279000
1	-4.035765000	3.660215000	0.958268000
1	-2.989823000	2.862211000	2.142326000
1	-2.446441000	4.343895000	1.332092000
6	5.151183000	-0.000019000	-0.615074000
1	6.197408000	-0.000023000	-0.910288000
6	-4.401707000	-1.204823000	-0.511176000
1	-4.928750000	-2.141500000	-0.671492000
6	4.482430000	-1.206611000	-0.428801000
1	5.014623000	-2.139819000	-0.584423000
6	-2.351163000	-2.571314000	0.065916000
1	-1.317328000	-2.368052000	0.357251000
6	-4.401692000	1.204857000	-0.511196000
1	-4.928722000	2.141538000	-0.671528000

6	2.388334000	-2.557823000	0.088117000
1	1.540077000	-2.393176000	0.761346000
6	-2.299451000	3.362002000	-1.255508000
1	-1.803637000	2.779797000	-2.038766000
1	-3.303670000	3.622554000	-1.610725000
1	-1.742130000	4.296552000	-1.118840000
6	-5.071332000	0.000020000	-0.703312000
1	-6.114725000	0.000023000	-1.008080000
6	3.236849000	-3.684244000	0.701359000
1	4.047317000	-4.002347000	0.035256000
1	3.683900000	-3.380968000	1.654918000
1	2.609210000	-4.563850000	0.885168000
6	1.810150000	-2.976221000	-1.280177000
1	1.151704000	-2.194627000	-1.672210000
1	2.614645000	-3.147719000	-2.005985000
1	1.234097000	-3.905423000	-1.187284000
6	3.236892000	3.684199000	0.701447000
1	3.683927000	3.380895000	1.655005000
1	4.047372000	4.002305000	0.035360000
1	2.609265000	4.563811000	0.885268000
6	1.810204000	2.976243000	-1.280121000
1	2.614708000	3.147750000	-2.005915000
1	1.151754000	2.194665000	-1.672180000
1	1.234159000	3.905448000	-1.187212000
6	-2.299538000	-3.362038000	-1.255435000
1	-3.303772000	-3.622593000	-1.610608000
1	-1.803744000	-2.779872000	-2.038735000
1	-1.742224000	-4.296589000	-1.118747000
6	-2.994950000	-3.404982000	1.190374000
1	-2.989795000	-2.862103000	2.142401000
1	-4.035789000	-3.660129000	0.958404000
1	-2.446467000	-4.343829000	1.332206000

I^{t}Bu

7	0.000001000	1.069084000	-0.298844000
7	-0.000001000	-1.069084000	-0.298844000
6	0.000000000	-0.678434000	-1.636250000
1	-0.000004000	-1.364774000	-2.467255000
6	0.000000000	0.678434000	-1.636250000
1	0.000004000	1.364774000	-2.467255000
6	-0.000009000	2.466826000	0.221488000
6	0.000000000	0.000000000	0.554851000
6	0.000009000	-2.466826000	0.221488000
6	0.000001000	3.469145000	-0.940204000
1	0.890696000	3.363388000	-1.569538000
1	-0.890680000	3.363387000	-1.569557000
1	-0.000004000	4.485741000	-0.534352000
6	1.262949000	2.659148000	1.079639000
1	2.166590000	2.542879000	0.470256000
1	1.273362000	3.660519000	1.525405000
1	1.287808000	1.910909000	1.875567000
6	-1.262982000	2.659144000	1.079610000
1	-1.273424000	3.660527000	1.525349000
1	-2.166612000	2.542843000	0.470217000
1	-1.287849000	1.910929000	1.875562000
6	-0.000001000	-3.469145000	-0.940204000
1	0.890680000	-3.363387000	-1.569557000

1	0.000004000	-4.485741000	-0.534352000
1	-0.890696000	-3.363388000	-1.569538000
6	1.262982000	-2.659144000	1.079610000
1	2.166612000	-2.542843000	0.470217000
1	1.287849000	-1.910929000	1.875562000
1	1.273424000	-3.660527000	1.525349000
6	-1.262949000	-2.659148000	1.079639000
1	-1.273362000	-3.660519000	1.525405000
1	-1.287808000	-1.910909000	1.875567000
1	-2.166590000	-2.542879000	0.470256000

IDipp=CH_2

7	-1.107513000	0.000000000	-0.580374000
7	1.107513000	0.000000000	-0.580374000
6	0.672941000	0.000000000	-1.916539000
1	1.380385000	0.000000000	-2.730545000
6	-0.672941000	0.000000000	-1.916539000
1	-1.380385000	0.000000000	-2.730545000
6	3.124521000	-1.233148000	0.065021000
6	-3.124521000	-1.233148000	0.065021000
6	-2.470071000	0.000000000	-0.146571000
6	0.000000000	0.000000000	0.280484000
6	4.457603000	-1.205780000	0.492091000
1	4.982399000	-2.141962000	0.663143000
6	-2.419545000	-2.569402000	-0.142542000
1	-1.421768000	-2.359829000	-0.538423000
6	2.470071000	0.000000000	-0.146571000
6	-3.124521000	1.233148000	0.065021000
6	3.124521000	1.233148000	0.065021000
6	2.419545000	-2.569402000	-0.142542000
1	1.421768000	-2.359829000	-0.538423000
6	-3.148488000	-3.448647000	-1.176330000
1	-4.154362000	-3.724727000	-0.838664000
1	-3.249755000	-2.933278000	-2.138153000
1	-2.590908000	-4.377391000	-1.345857000
6	5.120057000	0.000000000	0.704504000
1	6.154870000	0.000000000	1.037567000
6	-4.457603000	1.205780000	0.492091000
1	-4.982399000	2.141962000	0.663143000
6	4.457603000	1.205780000	0.492091000
1	4.982399000	2.141962000	0.663143000
6	-2.419545000	2.569402000	-0.142542000
1	-1.421768000	2.359829000	-0.538423000
6	-4.457603000	-1.205780000	0.492091000
1	-4.982399000	-2.141962000	0.663143000
6	2.419545000	2.569402000	-0.142542000
1	1.421768000	2.359829000	-0.538423000
6	-2.233624000	-3.314824000	1.193533000
1	-1.657312000	-2.706958000	1.898174000
1	-3.198204000	-3.557191000	1.656054000
1	-1.694029000	-4.256189000	1.033323000
6	-5.120057000	0.000000000	0.704504000
1	-6.154870000	0.000000000	1.037567000
6	3.148488000	3.448647000	-1.176330000
1	4.154362000	3.724727000	-0.838664000
1	3.249755000	2.933278000	-2.138153000
1	2.590908000	4.377391000	-1.345857000

6	2.233624000	3.314824000	1.193533000
1	1.657312000	2.706958000	1.898174000
1	3.198204000	3.557191000	1.656054000
1	1.694029000	4.256189000	1.033323000
6	3.148488000	-3.448647000	-1.176330000
1	3.249755000	-2.933278000	-2.138153000
1	4.154362000	-3.724727000	-0.838664000
1	2.590908000	-4.377391000	-1.345857000
6	2.233624000	-3.314824000	1.193533000
1	3.198204000	-3.557191000	1.656054000
1	1.657312000	-2.706958000	1.898174000
1	1.694029000	-4.256189000	1.033323000
6	-2.233624000	3.314824000	1.193533000
1	-3.198204000	3.557191000	1.656054000
1	-1.657312000	2.706958000	1.898174000
1	-1.694029000	4.256189000	1.033323000
6	-3.148488000	3.448647000	-1.176330000
1	-3.249755000	2.933278000	-2.138153000
1	-4.154362000	3.724727000	-0.838664000
1	-2.590908000	4.377391000	-1.345857000
6	0.000000000	0.000000000	1.639328000
1	-0.932042000	0.000000000	2.187351000
1	0.932042000	0.000000000	2.187351000

1·IMe

26	-1.720096000	-0.040406000	-0.097607000
15	0.072570000	1.499731000	-0.356636000
15	1.154619000	0.337982000	1.186607000
15	-0.143610000	-1.434909000	1.011489000
15	-0.350446000	0.159529000	-2.019846000
15	-0.504500000	-1.790120000	-1.113912000
7	3.730783000	1.131305000	0.297400000
7	3.639268000	-1.032435000	0.301858000
6	-3.096164000	1.288698000	0.768904000
6	-3.180734000	0.011545000	1.404686000
6	-3.363277000	1.111434000	-0.629220000
6	-3.503041000	-0.965370000	0.403690000
6	-3.617141000	-0.283337000	-0.855275000
6	4.917147000	-0.682567000	-0.138455000
6	2.907867000	0.081050000	0.558494000
6	4.971673000	0.681204000	-0.150305000
6	-4.027676000	-0.903502000	-2.159809000
1	-3.579013000	-0.382608000	-3.010813000
1	-5.119441000	-0.867680000	-2.280799000
1	-3.718089000	-1.950825000	-2.221333000
6	3.353516000	2.536110000	0.452633000
1	2.736772000	2.864011000	-0.387788000
1	4.259510000	3.139119000	0.515576000
1	2.776976000	2.651303000	1.373110000
6	-3.772197000	-2.421425000	0.653740000
1	-3.569680000	-3.025563000	-0.235345000
1	-4.821978000	-2.582423000	0.937278000
1	-3.147898000	-2.813117000	1.463213000
6	-3.050650000	-0.247139000	2.878604000
1	-2.671924000	-1.252944000	3.078970000
1	-4.026647000	-0.149453000	3.375482000
1	-2.364852000	0.460281000	3.354537000

6	-3.455991000	2.210248000	-1.648628000
1	-2.726268000	3.002889000	-1.453688000
1	-4.454820000	2.669223000	-1.639332000
1	-3.268570000	1.837217000	-2.659425000
6	3.219525000	-2.419029000	0.502058000
1	3.432025000	-2.997495000	-0.399774000
1	2.148374000	-2.446012000	0.696731000
1	3.758005000	-2.851898000	1.350939000
6	6.076422000	1.604306000	-0.546458000
1	5.771791000	2.279755000	-1.354628000
1	6.934291000	1.029577000	-0.903264000
1	6.420302000	2.221321000	0.292969000
6	-2.868620000	2.602635000	1.460615000
1	-2.224845000	2.493385000	2.338623000
1	-3.823836000	3.029013000	1.799331000
1	-2.394410000	3.330430000	0.796761000
6	5.942381000	-1.704112000	-0.503968000
1	6.168006000	-2.374144000	0.334505000
1	6.874625000	-1.215464000	-0.796591000
1	5.615993000	-2.327107000	-1.345642000

1·IMes

26	-2.482779000	0.000075000	-0.080739000
15	0.493850000	-0.000013000	0.757701000
15	-0.752160000	-1.641975000	0.015138000
15	-0.752063000	1.642020000	0.015133000
15	-1.516084000	-1.077167000	-1.947634000
15	-1.516019000	1.077251000	-1.947638000
7	3.034632000	-1.086698000	-0.183073000
7	3.034699000	1.086515000	-0.183073000
6	2.686262000	-2.485955000	-0.046368000
6	2.387545000	-3.220006000	-1.205084000
6	2.686416000	2.485793000	-0.046368000
6	2.239562000	-0.000067000	0.033190000
6	2.739309000	-3.072110000	1.227648000
6	2.315857000	-2.572156000	-2.566115000
1	1.446293000	-1.906753000	-2.631100000
1	2.210882000	-3.331104000	-3.346214000
1	3.206420000	-1.975321000	-2.793575000
6	2.739498000	3.071944000	1.227649000
6	2.387749000	3.219865000	-1.205083000
6	4.315400000	0.676629000	-0.536969000
1	5.091979000	1.393949000	-0.750276000
6	2.138384000	-5.206669000	0.199112000
6	2.121563000	-4.582945000	-1.052003000
1	1.881303000	-5.168201000	-1.936438000
6	2.455804000	-4.437043000	1.322079000
1	2.485397000	-4.908895000	2.301484000
6	2.456080000	4.436894000	1.322081000
1	2.485702000	4.908744000	2.301487000
6	4.315358000	-0.676891000	-0.536968000
1	5.091894000	-1.394259000	-0.750275000
6	-4.498786000	0.000158000	-0.497824000
6	3.083174000	-2.270386000	2.460061000
1	4.028915000	-1.727107000	2.344404000
1	3.177260000	-2.926388000	3.329917000
1	2.305577000	-1.528945000	2.679777000

6	2.316024000	2.572022000	-2.566116000
1	3.206547000	1.975124000	-2.793572000
1	2.211107000	3.330978000	-3.346215000
1	1.446414000	1.906679000	-2.631106000
6	2.138713000	5.206542000	0.199113000
6	-3.620714000	0.714506000	1.526867000
6	-4.163159000	1.161720000	0.276437000
6	3.083311000	2.270197000	2.460061000
1	2.305675000	1.528793000	2.679767000
1	3.177422000	2.926190000	3.329921000
1	4.029027000	1.726872000	2.344411000
6	2.121856000	4.582821000	-1.052002000
1	1.881637000	5.168093000	-1.936437000
6	-4.163251000	-1.161455000	0.276399000
6	1.797434000	-6.671390000	0.335960000
1	2.103376000	-7.239595000	-0.548769000
1	0.714646000	-6.808998000	0.452980000
1	2.280004000	-7.116797000	1.212121000
6	-3.620772000	-0.714326000	1.526844000
6	1.797857000	6.671286000	0.335963000
1	0.715080000	6.808961000	0.452999000
1	2.103822000	7.239469000	-0.548772000
1	2.280468000	7.116664000	1.212116000
6	-4.427050000	2.591003000	-0.101206000
1	-3.653996000	3.260204000	0.290042000
1	-5.392749000	2.929355000	0.300809000
1	-4.453409000	2.722831000	-1.186595000
6	-3.224411000	1.587910000	2.682822000
1	-2.398635000	1.152102000	3.253573000
1	-4.071159000	1.722412000	3.371534000
1	-2.904667000	2.578762000	2.349783000
6	-5.176194000	0.000208000	-1.838115000
1	-4.902595000	0.880735000	-2.426845000
1	-6.269236000	0.000287000	-1.722281000
1	-4.902723000	-0.880357000	-2.426845000
6	-3.224538000	-1.587800000	2.682769000
1	-2.904839000	-2.578655000	2.349696000
1	-4.071306000	-1.722285000	3.371459000
1	-2.398749000	-1.152058000	3.253554000
6	-4.427253000	-2.590705000	-0.101293000
1	-4.453563000	-2.722505000	-1.186687000
1	-5.393005000	-2.928977000	0.300659000
1	-3.654283000	-3.259985000	0.289982000

1·IDipp

26	-2.922441000	0.000009000	0.167590000
15	0.017436000	0.000229000	-0.638304000
15	-1.191578000	1.649187000	0.122535000
15	-1.191432000	-1.648982000	0.122212000
15	-2.004773000	-1.074580000	2.061233000
15	-2.004936000	1.074372000	2.061409000
7	2.669711000	-1.086519000	-0.060462000
7	2.669852000	1.086560000	-0.060295000
6	3.996356000	0.676512000	0.006058000
1	4.801340000	1.392123000	0.049364000
6	3.996276000	-0.676623000	0.005927000
1	4.801158000	-1.392345000	0.049247000

6	2.234832000	3.166389000	1.166187000
6	2.235184000	-3.166431000	1.166023000
6	2.303978000	-2.491545000	-0.069146000
6	1.844685000	0.000078000	-0.107734000
6	1.968183000	4.539477000	1.127771000
1	1.902274000	5.094058000	2.058391000
6	2.475145000	-2.472244000	2.504381000
1	2.431058000	-1.390189000	2.339560000
6	2.304092000	2.491570000	-0.069014000
6	2.123796000	-3.134394000	-1.308854000
6	2.124232000	3.134452000	-1.308735000
6	2.474572000	2.472084000	2.504527000
1	2.430213000	1.390046000	2.339641000
6	-4.015961000	0.714331000	-1.470069000
6	3.880285000	-2.805636000	3.048926000
1	3.981490000	-3.880859000	3.238019000
1	4.672002000	-2.516481000	2.348224000
1	4.058512000	-2.280142000	3.994366000
6	1.779118000	5.203800000	-0.080264000
1	1.568732000	6.269862000	-0.084302000
6	1.857630000	-4.508181000	-1.282521000
1	1.709579000	-5.038574000	-2.218105000
6	-4.593134000	1.161451000	-0.234973000
6	1.857895000	4.508224000	-1.282415000
1	1.710096000	5.038643000	-2.218024000
6	2.247495000	-2.408557000	-2.645524000
1	2.281089000	-1.332524000	-2.449512000
6	1.968718000	-4.539573000	1.127620000
1	1.903201000	-5.094194000	2.058246000
6	2.248308000	2.408724000	-2.645443000
1	2.282717000	1.332708000	-2.449456000
6	1.396438000	-2.808521000	3.549937000
1	0.393679000	-2.589872000	3.172796000
1	1.430784000	-3.862988000	3.847268000
1	1.558498000	-2.210092000	4.453706000
6	-4.015854000	-0.714189000	-1.470215000
6	1.779335000	-5.203848000	-0.080373000
1	1.569085000	-6.269937000	-0.084422000
6	-4.866206000	2.590937000	0.135583000
1	-4.925614000	2.722017000	1.219763000
1	-4.080158000	3.259191000	-0.230670000
1	-5.818428000	2.931258000	-0.295721000
6	-3.583222000	1.585801000	-2.614117000
1	-3.283268000	2.580335000	-2.273716000
1	-2.733513000	1.152029000	-3.150613000
1	-4.403719000	1.711427000	-3.335459000
6	3.562305000	2.792969000	-3.356105000
1	3.586194000	3.863364000	-3.591952000
1	4.437334000	2.569730000	-2.734637000
1	3.664394000	2.239528000	-4.296910000
6	-4.951610000	-0.000189000	0.528412000
6	1.033159000	2.651916000	-3.559470000
1	0.102530000	2.364324000	-3.061014000
1	0.951807000	3.702864000	-3.859829000
1	1.130611000	2.055649000	-4.474116000
6	3.879830000	2.805089000	3.049050000

1	4.671443000	2.515691000	2.348334000
1	3.981321000	3.880288000	3.238117000
1	4.057927000	2.279553000	3.994493000
6	1.396023000	2.808595000	3.550142000
1	1.430776000	3.862995000	3.847671000
1	0.393167000	2.590377000	3.173004000
1	1.557885000	2.209959000	4.453809000
6	-4.592973000	-1.161623000	-0.235207000
6	1.032666000	-2.652573000	-3.559748000
1	0.952205000	-3.703530000	-3.860339000
1	0.101726000	-2.365819000	-3.061385000
1	1.129766000	-2.056059000	-4.474269000
6	-5.665721000	-0.000415000	1.849486000
1	-5.408372000	-0.880839000	2.445590000
1	-5.409153000	0.880329000	2.445450000
1	-6.755081000	-0.000924000	1.703254000
6	-3.582979000	-1.585287000	-2.614500000
1	-2.732392000	-1.151988000	-3.149984000
1	-3.284274000	-2.580336000	-2.274518000
1	-4.402991000	-1.709640000	-3.336609000
6	3.561845000	-2.791897000	-3.356036000
1	4.436665000	-2.568003000	-2.734514000
1	3.586483000	-3.862298000	-3.591789000
1	3.663624000	-2.238452000	-4.296872000
6	-4.865738000	-2.591167000	0.135339000
1	-4.080166000	-3.259405000	-0.231950000
1	-4.923896000	-2.722455000	1.219560000
1	-5.818487000	-2.931340000	-0.294925000

1·I^{t}Bu

26	2.046498000	-0.018935000	-0.112880000
15	-0.961251000	0.070096000	0.988145000
15	0.289853000	1.523982000	-0.134012000
15	0.397634000	-1.595284000	0.412677000
15	0.883995000	0.696237000	-2.052296000
15	0.970490000	-1.424915000	-1.678503000
7	-3.451073000	1.104281000	-0.207119000
7	-3.453249000	-1.093194000	-0.200810000
6	-2.747896000	0.005271000	0.233750000
6	-4.488467000	-0.670185000	-1.018693000
1	-5.152276000	-1.352901000	-1.517791000
6	-4.484631000	0.677596000	-1.025215000
1	-5.142757000	1.359271000	-1.533962000
6	4.022551000	-0.061092000	-0.694815000
6	3.336167000	-0.411243000	1.493914000
6	3.787094000	-1.068360000	0.301385000
6	3.716177000	1.215734000	-0.114654000
6	3.292564000	0.994991000	1.237557000
6	4.056811000	-2.539177000	0.160426000
1	3.341541000	-3.136393000	0.735081000
1	5.064170000	-2.788568000	0.522798000
1	3.986733000	-2.862413000	-0.882116000
6	3.053114000	-1.077436000	2.810032000
1	2.313804000	-0.521252000	3.394216000
1	3.969882000	-1.147588000	3.412948000
1	2.664377000	-2.090329000	2.672905000
6	4.587018000	-0.293582000	-2.066946000

1	4.291447000	-1.269692000	-2.462638000
1	5.685307000	-0.257391000	-2.047084000
1	4.240613000	0.462426000	-2.777762000
6	2.955292000	2.063354000	2.238381000
1	2.500050000	2.934492000	1.758742000
1	3.860523000	2.401860000	2.762548000
1	2.250915000	1.700947000	2.993282000
6	3.901864000	2.555807000	-0.767150000
1	3.809593000	2.490137000	-1.855035000
1	4.895660000	2.966452000	-0.538741000
1	3.157727000	3.279895000	-0.420125000
6	-3.366192000	-2.556154000	0.216955000
6	-3.391875000	2.576926000	0.192124000
6	-4.805190000	-3.118311000	0.281517000
1	-5.268359000	-3.227898000	-0.703271000
1	-4.756563000	-4.119931000	0.718073000
1	-5.454270000	-2.504375000	0.914777000
6	-2.563980000	-3.337505000	-0.832886000
1	-2.535416000	-4.396517000	-0.554336000
1	-3.037941000	-3.257886000	-1.817751000
1	-1.538557000	-2.974743000	-0.908009000
6	-2.776826000	-2.676242000	1.629279000
1	-3.333145000	-2.057149000	2.341101000
1	-2.862733000	-3.719868000	1.947489000
1	-1.720081000	-2.416810000	1.672643000
6	-4.845429000	3.041500000	0.448318000
1	-5.456059000	3.074877000	-0.457865000
1	-5.344470000	2.404835000	1.186425000
1	-4.814006000	4.060334000	0.844710000
6	-2.623171000	2.787561000	1.503521000
1	-2.989031000	2.125826000	2.294692000
1	-1.549203000	2.651596000	1.391246000
1	-2.787938000	3.821340000	1.823862000
6	-2.779396000	3.382149000	-0.963539000
1	-2.797574000	4.447899000	-0.710689000
1	-1.742707000	3.088384000	-1.142343000
1	-3.352360000	3.244472000	-1.887371000

1·IDipp=CH_2

26	-3.483218000	-0.000098000	-0.449051000
15	-0.533729000	0.000059000	0.311609000
15	-1.740801000	-1.648107000	-0.437857000
15	-1.740848000	1.648078000	-0.438241000
15	-2.585421000	1.074736000	-2.361418000
15	-2.585267000	-1.075301000	-2.361269000
7	3.040603000	-1.092345000	0.622478000
7	3.040522000	1.092398000	0.622572000
6	4.107513000	0.676617000	1.413716000
1	4.759273000	1.389382000	1.891220000
6	4.107531000	-0.676551000	1.413704000
1	4.759353000	-1.389309000	1.891129000
6	2.000907000	3.223303000	1.277141000
6	2.001332000	-3.223338000	1.277233000
6	2.742984000	-2.481828000	0.333612000
6	2.394485000	0.000024000	0.122446000
6	1.770667000	4.572887000	0.986126000
1	1.198987000	5.175664000	1.683717000

6	1.499874000	-2.625266000	2.589422000
1	1.484275000	-1.535747000	2.480299000
6	2.742825000	2.481860000	0.333667000
6	3.252841000	-3.043516000	-0.855062000
6	3.252874000	3.043604000	-0.854892000
6	1.499298000	2.625209000	2.589263000
1	1.483665000	1.535699000	2.480108000
6	-4.568566000	-0.714492000	1.191496000
6	2.457447000	-2.976504000	3.748439000
1	2.502122000	-4.061268000	3.902033000
1	3.479149000	-2.626075000	3.563373000
1	2.108824000	-2.518636000	4.681276000
6	2.249104000	5.152965000	-0.184618000
1	2.047917000	6.200582000	-0.390573000
6	2.982313000	-4.396122000	-1.092643000
1	3.353771000	-4.861487000	-2.000719000
6	-5.149994000	-1.161653000	-0.041112000
6	2.982218000	4.396177000	-1.092544000
1	3.353826000	4.861579000	-2.000541000
6	4.101663000	-2.259805000	-1.852586000
1	4.121348000	-1.210906000	-1.540261000
6	1.771217000	-4.572963000	0.986286000
1	1.199756000	-5.175798000	1.684003000
6	4.102053000	2.260034000	-1.852225000
1	4.122196000	1.211211000	-1.539664000
6	0.063180000	-3.055538000	2.934626000
1	-0.623785000	-2.850646000	2.108894000
1	0.003041000	-4.122231000	3.180525000
1	-0.283532000	-2.499937000	3.813042000
6	-4.568339000	0.714461000	1.191511000
6	2.249497000	-5.152997000	-0.184540000
1	2.048419000	-6.200647000	-0.390434000
6	-5.421713000	-2.590921000	-0.412896000
1	-5.483656000	-2.719878000	-1.497157000
1	-4.632448000	-3.257659000	-0.050978000
1	-6.372038000	-2.934097000	0.020678000
6	-4.130240000	-1.586881000	2.332560000
1	-3.826648000	-2.578820000	1.987707000
1	-3.280505000	-1.151573000	2.867503000
1	-4.948653000	-1.718519000	3.055512000
6	5.560864000	2.760935000	-1.843945000
1	5.623352000	3.808767000	-2.158991000
1	6.004543000	2.687106000	-0.844610000
1	6.172910000	2.166930000	-2.532631000
6	-5.509785000	0.000167000	-0.804023000
6	3.513657000	2.297595000	-3.275433000
1	2.481548000	1.932995000	-3.294272000
1	3.516302000	3.312549000	-3.688010000
1	4.109858000	1.668133000	-3.946102000
6	2.456774000	2.976400000	3.748380000
1	3.478495000	2.625967000	3.563400000
1	2.501452000	4.061159000	3.902010000
1	2.108061000	2.518510000	4.681173000
6	0.062605000	3.055551000	2.934372000
1	0.002570000	4.122195000	3.180532000
1	-0.624291000	2.850956000	2.108507000

1	-0.284292000	2.499774000	3.812599000
6	-5.149685000	1.161838000	-0.041079000
6	3.513274000	-2.297911000	-3.275782000
1	3.516739000	-3.312880000	-3.688327000
1	2.480876000	-1.934131000	-3.294630000
1	4.108974000	-1.668007000	-3.946478000
6	-6.227784000	0.000120000	-2.122933000
1	-5.972968000	0.881176000	-2.719105000
1	-5.970676000	-0.879443000	-2.720330000
1	-7.316837000	-0.001407000	-1.973492000
6	-4.129632000	1.586746000	2.332499000
1	-3.281196000	1.150203000	2.868505000
1	-3.823878000	2.577927000	1.987343000
1	-4.948514000	1.720295000	3.054574000
6	5.560679000	-2.760098000	-1.844219000
1	6.004395000	-2.685754000	-0.844936000
1	5.623559000	-3.808014000	-2.158912000
1	6.172453000	-2.166081000	-2.533139000
6	-5.420975000	2.591233000	-0.412695000
1	-4.631537000	3.257682000	-0.050641000
1	-5.482818000	2.720374000	-1.496940000
1	-6.371217000	2.934613000	0.020890000
6	1.219804000	-0.000031000	-0.727557000
1	1.178835000	-0.895063000	-1.347598000
1	1.178826000	0.894895000	-1.347764000

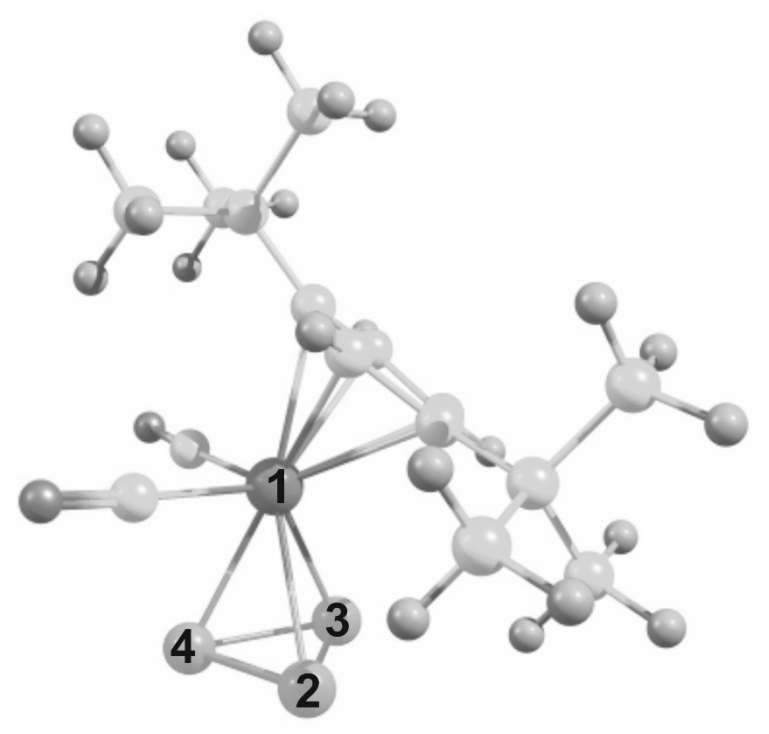

Figure S 10. Molecule model of $[Cp''Ta(CO)_2(\eta^3\text{-}P_3)]^-$ used for WBI calculations.

Table S 6. Wiberg bond indexes (WBI) for selected bonds in [Cp''Ta$(CO)_2(\eta^3$-$P_3)]^-$. B3LYP/def2-SVPD level of theory.

Bond	Bond distance, Å	WBI
Ta-P2	2.6433	0.8549
Ta-P3	2.6324	0.8705
Ta-P4	2.6802	0.7648
P2-P3	2.2129	1.0064
P2-P4	2.1954	1.0029
P3-P4	2.1951	1.0137

Usually for the single bonds (bond order one) WBI value is slightly less than 1.0. WBI slightly larger than 1.0 may indicate small additional stabilization compared to the single bond.

Wiberg bond index matrix in the NAO basis:

Atom	1	2	3	4	5	6	7	8	9
1. Ta	0.0000	0.8549	0.8705	0.7648	0.1125	0.1211	0.2602	0.3323	0.0113
2. P	0.8549	0.0000	1.0064	1.0029	0.0123	0.0303	0.0378	0.0044	0.0004
3. P	0.8705	1.0064	0.0000	1.0137	0.0326	0.0085	0.0051	0.0113	0.0009
4. P	0.7648	1.0029	1.0137	0.0000	0.0299	0.0383	0.0113	0.0110	0.0003
5. O	0.1125	0.0123	0.0326	0.0299	0.0000	0.0175	0.0015	0.0078	0.0001
6. O	0.1211	0.0303	0.0085	0.0383	0.0175	0.0000	0.0033	0.0029	0.0003
7. C	0.2602	0.0378	0.0051	0.0113	0.0015	0.0033	0.0000	1.2641	0.0051
8. C	0.3323	0.0044	0.0113	0.0110	0.0078	0.0029	1.2641	0.0000	0.8891
9. H	0.0113	0.0004	0.0009	0.0003	0.0001	0.0003	0.0051	0.8891	0.0000
10. C	0.3296	0.0103	0.0101	0.0093	0.0088	0.0102	0.0399	1.2286	0.0049
11. C	1.2928	0.0570	0.0265	0.0928	0.0340	1.9502	0.0106	0.0056	0.0006
12. C	0.2914	0.0032	0.0390	0.0108	0.0040	0.0010	1.2763	0.0369	0.0101
13. H	0.0118	0.0002	0.0009	0.0006	0.0003	0.0001	0.0050	0.0101	0.0003
14. C	0.0120	0.0013	0.0005	0.0009	0.0001	0.0002	0.9825	0.0135	0.0008
15. C	0.3425	0.0143	0.0059	0.0093	0.0047	0.0097	0.0395	0.0354	0.0100
16. H	0.0129	0.0009	0.0010	0.0005	0.0005	0.0002	0.0084	0.0098	0.0003
17. C	0.0137	0.0011	0.0006	0.0007	0.0004	0.0004	0.0072	0.0137	0.0008
18. C	0.0028	0.0034	0.0013	0.0018	0.0001	0.0002	0.0115	0.0032	0.0006
19. H	0.0002	0.0002	0.0001	0.0001	0.0000	0.0000	0.0009	0.0006	0.0008
20. H	0.0023	0.0064	0.0010	0.0009	0.0001	0.0002	0.0008	0.0002	0.0000
21. H	0.0007	0.0003	0.0001	0.0001	0.0000	0.0000	0.0117	0.0005	0.0001
22. C	1.2629	0.0320	0.0595	0.0663	1.9784	0.0348	0.0056	0.0190	0.0003
23. C	0.0016	0.0028	0.0012	0.0042	0.0001	0.0001	0.0111	0.0090	0.0003
24. H	0.0027	0.0082	0.0011	0.0016	0.0002	0.0003	0.0009	0.0003	0.0000
25. H	0.0001	0.0002	0.0001	0.0002	0.0000	0.0000	0.0007	0.0003	0.0000
26. H	0.0005	0.0001	0.0001	0.0002	0.0000	0.0000	0.0115	0.0002	0.0000
27. C	0.0066	0.0028	0.0002	0.0011	0.0001	0.0001	0.0159	0.0074	0.0002
28. H	0.0002	0.0001	0.0001	0.0001	0.0000	0.0000	0.0012	0.0003	0.0000
29. H	0.0001	0.0001	0.0000	0.0001	0.0000	0.0000	0.0011	0.0005	0.0001
30. H	0.0005	0.0004	0.0001	0.0002	0.0000	0.0000	0.0117	0.0012	0.0000
31. C	0.0094	0.0003	0.0003	0.0003	0.0007	0.0007	0.0013	0.0068	0.0002
32. H	0.0002	0.0000	0.0000	0.0000	0.0000	0.0000	0.0001	0.0006	0.0001
33. H	0.0003	0.0000	0.0000	0.0001	0.0000	0.0000	0.0001	0.0003	0.0000
34. H	0.0008	0.0000	0.0000	0.0001	0.0001	0.0001	0.0004	0.0012	0.0000
35. C	0.0015	0.0004	0.0001	0.0002	0.0001	0.0022	0.0006	0.0086	0.0003
36. H	0.0001	0.0000	0.0000	0.0000	0.0000	0.0000	0.0000	0.0003	0.0000
37. H	0.0021	0.0015	0.0001	0.0005	0.0000	0.0025	0.0001	0.0003	0.0000
38. H	0.0004	0.0001	0.0000	0.0000	0.0000	0.0001	0.0004	0.0002	0.0000
39. C	0.0033	0.0002	0.0012	0.0003	0.0007	0.0003	0.0011	0.0028	0.0005
40. H	0.0034	0.0003	0.0010	0.0006	0.0005	0.0002	0.0001	0.0003	0.0000

41.	H	0.0003	0.0000	0.0003	0.0000	0.0001	0.0000	0.0002	0.0005	0.0007
42.	H	0.0008	0.0000	0.0001	0.0000	0.0001	0.0000	0.0002	0.0004	0.0000

Atom		10	11	12	13	14	15	16	17	18
1.	Ta	0.3296	1.2928	0.2914	0.0118	0.0120	0.3425	0.0129	0.0137	0.0028
2.	P	0.0103	0.0570	0.0032	0.0002	0.0013	0.0143	0.0009	0.0011	0.0034
3.	P	0.0101	0.0265	0.0390	0.0009	0.0005	0.0059	0.0010	0.0006	0.0013
4.	P	0.0093	0.0928	0.0108	0.0006	0.0009	0.0093	0.0005	0.0007	0.0018
5.	O	0.0088	0.0340	0.0040	0.0003	0.0001	0.0047	0.0005	0.0004	0.0001
6.	O	0.0102	1.9502	0.0010	0.0001	0.0002	0.0097	0.0002	0.0004	0.0002
7.	C	0.0399	0.0106	1.2763	0.0050	0.9825	0.0395	0.0084	0.0072	0.0115
8.	C	1.2286	0.0056	0.0369	0.0101	0.0135	0.0354	0.0098	0.0137	0.0032
9.	H	0.0049	0.0006	0.0101	0.0003	0.0008	0.0100	0.0003	0.0008	0.0006
10.	C	0.0000	0.0206	0.0387	0.0084	0.0075	1.2295	0.0050	0.9805	0.0010
11.	C	0.0206	0.0000	0.0048	0.0003	0.0008	0.0215	0.0005	0.0011	0.0005
12.	C	0.0387	0.0048	0.0000	0.8896	0.0132	1.2645	0.0035	0.0074	0.0094
13.	H	0.0084	0.0003	0.8896	0.0000	0.0008	0.0034	0.0008	0.0002	0.0003
14.	C	0.0075	0.0008	0.0132	0.0008	0.0000	0.0077	0.0002	0.0002	0.9950
15.	C	1.2295	0.0215	1.2645	0.0034	0.0077	0.0000	0.8893	0.0128	0.0007
16.	H	0.0050	0.0005	0.0035	0.0008	0.0002	0.8893	0.0000	0.0008	0.0003
17.	C	0.9805	0.0011	0.0074	0.0002	0.0002	0.0128	0.0008	0.0000	0.0000
18.	C	0.0010	0.0005	0.0094	0.0003	0.9950	0.0007	0.0003	0.0000	0.0000
19.	H	0.0002	0.0001	0.0003	0.0000	0.0031	0.0000	0.0000	0.0000	0.9325
20.	H	0.0001	0.0008	0.0002	0.0000	0.0041	0.0001	0.0000	0.0000	0.9122
21.	H	0.0002	0.0001	0.0003	0.0000	0.0028	0.0005	0.0001	0.0000	0.9340
22.	C	0.0178	0.0563	0.0104	0.0007	0.0003	0.0081	0.0011	0.0010	0.0004
23.	C	0.0005	0.0003	0.0030	0.0007	0.9965	0.0009	0.0000	0.0002	0.0099
24.	H	0.0001	0.0006	0.0002	0.0001	0.0041	0.0001	0.0000	0.0000	0.0006
25.	H	0.0000	0.0000	0.0007	0.0006	0.0031	0.0002	0.0000	0.0000	0.0123
26.	H	0.0004	0.0000	0.0005	0.0001	0.0028	0.0002	0.0000	0.0001	0.0010
27.	C	0.0013	0.0003	0.0077	0.0001	0.9843	0.0015	0.0001	0.0001	0.0097
28.	H	0.0001	0.0000	0.0004	0.0001	0.0032	0.0001	0.0000	0.0000	0.0121
29.	H	0.0001	0.0000	0.0003	0.0000	0.0032	0.0001	0.0000	0.0000	0.0007
30.	H	0.0005	0.0000	0.0010	0.0000	0.0030	0.0006	0.0000	0.0000	0.0007
31.	C	0.0153	0.0010	0.0015	0.0001	0.0001	0.0066	0.0002	0.9840	0.0000
32.	H	0.0010	0.0001	0.0001	0.0000	0.0000	0.0002	0.0000	0.0032	0.0000
33.	H	0.0012	0.0001	0.0001	0.0000	0.0000	0.0004	0.0001	0.0032	0.0000
34.	H	0.0117	0.0002	0.0006	0.0000	0.0000	0.0007	0.0000	0.0029	0.0000
35.	C	0.0112	0.0011	0.0008	0.0000	0.0003	0.0027	0.0007	0.9974	0.0000
36.	H	0.0007	0.0001	0.0002	0.0000	0.0000	0.0007	0.0005	0.0032	0.0000
37.	H	0.0008	0.0020	0.0001	0.0000	0.0000	0.0003	0.0001	0.0041	0.0000
38.	H	0.0115	0.0001	0.0002	0.0000	0.0001	0.0005	0.0001	0.0029	0.0000
39.	C	0.0118	0.0008	0.0006	0.0003	0.0000	0.0094	0.0002	0.9947	0.0000
40.	H	0.0007	0.0003	0.0001	0.0000	0.0000	0.0004	0.0000	0.0041	0.0000
41.	H	0.0010	0.0000	0.0000	0.0000	0.0000	0.0003	0.0000	0.0032	0.0000
42.	H	0.0119	0.0001	0.0005	0.0001	0.0000	0.0003	0.0000	0.0027	0.0000

Atom		19	20	21	22	23	24	25	26	27
1.	Ta	0.0002	0.0023	0.0007	1.2629	0.0016	0.0027	0.0001	0.0005	0.0066
2.	P	0.0002	0.0064	0.0003	0.0320	0.0028	0.0082	0.0002	0.0001	0.0028
3.	P	0.0001	0.0010	0.0001	0.0595	0.0012	0.0011	0.0001	0.0001	0.0002
4.	P	0.0001	0.0009	0.0001	0.0663	0.0042	0.0016	0.0002	0.0002	0.0011
5.	O	0.0000	0.0001	0.0000	1.9784	0.0001	0.0002	0.0000	0.0000	0.0001
6.	O	0.0000	0.0002	0.0000	0.0348	0.0001	0.0003	0.0000	0.0000	0.0001
7.	C	0.0009	0.0008	0.0117	0.0056	0.0111	0.0009	0.0007	0.0115	0.0159
8.	C	0.0006	0.0002	0.0005	0.0190	0.0090	0.0003	0.0003	0.0002	0.0074
9.	H	0.0008	0.0000	0.0001	0.0003	0.0003	0.0000	0.0000	0.0000	0.0002
10.	C	0.0002	0.0001	0.0002	0.0178	0.0005	0.0001	0.0000	0.0004	0.0013
11.	C	0.0001	0.0008	0.0001	0.0563	0.0003	0.0006	0.0000	0.0000	0.0003
12.	C	0.0003	0.0002	0.0003	0.0104	0.0030	0.0002	0.0007	0.0005	0.0077
13.	H	0.0000	0.0000	0.0000	0.0007	0.0007	0.0001	0.0006	0.0001	0.0001
14.	C	0.0031	0.0041	0.0028	0.0003	0.9965	0.0041	0.0031	0.0028	0.9843
15.	C	0.0000	0.0001	0.0005	0.0081	0.0009	0.0001	0.0002	0.0002	0.0015
16.	H	0.0000	0.0000	0.0001	0.0011	0.0000	0.0000	0.0000	0.0000	0.0001
17.	C	0.0000	0.0000	0.0000	0.0010	0.0002	0.0000	0.0000	0.0001	0.0001
18.	C	0.9325	0.9122	0.9340	0.0004	0.0099	0.0006	0.0123	0.0010	0.0097
19.	H	0.0000	0.0012	0.0006	0.0000	0.0122	0.0002	0.0011	0.0003	0.0008
20.	H	0.0012	0.0000	0.0010	0.0003	0.0008	0.0002	0.0002	0.0000	0.0110
21.	H	0.0006	0.0010	0.0000	0.0000	0.0009	0.0000	0.0002	0.0005	0.0009
22.	C	0.0000	0.0003	0.0000	0.0000	0.0002	0.0002	0.0000	0.0000	0.0002
23.	C	0.0122	0.0008	0.0009	0.0002	0.0000	0.9116	0.9323	0.9337	0.0097
24.	H	0.0002	0.0002	0.0000	0.0002	0.9116	0.0000	0.0011	0.0010	0.0107
25.	H	0.0011	0.0002	0.0002	0.0000	0.9323	0.0011	0.0000	0.0006	0.0010
26.	H	0.0003	0.0000	0.0005	0.0000	0.9337	0.0010	0.0006	0.0000	0.0008
27.	C	0.0008	0.0110	0.0009	0.0002	0.0097	0.0107	0.0010	0.0008	0.0000

28.	H	0.0002	0.0010	0.0002	0.0000	0.0006	0.0002	0.0004	0.0000	0.9305
29.	H	0.0003	0.0002	0.0000	0.0000	0.0120	0.0010	0.0002	0.0002	0.9311
30.	H	0.0000	0.0002	0.0004	0.0000	0.0008	0.0002	0.0000	0.0004	0.9325
31.	C	0.0000	0.0000	0.0000	0.0010	0.0000	0.0000	0.0000	0.0000	0.0001
32.	H	0.0000	0.0000	0.0000	0.0000	0.0000	0.0000	0.0000	0.0000	0.0000
33.	H	0.0000	0.0000	0.0000	0.0000	0.0000	0.0000	0.0000	0.0000	0.0000
34.	H	0.0000	0.0000	0.0000	0.0002	0.0000	0.0000	0.0000	0.0000	0.0000
35.	C	0.0000	0.0000	0.0000	0.0002	0.0000	0.0000	0.0000	0.0000	0.0000
36.	H	0.0000	0.0000	0.0000	0.0000	0.0000	0.0000	0.0000	0.0000	0.0000
37.	H	0.0000	0.0000	0.0000	0.0001	0.0000	0.0000	0.0000	0.0000	0.0000
38.	H	0.0000	0.0000	0.0000	0.0000	0.0000	0.0000	0.0000	0.0000	0.0000
39.	C	0.0000	0.0000	0.0000	0.0013	0.0000	0.0000	0.0000	0.0000	0.0000
40.	H	0.0000	0.0000	0.0000	0.0013	0.0000	0.0000	0.0000	0.0000	0.0000
41.	H	0.0000	0.0000	0.0000	0.0002	0.0000	0.0000	0.0000	0.0000	0.0000
42.	H	0.0000	0.0000	0.0000	0.0002	0.0000	0.0000	0.0000	0.0000	0.0000

Atom	28	29	30	31	32	33	34	35	36
1. Ta	0.0002	0.0001	0.0005	0.0094	0.0002	0.0003	0.0008	0.0015	0.0001
2. P	0.0001	0.0001	0.0004	0.0003	0.0000	0.0000	0.0000	0.0004	0.0000
3. P	0.0001	0.0000	0.0001	0.0003	0.0000	0.0000	0.0000	0.0001	0.0000
4. P	0.0001	0.0001	0.0002	0.0003	0.0000	0.0001	0.0001	0.0002	0.0000
5. O	0.0000	0.0000	0.0000	0.0007	0.0000	0.0000	0.0001	0.0001	0.0000
6. O	0.0000	0.0000	0.0000	0.0007	0.0000	0.0000	0.0001	0.0022	0.0000
7. C	0.0012	0.0011	0.0117	0.0013	0.0001	0.0001	0.0004	0.0006	0.0000
8. C	0.0003	0.0005	0.0012	0.0068	0.0006	0.0003	0.0012	0.0086	0.0003
9. H	0.0000	0.0001	0.0000	0.0002	0.0001	0.0000	0.0000	0.0003	0.0000
10. C	0.0001	0.0001	0.0005	0.0153	0.0010	0.0012	0.0117	0.0112	0.0007
11. C	0.0000	0.0000	0.0000	0.0010	0.0001	0.0001	0.0002	0.0011	0.0001
12. C	0.0004	0.0003	0.0010	0.0015	0.0001	0.0001	0.0006	0.0008	0.0002
13. H	0.0001	0.0000	0.0000	0.0001	0.0000	0.0000	0.0000	0.0000	0.0000
14. C	0.0032	0.0032	0.0030	0.0001	0.0000	0.0000	0.0000	0.0003	0.0000
15. C	0.0001	0.0001	0.0006	0.0066	0.0002	0.0004	0.0007	0.0027	0.0007
16. H	0.0000	0.0000	0.0000	0.0002	0.0000	0.0001	0.0000	0.0007	0.0005
17. C	0.0000	0.0000	0.0000	0.9840	0.0032	0.0032	0.0029	0.9974	0.0032
18. C	0.0121	0.0007	0.0007	0.0000	0.0000	0.0000	0.0000	0.0000	0.0000
19. H	0.0002	0.0003	0.0000	0.0000	0.0000	0.0000	0.0000	0.0000	0.0000
20. H	0.0010	0.0002	0.0002	0.0000	0.0000	0.0000	0.0000	0.0000	0.0000
21. H	0.0002	0.0000	0.0004	0.0000	0.0000	0.0000	0.0000	0.0000	0.0000
22. C	0.0000	0.0000	0.0000	0.0010	0.0000	0.0000	0.0002	0.0002	0.0000
23. C	0.0006	0.0120	0.0008	0.0000	0.0000	0.0000	0.0000	0.0000	0.0000
24. H	0.0002	0.0010	0.0002	0.0000	0.0000	0.0000	0.0000	0.0000	0.0000
25. H	0.0004	0.0002	0.0000	0.0000	0.0000	0.0000	0.0000	0.0000	0.0000
26. H	0.0000	0.0002	0.0004	0.0000	0.0000	0.0000	0.0000	0.0000	0.0000
27. C	0.9305	0.9311	0.9325	0.0001	0.0000	0.0000	0.0000	0.0000	0.0000
28. H	0.0000	0.0006	0.0005	0.0000	0.0000	0.0000	0.0000	0.0000	0.0000
29. H	0.0006	0.0000	0.0005	0.0000	0.0001	0.0000	0.0000	0.0000	0.0000
30. H	0.0005	0.0005	0.0000	0.0000	0.0000	0.0000	0.0000	0.0000	0.0000
31. C	0.0000	0.0000	0.0000	0.0000	0.9310	0.9303	0.9331	0.0095	0.0009
32. H	0.0000	0.0001	0.0000	0.9310	0.0000	0.0006	0.0005	0.0118	0.0002
33. H	0.0000	0.0000	0.0000	0.9303	0.0006	0.0000	0.0005	0.0007	0.0004
34. H	0.0000	0.0000	0.0000	0.9331	0.0005	0.0005	0.0000	0.0008	0.0000
35. C	0.0000	0.0000	0.0000	0.0095	0.0118	0.0007	0.0008	0.0000	0.9318
36. H	0.0000	0.0000	0.0000	0.0009	0.0002	0.0004	0.0000	0.9318	0.0000
37. H	0.0000	0.0000	0.0000	0.0111	0.0010	0.0002	0.0002	0.9181	0.0011
38. H	0.0000	0.0000	0.0000	0.0008	0.0002	0.0000	0.0004	0.9333	0.0006
39. C	0.0000	0.0000	0.0000	0.0096	0.0007	0.0120	0.0006	0.0100	0.0123
40. H	0.0000	0.0000	0.0000	0.0114	0.0002	0.0010	0.0002	0.0010	0.0003
41. H	0.0000	0.0000	0.0000	0.0007	0.0003	0.0001	0.0000	0.0121	0.0011
42. H	0.0000	0.0000	0.0000	0.0010	0.0000	0.0003	0.0004	0.0008	0.0002

Atom	37	38	39	40	41	42
1. Ta	0.0021	0.0004	0.0033	0.0034	0.0003	0.0008
2. P	0.0015	0.0001	0.0002	0.0003	0.0000	0.0000
3. P	0.0001	0.0000	0.0012	0.0010	0.0003	0.0001
4. P	0.0005	0.0000	0.0003	0.0006	0.0000	0.0000
5. O	0.0000	0.0000	0.0007	0.0005	0.0001	0.0001
6. O	0.0025	0.0001	0.0003	0.0002	0.0000	0.0000
7. C	0.0001	0.0004	0.0011	0.0001	0.0002	0.0002
8. C	0.0003	0.0002	0.0028	0.0003	0.0005	0.0004
9. H	0.0000	0.0000	0.0005	0.0000	0.0007	0.0000
10. C	0.0008	0.0115	0.0118	0.0007	0.0010	0.0119
11. C	0.0020	0.0001	0.0008	0.0003	0.0000	0.0001
12. C	0.0001	0.0002	0.0006	0.0001	0.0000	0.0005
13. H	0.0000	0.0000	0.0003	0.0000	0.0000	0.0001
14. C	0.0000	0.0001	0.0000	0.0000	0.0000	0.0000

15.	C	0.0003	0.0005	0.0094	0.0004	0.0003	0.0003
16.	H	0.0001	0.0001	0.0002	0.0000	0.0000	0.0000
17.	C	0.0041	0.0029	0.9947	0.0041	0.0032	0.0027
18.	C	0.0000	0.0000	0.0000	0.0000	0.0000	0.0000
19.	H	0.0000	0.0000	0.0000	0.0000	0.0000	0.0000
20.	H	0.0000	0.0000	0.0000	0.0000	0.0000	0.0000
21.	H	0.0000	0.0000	0.0000	0.0000	0.0000	0.0000
22.	C	0.0001	0.0000	0.0013	0.0013	0.0002	0.0002
23.	C	0.0000	0.0000	0.0000	0.0000	0.0000	0.0000
24.	H	0.0000	0.0000	0.0000	0.0000	0.0000	0.0000
25.	H	0.0000	0.0000	0.0000	0.0000	0.0000	0.0000
26.	H	0.0000	0.0000	0.0000	0.0000	0.0000	0.0000
27.	C	0.0000	0.0000	0.0000	0.0000	0.0000	0.0000
28.	H	0.0000	0.0000	0.0000	0.0000	0.0000	0.0000
29.	H	0.0000	0.0000	0.0000	0.0000	0.0000	0.0000
30.	H	0.0000	0.0000	0.0000	0.0000	0.0000	0.0000
31.	C	0.0111	0.0008	0.0096	0.0114	0.0007	0.0010
32.	H	0.0010	0.0002	0.0007	0.0002	0.0003	0.0000
33.	H	0.0002	0.0000	0.0120	0.0010	0.0001	0.0003
34.	H	0.0002	0.0004	0.0006	0.0002	0.0000	0.0004
35.	C	0.9181	0.9333	0.0100	0.0010	0.0121	0.0008
36.	H	0.0011	0.0006	0.0123	0.0003	0.0011	0.0002
37.	H	0.0000	0.0010	0.0006	0.0002	0.0001	0.0000
38.	H	0.0010	0.0000	0.0010	0.0000	0.0003	0.0005
39.	C	0.0006	0.0010	0.0000	0.9205	0.9307	0.9339
40.	H	0.0002	0.0000	0.9205	0.0000	0.0013	0.0009
41.	H	0.0001	0.0003	0.9307	0.0013	0.0000	0.0006
42.	H	0.0000	0.0005	0.9339	0.0009	0.0006	0.0000

Wiberg bond index, Totals by atom:

Atom		l			
1.	Ta	6.9386	22.	C	3.5607
2.	P	3.0977	23.	C	3.8573
3.	P	3.1015	24.	H	0.9476
4.	P	3.0761	25.	H	0.9557
5.	O	2.2486	26.	H	0.9553
6.	O	2.2365	27.	C	3.8687
7.	C	4.0470	28.	H	0.9521
8.	C	3.9413	29.	H	0.9527
9.	H	0.9398	30.	H	0.9556
10.	C	4.0427	31.	C	3.8691
11.	C	3.5848	32.	H	0.9526
12.	C	3.9334	33.	H	0.9521
13.	H	0.9361	34.	H	0.9560
14.	C	4.0484	35.	C	3.8583
15.	C	3.9353	36.	H	0.9549
16.	H	0.9382	37.	H	0.9483
17.	C	4.0488	38.	H	0.9547
18.	C	3.8584	39.	C	3.8618
19.	H	0.9558	40.	H	0.9502
20.	H	0.9456	41.	H	0.9544
21.	H	0.9561	42.	H	0.9562

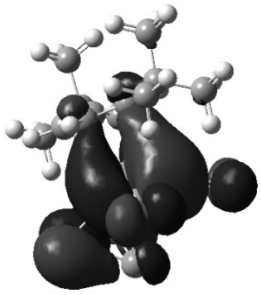

HOMO

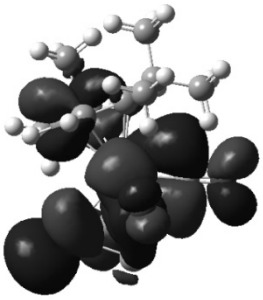

LUMO

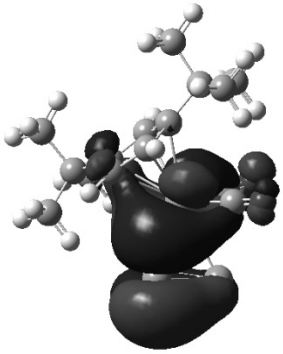

HOMO-1

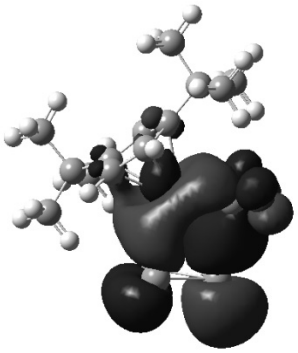

HOMO-2

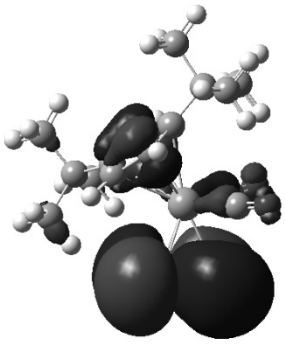

HOMO-3

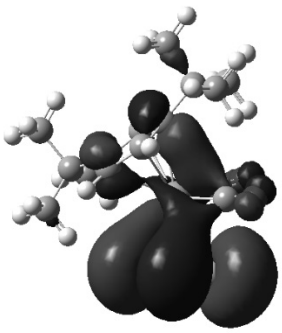

HOMO-4

Figure S 11. HOMO and LUMO and other selected MOs of the anion of **6** (= [Cp''Ta(CO)$_2$(η^3-P$_3$)]$^-$). B3LYP/def2-SVPD level of theory.

References:

[1] O. J. Scherer, T. Brück, *Angew. Chem. Int. Ed.* **1987**, *26*, 59-59.

[2] O. J. Scherer, R. Winter, G. Wolmershäuser, *Z. Anorg. Allg. Chem.* **1993**, *619*, 827-835.

[3] N. Kuhn, T. Kratz, *Synthesis* **1993**, *6*, 561-562.

[4] A. J. Arduengo III, H. C. R. Dias, R. L. Harlow, M. Kline, *J. Am. Chem. Soc.* **1992**, *114*, 5530-5534.

[5] A. J. Arduengo III, R. Krafczyk, R. Schmutzler, H. A. Craig, G. Jens R, W. J. Marshall, M. Unverzagt, *Tetrahedron* **1999**, *55*, 14523-14536.

[6] J. W. Runyon, O. Steinhof, H. V. R. Dias, J. C. Calabrese, W. J. Marshall, A. J. Arduengo, *Aust. J. Chem.* **2011**, *64*, 1165-1172.

[7] K. Powers, C. Hering-Junghans, R. McDonald, M. J. Ferguson, E. Rivard, *Polyhedron* **2016**, *108*, 8-14.

[8] CrysAlisPro Software System, Rigaku Oxford Diffraction, (**2018**).

[9] a) L. J. Bourhis, O. V. Dolomanov, R. J. Gildea, J. A. K. Howard, H. Puschmann, The Anatomy of a Comprehensive Constrained, Restrained, Refinement Program for the Modern Computing Environment - **Olex2** Disected, *Acta Cryst. A* **2015**, A71, 59–71; b) O. V. Dolomanov, L. J. Bourhis, R. J. Gildea, J. A. K. Howard, H. Puschmann, Olex2: A complete structure solution, refinement and analysis program, *J. Appl. Cryst.* **2009**, 42, 339–341.

[10] G. M. Sheldrick, ShelXT-Integrated space-group and crystal-structure determination, *Acta Cryst.* **2015**, A71, 3–8.

[11] G. M. Sheldrick, Crystal structure refinement with ShelXL, *Acta Cryst.* **2015**, C71, 3–8.

[12] a) A. D. Becke, *J. Chem. Phys.* **1993**, *98*, 5648-5652; b) C. Lee, W. Yang, R. G. Parr, *Phys. Rev. B.* **1988**, *37*, 785.

[13] M. J. Frisch, G. W. Trucks, H. B. Schlegel, G. E. Scuseria, M. A. Robb, J. R. Cheeseman, G. Scalmani, V. Barone, B. Mennucci, G. A. Petersson, H. Nakatsuji, M. Caricato, X. Li, H. P. Hratchian, A. F. Izmaylov, J. Bloino, G. Zheng, J. L. Sonnenberg, M. Hada, M. Ehara, K. Toyota, R. Fukuda, J. Hasegawa, M. Ishida, T. Nakajima, Y. Honda, O. Kitao, H. Nakai, T. Vreven, J. A. Montgomery, Jr., J. E. Peralta, F. Ogliaro, M. Bearpark, J. J. Heyd, E. Brothers, K. N. Kudin, V. N. Staroverov, T. Keith, R. Kobayashi, J. Normand, K. Raghavachari, A. Rendell, J. C. Burant, S. S. Iyengar, J. Tomasi, M. Cossi, N. Rega, J. M. Millam, M. Klene, J. E. Knox, J. B. Cross, V. Bakken, C. Adamo, J. Jaramillo, R. Gomperts, R. E. Stratmann, O. Yazyev, A. J. Austin, R. Cammi, C. Pomelli, J. W. Ochterski, R. L. Martin, K. Morokuma, V. G. Zakrzewski, G. A. Voth, P. Salvador, J. J. Dannenberg, S. Dapprich, A. D. Daniels, O. Farkas, J. B. Foresman, J. V. Ortiz, J. Cioslowski, and D. J. Fox, Gaussian 09, Revision E.01, Gaussian, Inc., Wallingford CT, **2013**.

4. The Reactivity of $[Cp_2Mo_2(CO)_4(\mu,\eta^{2:2}\text{-}P_2)]$ and $[Cp''Ta(CO)_2(\eta^4\text{-}P_4)]$ towards Hydroxide and *tert*-Butyl Nucleophiles

Felix Riedlberger, Michael Seidl and Manfred Scheer

- All compounds were synthesized and characterized by Felix Riedlberger.
- The manuscript was written by Felix Riedlberger.
- Figures were made by Felix Riedlberger.
- X-ray structure analyses and refinements were performed by Felix Riedlberger and finally checked by Michael Seidl.

4.1 Introduction

Abstract: *The reactions of [$Cp_2Mo_2(CO)_4(\mu,\eta^{2:2}\text{-}P_2)$] (**1**) and [$(Cp''Ta(CO)_2(\eta^4\text{-}P_4)$] (**2**), respectively, towards the anions OH^- and $^tBu^-$ are reported. While the reaction of **1** with KOH gives the anionic complex [$Cp_2Mo_2(CO)_4(\mu\text{-}PH_2)]^-$ (**3**) under a formal phosphorus abstraction, **1** reacts with Li^tBu under the alkylation leading to the formation of [$Cp_2Mo_2(CO)_4(\mu,\eta^{2:1}\text{-}PP^tBu)]^-$ (**4**). The reaction of **2** with [IDipp-H][OH] ($[IDipp\text{-}H]^+$ = 1,3-bis-(2,6-diisopropyl-phenyl)imidazolium) and Li^tBu yield [$Cp''Ta(CO)_2(\eta^3\text{-}P_4OH)]^-$ (**5**) and [$Cp''Ta(CO)_2(\eta^3\text{-}P_4{}^tBu)]^-$ (**6**), respectively. Compounds **3**, **4**, **5** and **6** were comprehensively characterized by NMR spectroscopy and X-ray structure analysis.*

White phosphorus P_4 can be activated with different methods. When P_4 is reacted with 2,4,6-tri-*tert*-butylphenyllithium and 1-bromo-2,4,6-tri-*tert*-butylbenzene, a butterfly-like phosphorus moiety, which is stabilized by two 2,4,6-tri-*tert*-butylphenyl residues is obtained.[1] Another way of P_4 activation can be obtained by a titanium halogen atom sink to remove the bromine atom from PhBr to yield PPh_3 in excellent yields.[2] The polyphosphorus ligand complex [$Cp_2Mo_2(CO)_4(\mu,\eta^{2:2}\text{-}P_2)$] (**1**) can form dimers with coinage metal salts,[3] 1D polymers with copper halides[4] and even 2D polymers with silver cations and organic linkers.[5] Not only the coordination chemistry of **1** is already investigated, but also its oxidation and reduction behavior. The oxidation of **1** with thiantrenium salt yields unprecedented P_4^{2+} chains.[6] The reaction of **1** with [$Cp^*_2Ln(thf)_2$] (Ln = Sm, Yb) leads to the reduction of the P_2 unit and the formation of the 16-membered bicyclic compounds [$(Cp^*_2Ln)_2P_2(CpMo(CO)_2)_4$] (Ln = Sm, Yb) as major products. In case of samarocene, two minor products, the *cyclo*-P_4 complex [$(Cp^*_2Sm)_2P_4(CpMo(CO)_2)_2$] and the *cyclo*-$P_5$ complex [$(Cp^*_2Sm)_3P_5(CpMo(CO)_2)_3$], are formed as well, revealing that in addition to the reduction of **1** a rearrangement takes place.[7] Out of the numerous polyphosphorus ligand complexes[8] only few examples contain a *cyclo*-P_4 unit and hence their reactivity is investigated to a lesser extent. Three of the known *cyclo*-P_4 complexes contain a group five element, which are [$(Cp^*Nb(CO)_2(\eta^4\text{-}P_4)$][9] (Cp* = pentamethylcyclopentadienyl), [$(Cp''Ta(CO)_2(\eta^4\text{-}P_4)$][10] (Cp'' = 1,3-di-*tert*-butylcyclopentadienyl) (**2**), and [$(Cp^*V(CO)_2(\eta^4\text{-}P_4)$].[11] After these pioneering results, it took over two decades to discover other *cyclo*-P_4 ligand complexes. In 2017 [$Cp'''Co(\eta^4\text{-}P_4)$][12] (Cp''' = 1,2,4-tri-*tert*-butylcyclopentadienyl) was published followed by the iron complex [$(^{Ph}PP_2{}^{Cy})Fe(\eta^4\text{-}P_4)$][13] and by the molybdenum complex [$(Ar^{Dipp2}NC)Mo(CO)_2(\eta^4\text{-}P_4)$] ($Ar^{Dipp2}$ = 2,6-(2,6-(*i*-Pr)$_2C_6H_3$)$_2C_6H_3$)).[14] The reactivity of [$(Cp''Ta(CO)_2(\eta^4\text{-}P_4)$] (**2**) towards Lewis acids was studied inter alia by our group. It has been shown that complex **2** can form spherical molecules with copper halides.[15] Although the coordination behavior of **1** and **2** and the redox properties of **1** have been extensively studied, their reactivity towards nucleophiles has not been investigated yet. This might be a way for obtaining organo phosphorus moieties. Herein, we report on the reactivity of [$Cp_2Mo_2(CO)_4(\mu,\eta^{2:2}\text{-}P_2)$] (**1**) and [$(Cp''Ta(CO)_2(\eta^4\text{-}P_4)$] (**2**) towards the nucleophiles OH^- and $^tBu^-$, which reveal a unique way of functionalization.

4.2 Results and Discussion

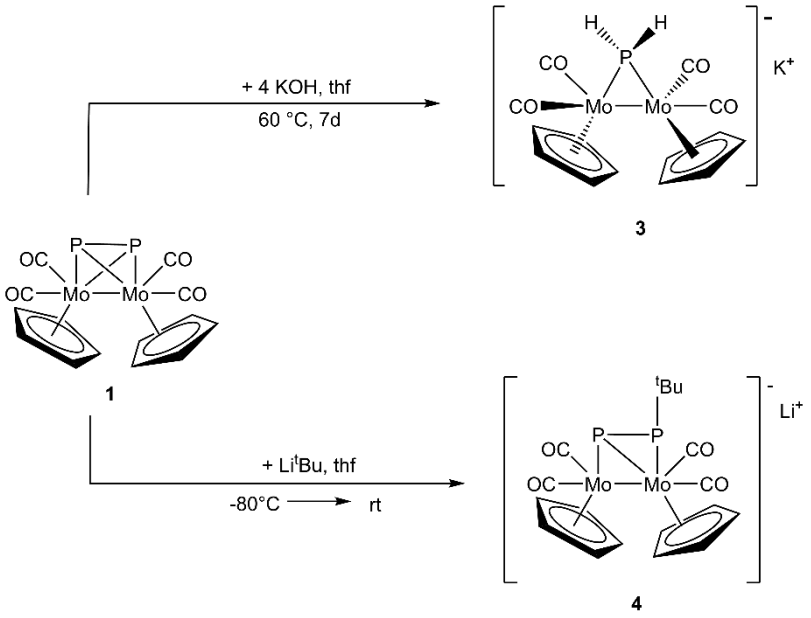

Scheme 1. Reactivity of **1** towards KOH and Li^{t}Bu.

$[Cp_2Mo_2(CO)_4(\mu,\eta^{2:2}\text{-}P_2)]$ (**1**) was reacted with an excess of KOH in thf at 60 °C for seven days. At room temperature, no reaction is obtained, which is surprising in view of the easy reaction of **1** with Li^{t}Bu. The ^{31}P NMR spectra of the reaction mixture show still unreacted **1** after several days. After 7 seven days, the ^{31}P NMR spectra show the exclusively formation of $[Cp_2Mo_2(CO)_4(\mu\text{-}PH_2)]^-$ (**3**). After workup $[K(thf)_4]$[**3**] can be isolated in a crystalline yield of 81% (Figure 1). The ^{31}P NMR spectra of the reaction mixture show no signal of the abstracted P atom in a range from 300 to –300 ppm. Compound **3** was already synthesized by *Mays et al.*[16] and our group,[17] but it was not isolated in pure form or further characterized besides by ^{31}P NMR spectroscopy. *Mays* used the synthesis of **1** with KOH and added HBF_4 to yield $[\{CpMo(CO)_2\}_2(\mu\text{-}H)(\mu\text{-}PH_2)]$ (**A**), whereas our group described a high yield one-pot reaction for **A** using $[CpMo(CO)_2]_2$, $LiP(SiMe_3)_2$, MeOH and HBF_4. The ^{31}P NMR spectrum of the reaction mixture of **3** shows a triplett at 49.8 ppm with a coupling constant $^1J_{PH}$ of 318 Hz, whereas the $^{31}P\{^1H\}$ NMR spectrum shows a singlet at 49.8 ppm. The ^{1}H NMR spectrum of the reaction mixture shows a singlet at 4.83 ppm for the Cp ligands and a doublet at 4.44 ppm with a coupling constant of 318 Hz for the PH_2 unit. The nature of the eliminated phosphorus atom from **1** could not be identified neither by ^{31}P NMR spectroscopy of the reaction mixture nor by other analytical methods. Single crystals of $[K(thf)_4]$[**3**] suitable for X-ray diffractions could be obtained by a saturated solution in thf layered with *n*-hexane and stored at 4°C. The X-ray structure analysis shows a three membered ring with two molybdenum atoms and one phosphorus atom to which two hydrogen atoms are bonded (Figure 1). The Mo-Mo distance in **3** with 3.1826(10) Å is slightly longer than that in **1** (Mo-Mo 3.022(1) Å). This lengthening of the Mo-Mo bond length is probably due to the increase of the ring strain in **3** compared to **1**.

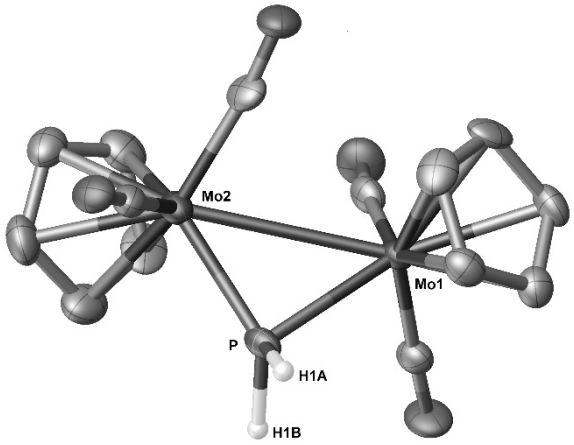

Figure 1. Molecular structure in the solid state of **3**. Thermal ellipsoids are shown at 50% probability level. Hydrogen atoms bonded to carbon are omitted for clarity. Selected bond lengths [Å] and angles [°]: Mo1-P 2.375(2), Mo2-P 2.378(2), Mo1-Mo2 3.1826(10), P-Mo1-Mo2 48.00(6), P-Mo2-Mo1 47.93(6), Mo1-P-Mo2 84.07(8), H1A-P-H1B 104(8).

When Li^{t}Bu is added to an orange solution of $[Cp_2Mo_2(CO)_4(\mu,\eta^{2:2}\text{-}P_2)]$ (**1**) at -80°C, an immediate color change to red-brown is observed. After work-up, $[Li(dme)_3][\mathbf{4}]$ (**4** = $[Cp_2Mo_2(CO)_4(\mu,\eta^{2:1}\text{-}PP^tBu)]^-$), can be isolated as dark red crystals in 38% yield. The $^{31}P\{^1H\}$ NMR spectrum of the reaction mixture shows only two doublets at 191.9 and 59.8 ppm of **4** with a $^1J_{PP}$ coupling constant of 454 Hz. In the ^{31}P NMR spectrum of **4** the signal centered at 191.9 ppm is considerably broadened as a consequence of the unresolved coupling to the hydrogen atoms of the *tert*-butyl substituents. All efforts to obtain good quality crystals of **4** for X-ray structure determination were not successful, since the crystals lose some solvents molecules and lose crystality. However, we were able to record a data set from which the atom connectivity of **4** could be unambiguously determined (Figure 2).

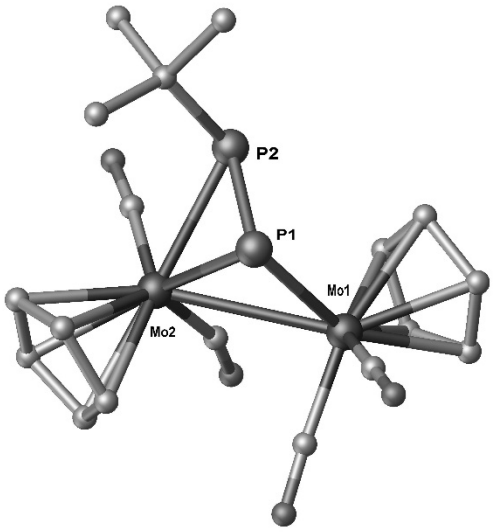

Figure 2. The molecule structure in the solid state of **4**. The H atoms are omitted for clarity.

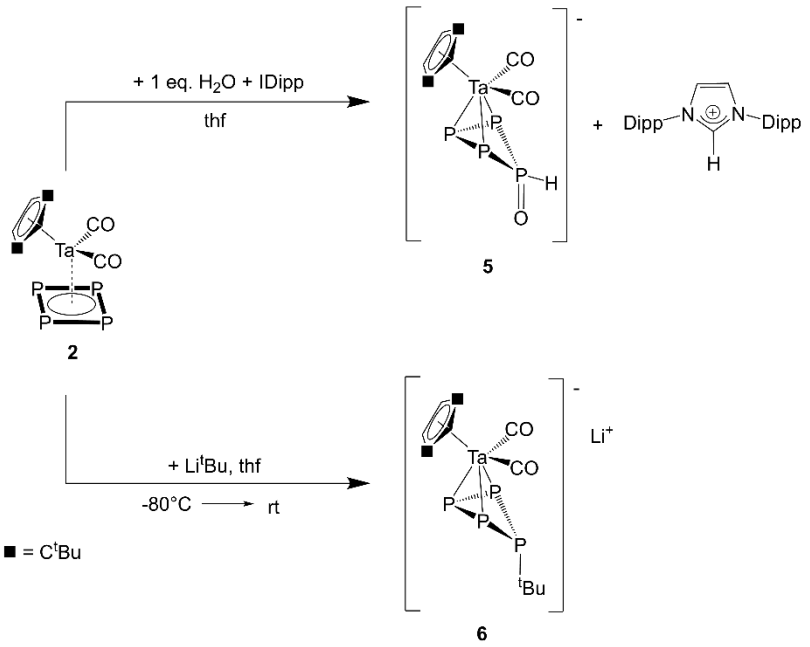

Scheme 2. Reactivity of **2** towards [IDipp-H][OH] and Li^{t}Bu.

After these successful attempts of nucleophilic functionalization, the question arose, if the *cyclo*-P_4 complex [Cp''Ta(CO)$_2$(η^4-P_4)] (**2**) can be functionalized as well with nucleophiles. All attempts to produce the anionic complex [Cp''Ta(CO)$_2$(η^3-P_4OH)]$^-$ (**5**) in reactions of **2** with KOH were unselective. Several byproducts were formed and a separation of the produced mixture was not successful regardless of numerous attempts. Therefore, a different source for the OH^- anions was used, the *in situ* generated imidazolium salt [IDipp-H][OH] (IDipp = 1,3-bis(2,6-diisopropylphenyl)-imidazole-2-ylidene). For this an equimolar amount of water was reacted with the NHC (= N-heterocyclic carbene). With the resulting counter cation [IDipp-H]$^+$ of OH^-, the reaction with **2** was selective to obtain [IDipp-H][**5**] in 81% yield. The $^{31}P\{^1H\}$ NMR spectrum of **2** shows an AMM'X spin system, with three distinct multiplets centered at 60.1, 40.2 and -114.8 ppm. The signals exhibit an integral ratio of 1:2:1, and a coupling pattern which indicates an intact P_4 ring. In the ^{31}P NMR spectrum the signal centered at 60.1 show a further coupling with a $^1J_{PH}$ coupling constant of 362.3 Hz. Both ^{31}P NMR spectra have been simulated and all coupling constants are given in the supporting information. The ^1H NMR spectrum of [IDipp-H][**5**] shows a doublet of triplets of doublets at 6.40 ppm with the three coupling constants $^1J_{PH}$ 362.3 Hz, $^2J_{PH}$ 21.2 Hz and $^3J_{PH}$ 4.3 Hz. This high coupling constant between the phosphorus atom and the hydrogen atom indicates a direct bonding between the phosphorus atom and the hydrogen atom. This evidence is proofed by the molecular structure of **5** in the solid state. X-ray structure investigations of [IDipp-H][**5**] show a *cyclo*-P_4 ring with three phosphorus atoms coordinating to the tantalum atom (Figure 3). The fourth phosphorus atom is bend and bears an oxygen atom in the *endo*-position and a hydrogen atom in the *exo*-position. The position of the hydrogen atom at the phosphorus atom could be located from the difference Fourier map and was freely refined. There is no big difference between the Ta-P and P-P distances in **2** and **5**, respectively.

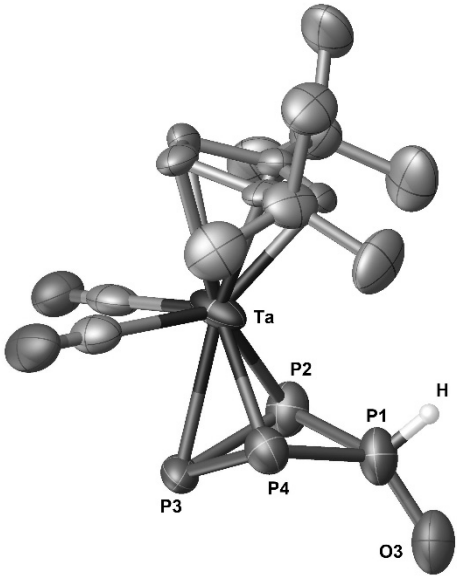

Figure 3. Molecular structure in the solid state of **5**. Thermal ellipsoids are shown at 50% probability level. Hydrogen atoms bonded to carbon are omitted for clarity. Selected bond lengths [Å] and angles [°]: Ta-P2 2.447(7), Ta-P3 2.514(3), Ta-P4 2.541(5), P1-P2 2.171(3), P2-P3 2.208(3), P3-P4 2.208(3), P4-P1 2.169(3), P1-O3 1.511(7), P1-P2-P3 84.21(13), P2-P3-P4 88.11(11), P3-P4-P1 84.23(12), P4-P1-P2 90.07(12).

When Li^{t}Bu is added to a solution of [Cp''Ta(CO)$_2$(η^4-P$_4$)] in thf at -80°C an immediate color change from sunny yellow to red is maintained. After workup, crystals of [Li(thf)$_4$][**6**] (**6** = [Cp''Ta(CO)$_2$(η^3-P$_4$^{t}Bu)]$^-$) can be isolated in 53% yield. The ^{31}P{^{1}H} NMR spectrum of compound **6** shows an AMX$_2$ spin system with the three signals centered at 108.1, -15.1 and -89.8 ppm with an integral ratio of 1:1:2, respectively. This is an indication of an intact P$_4$ ring. Single crystals of [Li(thf)$_4$][**6**] were obtained from a saturated solution in thf layered with *n*-hexane and stored at 4°C. The structure of **6** reveal a *cyclo*-P$_4$ ring, similar to that found in **5**, which coordinated in a η^3 fashion to a Cp''Ta(CO)$_2$ fragment (Figure 4). The fourth phosphorus atom is not bonded to the tantalum but form a new bond to the ^{t}Bu unit in *endo*-position. The Ta-P distances in **6** are very similar to the corresponding distances in **5**. The distance between the phosphorus atom and the carbon atom is 1.903(4) Å and is characteristic for a P-C single bond.[18]

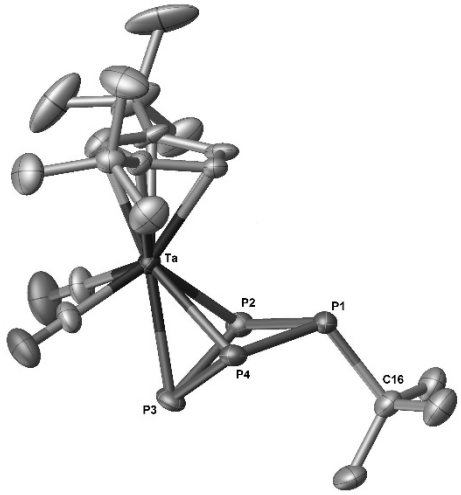

Figure 4. Molecular structure in the solid state of **6**. Thermal ellipsoids are shown at 50% probability level. Hydrogen atoms bonded to carbon are omitted for clarity. Selected bond lengths [Å] and angles [°]: Ta-P2 2.6046(10), Ta-P3 2.5778(9), Ta-P4 2.5971(10), P1-P2 2.2047(14), P2-P3 2.2074(14), P3-P4 2.005(14), P4-P1 2.2167(14), P1-C16 1.903(4), P1-P2-P3 91.63(5), P2-P3-P4 84.02(5), P3-P4-P1 91.50(5), P4-P1-P2 83.70(5).

4.3 Conclusion and References

In summary, we have shown that $[Cp_2Mo_2(CO)_4(\mu,\eta^{2:2}\text{-}P_2)]$ (**1**) and $[Cp''Ta(CO)_2(\eta^4\text{-}P_4)]$ (**2**) reveal a different reactivity towards hydroxide and *tert*-butyl anions. This gives access to novel functionalized compounds such as $[Cp_2Mo_2(CO)_4(\mu\text{-}PH_2)]^-$ (**3**), $[Cp_2Mo_2(CO)_4(\mu,\eta^{2:1}\text{-}PP^tBu)]^-$ (**4**), $[Cp''Ta(CO)_2(\eta^3\text{-}P_4OH)]^-$ (**5**) and $[Cp''Ta(CO)_2(\eta^3\text{-}P_4{}^tBu)]^-$ (**6**). This shows, that **1** and **2** can be used not only as building block in supramolecular coordination chemistry with transition metals but also as starting materials for the synthesis of functionalized complexes. The most interesting result is the formation of complex **3** with a phosphorus atom being abstracted from **1**. This exhibits the potential of P_n ligand complexes to release a phosphorus atom which can be functionalized to useful P containing products.

References:

[1] R. Riedel, H.-D. Hausen, E. Fluck, *Angew. Chem. Int. Ed.* **1985**, *24*, 1056-1057.
[2] B. M. Cossairt, C. C. Cummins, *New Journal of Chemistry* **2010**, *34*, 1533.
[3] M. Scheer, L. J. Gregoriades, M. Zabel, J. Bai, I. Krossing, G. Brunklaus, H. Eckert, *Chem. Eur. J.* **2008**, *14*, 282-295.
[4] M. Scheer, L. Gregoriades, J. Bai, M. Sierka, G. Brunklaus, H. Eckert, *Chem. Eur. J.* **2005**, *11*, 2163-2169.
[5] B. Attenberger, S. Welsch, M. Zabel, E. Peresypkina, M. Scheer, *Angew. Chem. Int. Ed.* **2011**, *50*, 11516-11519.
[6] L. Dütsch, M. Fleischmann, S. Welsch, G. Balazs, W. Kremer, M. Scheer, *Angew. Chem. Int. Ed.* **2018**, *57*, 3256-3261.
[7] N. Arleth, M. T. Gamer, R. Koppe, N. A. Pushkarevsky, S. N. Konchenko, M. Fleischmann, M. Bodensteiner, M. Scheer, P. W. Roesky, *Chem Sci* **2015**, *6*, 7179-7184.
[8] a) M. Scheer, G. Balázs, A. Seitz, *Chem. Rev.* **2010**, *110*, 4236-4256; b) M. Caporali, L. Gonsalvi, A. Rossin, M. Peruzzini, *Chem. Rev.* **2010**, *110*, 4178-4235; c) O. J. Scherer, *Acc. Chem. Res.* **1999**, *32*, 751-762.
[9] O. J. Scherer, J. Vondung, G. Wolmershäuser, *Angew. Chem. Int. Ed.* **1989**, *28*, 1355-1357.
[10] O. J. Scherer, R. Winter, G. Wolmershäuser, *Z. Anorg. Allg. Chem.* **1993**, *619*, 827-835.
[11] M. Herberhold, G. Frohmader, W. Milius, *J. Organomet. Chem.* **1996**, *522*, 185-196.
[12] F. Dielmann, A. Timoshkin, M. Piesch, G. Balázs, M. Scheer, *Angew. Chem. Int. Ed.* **2017**, *56*, 1671-1675.
[13] A. Cavaillé, N. Saffon-Merceron, N. Nebra, M. Fustier-Boutignon, N. Mézailles, *Angew. Chem. Int. Ed.* **2018**, *57*, 1874-1878.
[14] K. A. Mandla, C. E. Moore, A. L. Rheingold, J. S. Figueroa, *Angew. Chem. Int. Ed.* **2019**, *58*, 1779-1783.
[15] a) F. Dielmann, E. V. Peresypkina, B. Krämer, F. Hastreiter, B. P. Johnson, M. Zabel, C. Heindl, M. Scheer, *Angew. Chem. Int. Ed.* **2016**, *55*, 14833-14837; b) B. P. Johnson, F. Dielmann, G. Balázs, M. Sierka, M. Scheer, *Angew. Chem. Int. Ed.* **2006**, *45*, 2473-2475.
[16] J. E. Davies, M. J. Mays, P. R. Raithby, G. P. Shields, P. K. Tompkin, *Chem. Commun.* **1997**, 361-362.
[17] U. Vogel, M. Scheer, *Z. Anorg. Allg. Chem.* **2003**, *629*, 1491-1495.
[18] P. Pyykkö, M. Atsumi, *Chemistry* **2009**, *15*, 12770-12779.

4.4 Supporting Information

Experimental details: complex syntheses and characterization

General procedures: All manipulations were performed with rigorous exclusion of oxygen and moisture in Schlenk-type glassware on a dual manifold Schlenk line in Argon atmosphere or in Argon filled glove box with a high-capacity recirculator (<0.1 ppm O_2). Toluene thf, dme and *n*-hexane were dried using conventional techniques, degassed and saturated with Argon. Deuterated solvents were degassed, dried and distilled prior to use. The complexes $[Cp_2Mo_2(CO)_4(\mu,\eta^{2:2}\text{-}P_2)]$[1] (**1**) and $[Cp''Ta(CO)_2(\eta^4\text{-}P_4)]$[2] (**2**) and the NHC IDipp[3] were prepared according to its published procedure. NMR spectra were recorded on a Bruker Avance 300 MHz and Bruker Avance 400 MHz spectrometers. Chemical shifts are given in ppm; they are referenced to TMS for ^1H and ^{13}C, and 85% H_3PO_4 for ^{31}P as external standard. Elemental analyses (CHN) were determined using in-house facility.

Synthesis of $[K(thf)_4][3]$, [3] = $[Cp_2Mo_2(CO)_4(\mu\text{-}PH_2)]^-$: 100 mg (0.20 mmol) $[Cp_2Mo_2(CO)_4(\mu,\eta^{2:2}\text{-}P_2)]$ (**1**) and 40 mg (0.71 mmol) KOH are dissolved in 20 mL thf and stirred for seven days at 60 °C. The color of the solution is changing from orange to bordeaux. The solution was reduced to 3 mL, layered with *n*-hexane and crystalized at 4 °C. After five days clear dark plates can be isolated of $[K(thf)_4][Mo_2Cp_2(CO)_4(\mu\text{-}PH_2)]$ (130 mg, 0.163 mmol, 81% yield).

^1H NMR (thf-d_8, 300 K): δ [ppm] = 4.44 (d, 2H, $^1J_{PH}$ = 318 Hz, PH_2), 4.83 (s, 10H, C_5H_5).

$^1H\{^{31}P\}$ NMR (thf-d_8, 300 K): δ [ppm] = 4.44 (s, 2H, PH_2), 4.83 (s, 10H, C_5H_5).

$^{31}P\{^1H\}$ NMR (thf-d_8, 300 K): δ [ppm] = 49.8 (s, 1P).

^{31}P NMR (thf-d_8, 300 K): δ [ppm] = 49.8 (t, $^1J_{PH}$ = 318 Hz, 1P).

EI-MS (dme): *m*/*z* = 466.8 (100%, $[Cp_2Mo_2(CO)_4(\mu\text{-}PH_2)]^-$).

EA calculated for $C_{14}H_{12}KMo_2O_4P$ (506,19 g·mol^{-1}): C: 33.22, H: 2.39; found [%]: C: 33.74, H: 2.71.

Synthesis of $[Li(dme)_3][4]$, [4] = $[Cp_2Mo_2(CO)_4(\mu,\eta^{2:1}\text{-}PP^tBu)]^-$: 80 mg (0.16 mmol) $[Cp_2Mo_2(CO)_4(\mu,\eta^{2:2}\text{-}P_2)]$ (**1**) are dissolved in 15 mL thf, cooled to -80°C and 21 mg (0.32 mmol, 0.19 mL) Li^{t}Bu in *n*-pentane is added. An instant color change from orange to brown is observed. After the solution was heated to ambient temperature overnight, all volatiles are removed, the oily residue is dissolved in 3 mL dme and layered with 9 mL *n*-hexane. Red brownish crystal blocks of $[Li(dme)_3][Mo_2Cp_2(CO)_4(\mu,\eta^{2:1}\text{-}PP^tBu)]$ (50 mg, 0.060 mmol, 38% yield) are obtained after storage for five days at 4 °C.

^{1}H NMR (thf-d_8, 300 K): δ [ppm] = 0.81 (d, 9H, ^{t}Bu), 4.58 (s, 5H, C_5H_5), 4.85 (s, 5H, C_5H_5).

^{31}P{^{1}H} NMR (thf-d_8, 300 K): δ [ppm] = 191.9 (d, $^{1}J_{PP}$ = 454 Hz, *P*-P-^{t}Bu), 59.8 (d, $^{1}J_{PP}$ = 454 Hz, P-*P*-^{t}Bu).

^{31}P NMR (thf-d_8, 300 K): δ [ppm] = 191.9 (d, $^{1}J_{PP}$ = 454 Hz, *P*-P-^{t}Bu), 59.8 (m, $^{1}J_{PP}$ = 454 Hz, P-*P*-^{t}Bu). The exact $^{3}J_{PH}$ coupling constant could not be determined.

EI-MS (dme) *m/z* = 552.9 (100%, $[Cp_2Mo_2(CO)_4(\mu,\eta^{2:1}\text{-}PP^{t}Bu)]^-$).

EA calculated for $C_{27.2}H_{37.4}LiMo_2O_{6.3}P_2$ (725.95 g·mol^{-1}): C: 45.00, H: 5.19; found [%]: C: 44.70, H: 5.19.

Synthesis of [IDipp-H][5], [5] = [Cp''Ta(CO)$_2$(η^3-P$_4$OH)]$^-$: 80 mg (0.15 mmol) of [Cp''Ta(CO)$_2$(η^4-P$_4$)] (**2**) were dissolved and 5 mL of a stock solution of H_2O in thf (c = 0.029 mmol·mL^{-1}) were added. No color change was observed. Afterwards, 58 mg (0.15 mmol) of IDipp were dissolved in thf and added to the sunny yellow solution of **1** and H_2O. A light color change to light brown was observed and the solution was stirred for three days, were the brown coloring of the solution got intensified. After removing all volatiles in vaccuo, the brown residue was dissolved in 3 mL dme, was layered by 15 mL *n*-hexane and stored at 4°C to obtain brown blocks of [IDipp-H][Cp''Ta(CO)$_2$(η^3-P$_4$OH)] (114 mg, 0.12 mmol, 81% yield).

^{1}H NMR (thf-d_8, 300 K): δ [ppm] = 1.28 (s, 18H, Cp'' ^{t}Bu), 1.32 (d, 12H, Dipp ^{i}Pr, $^{3}J_{HH}$ = 6.8 Hz), 1.36 (d, 12H, Dipp ^{i}Pr, $^{3}J_{HH}$ = 6.8 Hz), 2.65 (sept, 4H, Dipp ^{i}Pr, $^{3}J_{HH}$ = 6.8 Hz), 5.35 (d, 2H, CH, $^{4}J_{HH}$ = 2.0 Hz), 5.59 (t, 1H, CH, $^{4}J_{HH}$ = 2.0 Hz), 6.40 (dtd, 1H, H-P, $^{1}J_{PH}$ = 362.3 Hz, $^{2}J_{PH}$ = 21.2 Hz, $^{3}J_{PH}$ = 4.3 Hz), 8.41 (s, 2H, H-CN), 11.64 (s, 1H, N2C-H).

^{31}P{^{1}H} NMR (thf-d_8, 300 K): δ [ppm] = 60.1 (t, 1P, P_A), 40.2 (t, 2P, $P_{M,M'}$), -114.8 (t, 1P, P_x).

For coupling constants see Table S 1.

^{31}P NMR (thf-d_8, 300 K): δ [ppm] = 60.1 (m, 1P, P_A), 40.2 (td, 2P, $P_{M,M'}$), -114.8 (t, 1P, P_x). For coupling constants see Table S 2.

EI-MS (dme): anion mode: *m/z* = 555.00 (100 %, $[M]^-$), cation mode: *m/z* = 389.29 (100%, $[(IDipp\text{-}H]^+$).

EA: due to the high sensitivity of [IDipp-H][Cp''Ta(CO)$_2$(η^3-P$_4$OH)] towards moisture and air, it was not possible to obtain an exact elemental analysis. Although several samples were used.

Synthesis of [Li(thf)$_4$][6], [6] = [Cp''Ta(CO)$_2$(η^3-P$_4$^{t}Bu)]$^-$: A solution of 100 mg (0.18 mmol) [Cp''Ta(CO)$_2$(η^4-P$_4$)] (**2**) in 20 mL thf is cooled down to -80 °C and 0.16 mL (0.18 mmol) ^{t}BuLi in *n*-pentane was added. An instant color change from sunny yellow to red is obtained. The reaction mixture is warmed up to ambient room temperature overnight. The solution was reduced to 3 mL and layered with 10 mL n-hexane. Clear light brown plates of [Li(thf)$_4$][Cp''Ta(CO)$_2$(η^3-P$_4$^{t}Bu)] (85 mg, 0.096 mmol, 53%) are formed after 4 days at 4°C.

^{1}H NMR (thf/C_6D_6 capillary, 300 K): δ [ppm] = 1.61 (s, 18H, Cp'' ^{t}Bu), 1.77 (d, 9H, P-^{t}Bu), 6.03 (t, 1H, CH, $^4J_{HH}$ = 2.0 Hz), 6.16 (d, 2H, CH, $^4J_{HH}$ = 2.0 Hz).

^{31}P{^{1}H} NMR (thf/C_6D_6 capillary, 300 K): δ [ppm] = 108.1 (dt, P_A), -15.1 (dt, P_M), -89.8 (dd, $P_{X,X}$). For coupling constants see Table S 3.

^{31}P NMR (thf/C_6D_6 capillary, 300 K): δ [ppm] = 108.1 (m, P_A), -15.1 (dt, P_M), -89.8 (dd, $P_{X,X}$), the phosphorus phosphorus coupling are the same like in the ^{31}P{^{1}H} NMR spectrum. The exact $^3J_{PH}$ coupling constant could not be determined.

EI-MS (dme): *m*/*z* = 1197.4 (100%, {[Cp''Ta(CO)$_2$(η^3-P$_4$-^{t}Bu)]$_2$+[Li$^+$]}$^-$).

EA calculated for $C_{19}H_{30}O_2P_4TaLi$ (602,22 g·mol^{-1}): C: 37.89, H: 5.02; found [%]: C: 37.69, H: 4.95.

Experimental and simulated NMR spectra

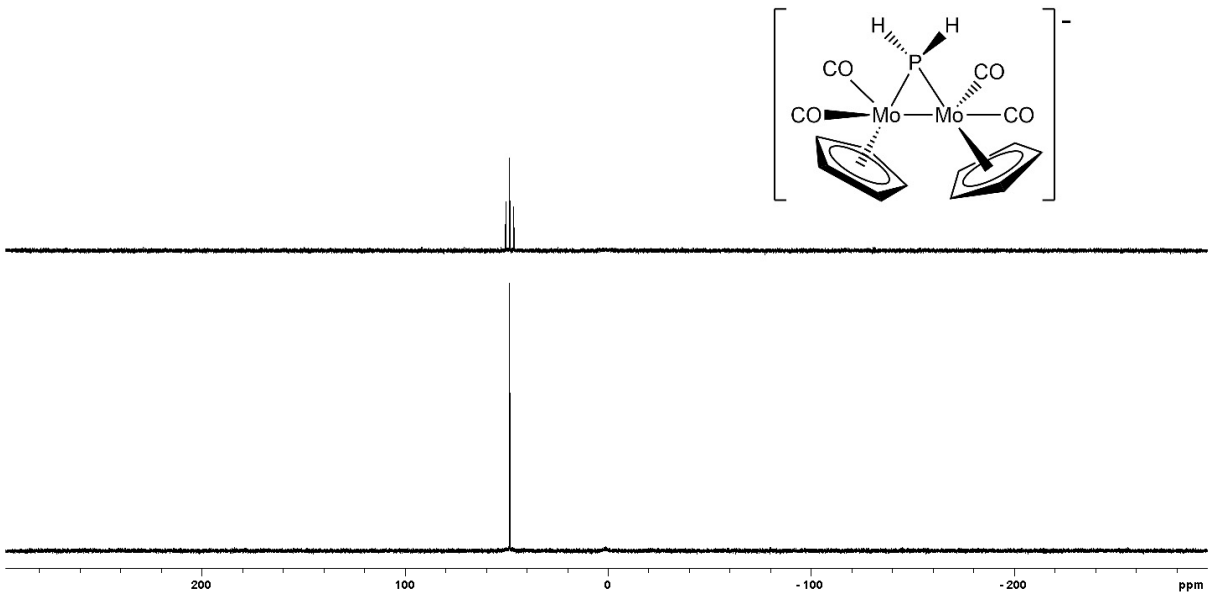

Figure S 1. ^{31}P NMR spectrum (top) and $^{31}P\{^{1}H\}$ NMR spectrum (bottom) of compound **3** at 300 K in thf-d_8.

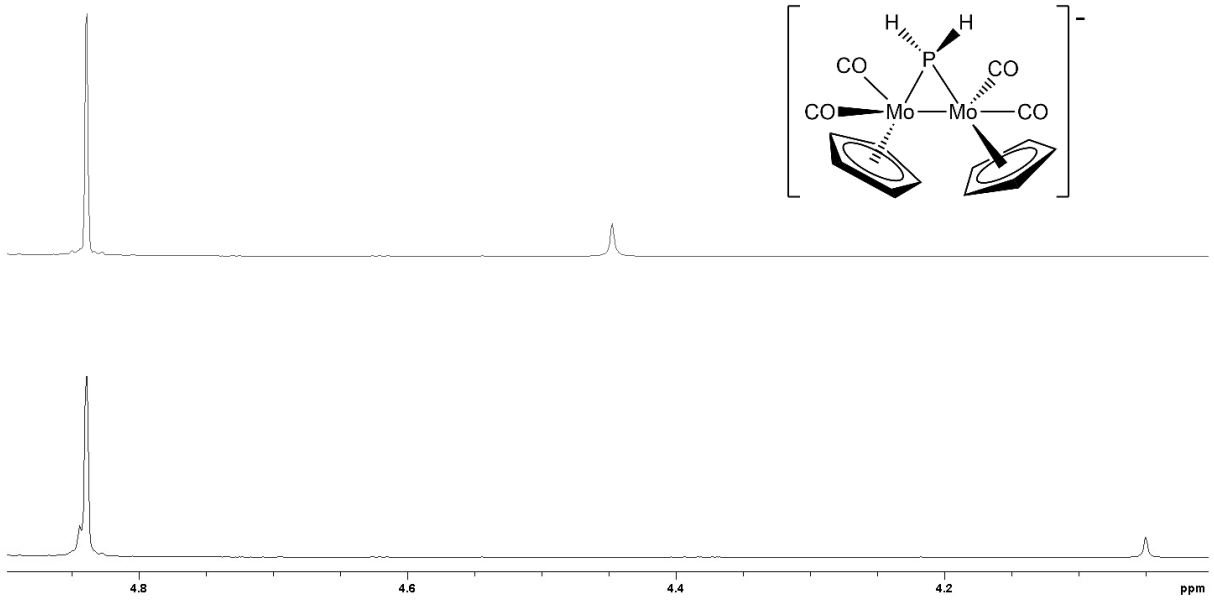

Figure S 2. $^{1}H\{^{31}P\}$ NMR spectrum (top) and ^{1}H NMR spectrum (bottom) from 4.9 to 4.0 ppm of **3** at 300 K in thf-d_8.

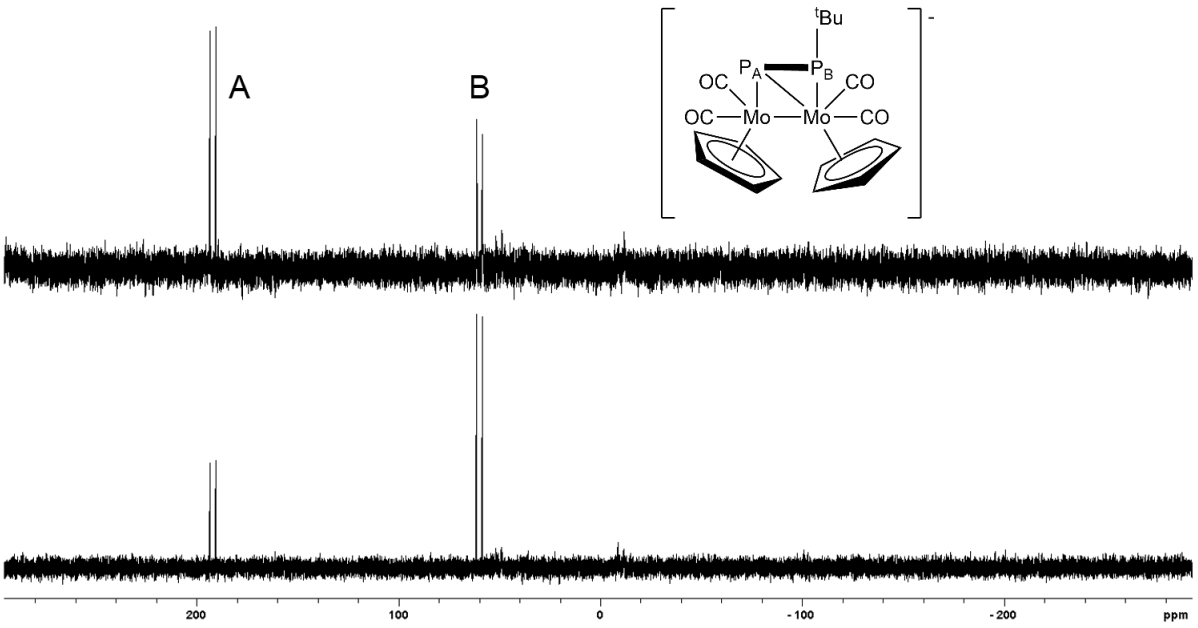

Figure S 3. ^{31}P NMR spectrum (top) and $^{31}P\{^{1}H\}$ NMR spectrum (bottom) of **4** at 300 K in thf-d_8.

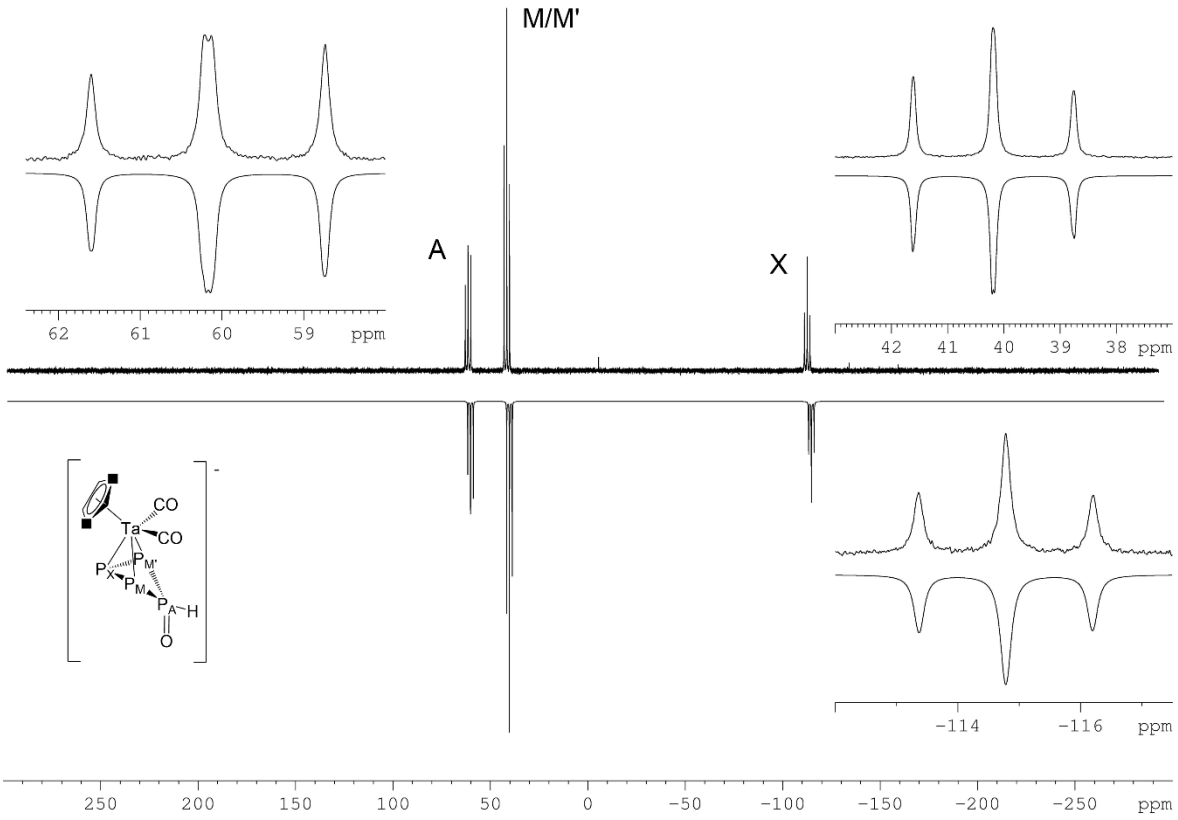

Figure S 4. Experimental (top) and simulated (bottom) $^{31}P\{^{1}H\}$ NMR spectrum of **5** at 300 K in thf-d_8.

Table S 1. $^{31}P\{^{1}H\}$ NMR chemical shifts and coupling constants for **5** obtained from the simulation.

***J* (Hz)**				***δ* (ppm)**	
$^{1}J_{P_A,P_M}$	230.2	$^{1}J_{P_M,P_X}$	232.4	P_A	60.1
$^{1}J_{P_A,P_{M'}}$	233.2	$^{1}J_{P_{M'},P_X}$	226.3	P_M, $P_{M'}$	40.2
$^{2}J_{P_A,P_X}$	7.5	$^{2}J_{P_M,P_{M'}}$	0.5	P_X	-114.8

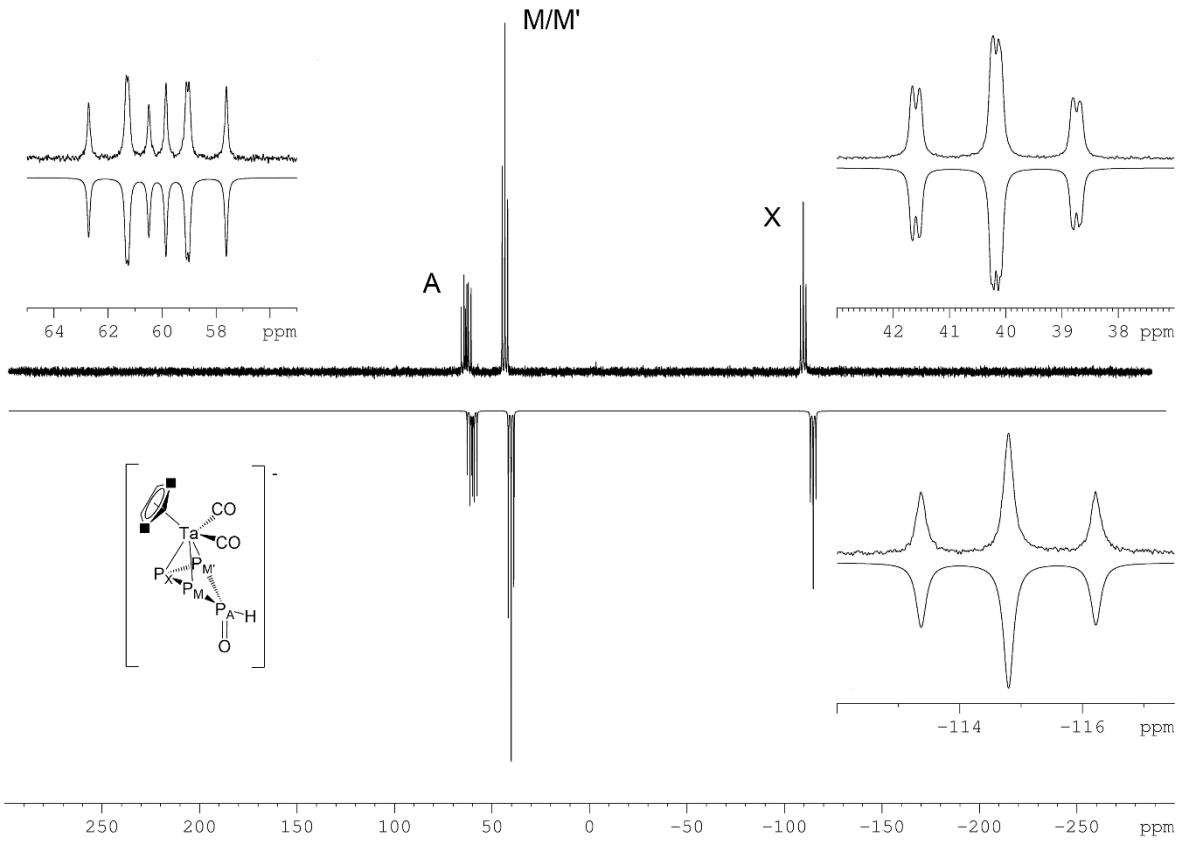

Figure S 5. Experimental (top) and simulated (bottom) ^{31}P NMR spectrum of **5** at 300 K in thf-d_8.

Table S 2. ^{31}P NMR chemical shifts and coupling constants for **5** obtained from the simulation.

***J* (Hz)**				***δ* (ppm)**	
$^1J_{P_A,P_M}$	232.2	$^1J_{P_M,P_X}$	231.6	P_A	60.1
$^1J_{P_A,P_{M'}}$	232.2	$^1J_{P_{M'},P_X}$	230.1	P_M, $P_{M'}$	40.2
$^2J_{P_A,P_X}$	3.5	$^2J_{P_M,P_{M'}}$	-4.0	P_X	-114.8
$^1J_{P_A,H}$	362.3	$^2J_{P_{M'},H}$	21.4		
$^2J_{P_M,H}$	21.0	$^3J_{P_X,H}$	4.3		

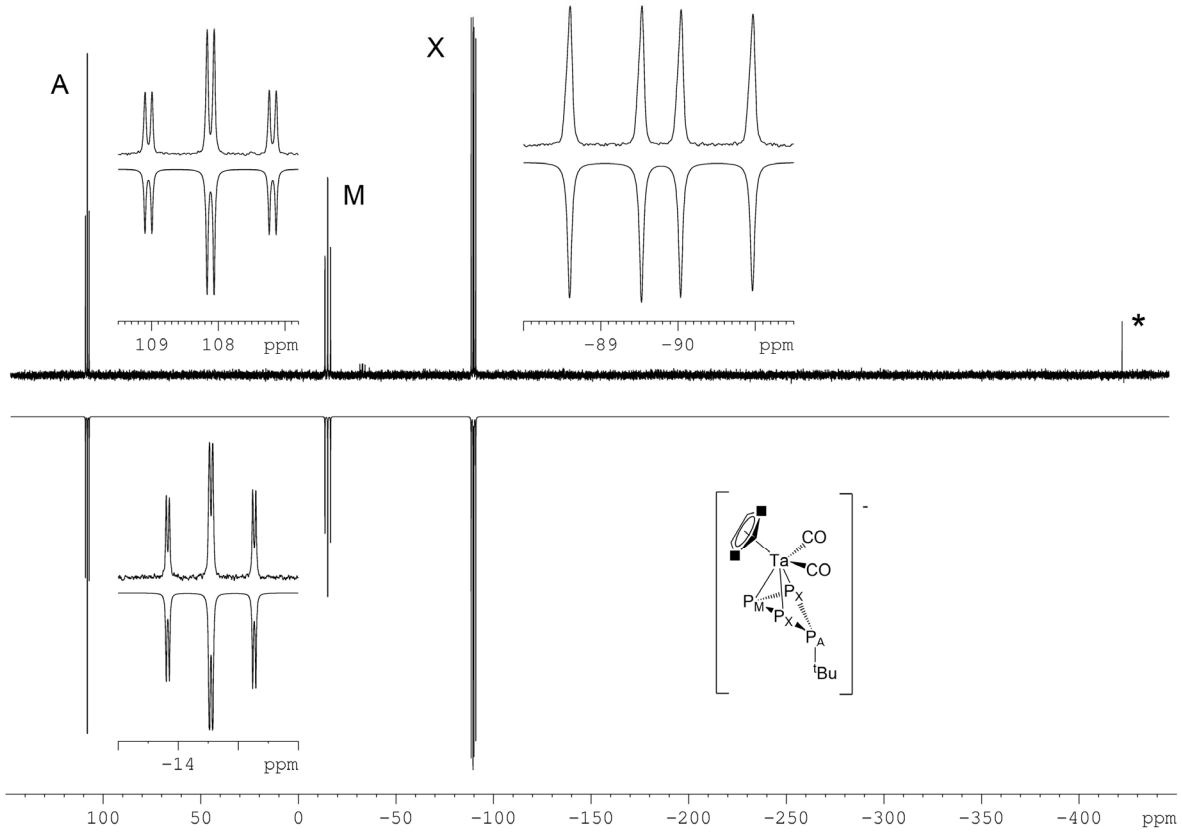

Figure S 6. Experimental (top) and simulated (bottom) $^{31}P\{^1H\}$ NMR spectrum of **6** at 300 K in thf with a C_6D_6 capillary. Impurities are marked with *.

Table S 3. ^{31}P NMR chemical shifts and coupling constants for **6** obtained from the simulation.

***J* (Hz)**		***δ* (ppm)**	
$^2J_{P_A,P_M}$	16.8	P_A	108.1
$^1J_{P_M,P_X}$	150.8	P_M	-15.1
$^1J_{P_A,P_X}$	232.9	P_X	-89.8

Details on X-ray structure determinations

All single crystal structure analyses were performed using Agilent Technologies diffractometer (GV50, TitanS2 detector) with $Cu_{K\alpha}$ radiation. Frames integration and data reduction were performed with the CrysAlisPro (Version 1.171.37.34 ([K(thf)$_4$][**3**]), 1.171.41.54a ([IDipp-H][**5**], [Li(thf)$_4$][**6**][4] software package. Using Olex2,[5] structures **5** and **6** were solved by ShelXT,[6] Structure **3** was solved with SIR97[7] and a least-square refinement on F^2 was carried out with ShelXL for all structures.[8] All non-hydrogen atoms were refined anisotropically. Hydrogen atoms at the carbon atoms were located in idealized positions and refined isotropically according to the riding model.

The images showing the compounds **3**-**6** were generated using **Olex2**.[5]

Compound 3: One CO ligand, the potassium atom and the thf molecules are disordered over two positions (56:44). The restraints SADI and SIMU were applied to describe these disorders.

Compound 5: The Cp'' ligand is disordered over two positions (80:20) and the Ta atom is disordered over two positions (58:42). The restraints SADI and SIMU were applied to describe these disorders.

Compound 6: One thf molecule is disordered over two positions (52:48) and the restraints SADI and SIMU were applied to describe these disorders.

Table S 4: Crystallographic data and detail of the compounds $[K(thf)_4][\mathbf{3}]$, [IDipp-H][**5**] and $[Li(thf)_4][\mathbf{6}]$.

Compound	$[K(thf)_4][\mathbf{3}]$	[IDipp-H][**5**]	$[Li(thf)_4][\mathbf{6}]$
File Name	FR033	FR110	FR073
CCDC			
Formula	$C_{60}H_{72}K_3Mo_6O_{16.5}P_3$	$C_{46}H_{69}N_2O_4P_4Ta$	$C_{35}H_{61}LiO_6P_4Ta$
$D_{calc.}$/ g cm^{-3}	1.768	1.366	1.426
μ/mm^{-1}	11.430	5.631	6.664
Formula Weight	1843.02	1018.86	889.60
Color	clear dark red	brown	clear light brown
Shape	plate	block	plate
Max size/mm	0.41	0.18×0.07×0.05	0.61×0.35×0.06
Mid size/mm	0.39	122.99(19)	123.00(10)
Min size/mm	0.08	orthorhombic	monoclinic
T/K	122.99(13)	*Pbca*	$P2_1/n$
Crystal System	monoclinic	19.8677(4)	11.86250(10)
Space Group	*C*2	17.9409(3)	21.7618(3)
a/Å	43.5147(8)	27.8048(6)	16.0909(2)
b/Å	7.94643(15)	90	90
c/Å	20.3986(3)	90	94.0170(10)
α/°	90	90	90
β/°	100.9442(15)	9910.9(3)	4143.65(8)
γ/°	90	8	4
V/Å^3	6925.3(2)	1	1
Z	4	1.54184	1.54184
Z'	1	Cu K_a	Cu K_a
Q_{min}/°	1.54184	3.179	3.421
Q_{max}/°	CuK_a	74.366	74.316
Measured Reflexes	2.723	50470	27131
Independent Reflexes	74.437	9939	8180
Reflections with I > 2(I)	53433	8929	7348
R_{int}	12674	0.0528	0.1071
Parameters	11748	631	488
Restraints	0.0796	220	148
Largest Peak	1116	1.476	2.009
Deepest Hole	562	-1.204	-2.103
GooF	1.066	1.176	1.031
wR2 (all data)	-0.901	0.1519	0.1366
wR2	1.046	0.1496	0.1318
R1 (all data)	0.1196	0.0825	0.0542
R1	0.1144	0.0772	0.0503
Flack Parameter	0.274(18)	-	-
Hooft Parameter	0.286(7)	-	-

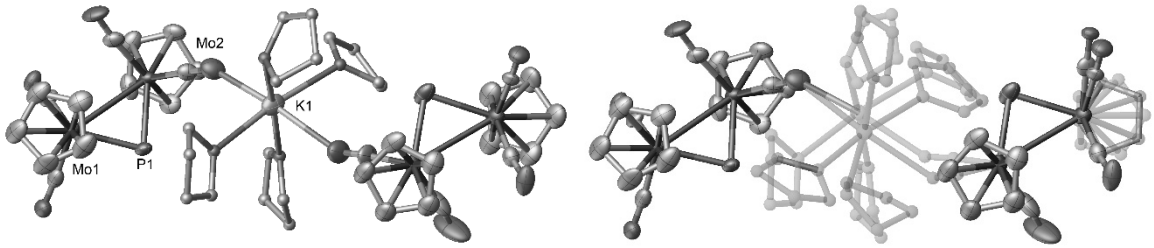

Figure S 7. Molecular structure of $[K(thf)_4][\mathbf{3}]$ in the solid state. All thf molecules are drawn in the balls and sticks model. H atoms omitted for clarity. Selected distances [Å] and angles [°]: Mo1-P1 2.375(2), Mo2-P1 2.378(2), Mo1-Mo2 3.1826(10), P1-Mo1-Mo2 48.00(6), P1-Mo2-Mo1 47.93(6), Mo1-P1-Mo2 84.07(8).

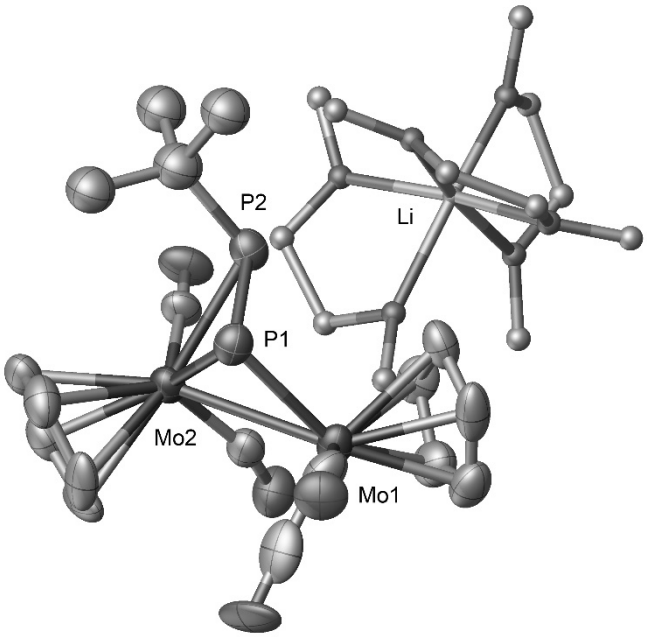

Figure S 8. Molecular structure of $[Li(dme)_3][\mathbf{4}]$ in the solid state. H atoms are omitted for clarity. However, it should be kept in mind, that the data quality of the measurement was low. Picture is shown to verify the certain atom connectivity.

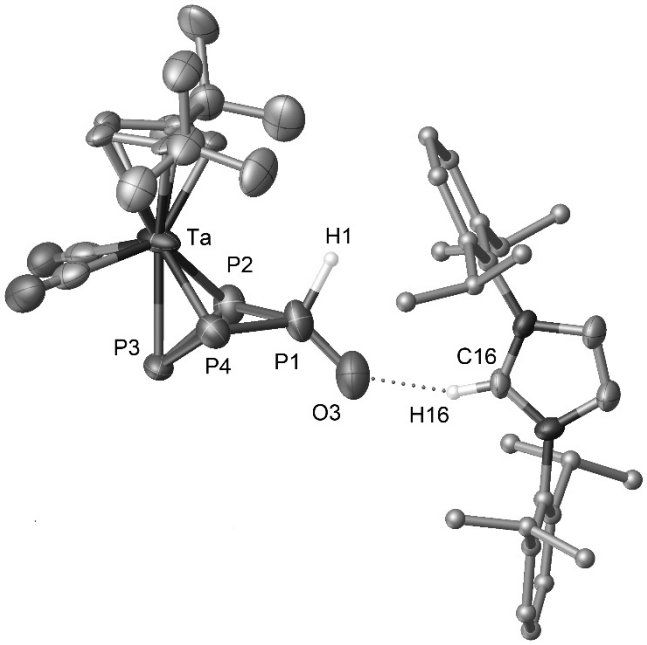

Figure S 9. Molecular structure of [IDipp-H][**5**] in the solid state. The Dipp ligands are drawn in the balls and sticks model. Except the phosphorus bound H atom and the Carbene C bound H atom, are all H atoms omitted for clarity. Selected distances [Å] and angles [°]: Ta-P2 2.447(7), Ta-P3 2.514(3), Ta-P4 2.541(5), P1-P2 2.171(3), P2-P3 2.208(3), P3-P4 2.208(3), P4-P1 2.169(3), P1-O3 1.511(7), P1-P2-P3 84.21(13), P2-P3-P4 88.11(11), P3-P4-P1 84.23(12), P4-P1-P2 90.07(12).

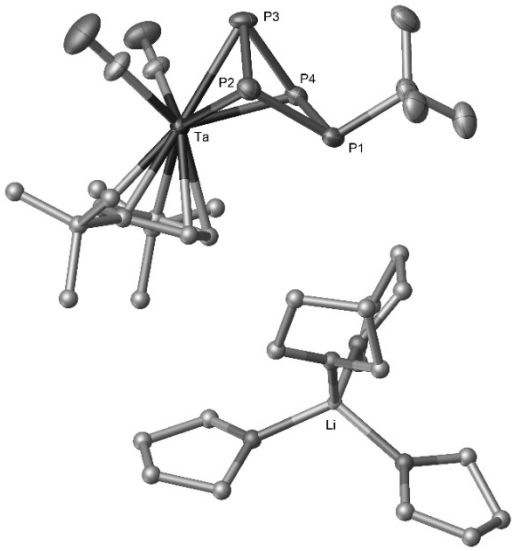

Figure S 10. Molecular structure of $[Li(thf)_4]$[**6**] in the solid state. H atoms are omitted for clarity. The Cp'' ligand, the Li atom and all thf molecules are drawn in balls and sticks model. Selected distances [Å] and angles [°]: Ta-P2 2.6046(10), Ta-P3 2.5778(9), Ta-P4 2.5971(10), P1-P2 2.2047(14), P2-P3 2.2074(14), P3-P4 2.005(14), P4-P1 2.2167(14), P1-C16 1.903(4), P1-P2-P3 91.63(5), P2-P3-P4 84.02(5), P3-P4-P1 91.50(5), P4-P1-P2 83.70(5).

References:

[1] O. J. Scherer, H. Sitzmann, G. Wolmershäuser, *J. Organomet. Chem.* **1984**, *268*, C9-C12.

[2] O. J. Scherer, R. Winter, G. Wolmershäuser, *Z. Anorg. Allg. Chem.* **1993**, *619*, 827-835.

[3] A. J. Arduengo III, R. Krafczyk, R. Schmutzler, H. A. Craig, G. Jens R, W. J. Marshall, M. Unverzagt, *Tetrahedron* **1999**, *55*, 14523-14536.

[4] CrysAlisPro Software System, Rigaku Oxford Diffraction, (**2018**).

[5] a) L. J. Bourhis, O. V. Dolomanov, R. J. Gildea, J. A. K. Howard, H. Puschmann, The Anatomy of a Comprehensive Constrained, Restrained, Refinement Program for the Modern Computing Environment - **Olex2** Disected, *Acta Cryst. A* **2015**, A71, 59–71; b) O. V. Dolomanov, L. J. Bourhis, R. J. Gildea, J. A. K. Howard, H. Puschmann, Olex2: A complete structure solution, refinement and analysis program, *J. Appl. Cryst.* **2009**, 42, 339–341.

[6] G. M. Sheldrick, ShelXT-Integrated space-group and crystal-structure determination, *Acta Cryst.* **2015**, A71, 3–8.

[7] Burla *et al.*, **2007**.

[8] G. M. Sheldrick, Crystal structure refinement with ShelXL, *Acta Cryst.* **2015**, C71, 3–8.

5. Functionalization of [Cp*Fe(η^5-P_5)] by successive Reactions with Main Group Nucleophiles and Electrophiles containing Functional Groups

Felix Riedlberger, Michael Seidl and Manfred Scheer

- All compounds were synthesized and characterized by Felix Riedlberger.
- The manuscript was written by Felix Riedlberger.
- Figures were made by Felix Riedlberger.
- X-ray structure analyses and refinements were performed by Felix Riedlberger and finally checked by Michael Seidl.

5.1 Introduction

Abstract: *The reactions of different nucleophiles with [Cp*Fe(η^5-P_5)] (**1**) (Cp* = pentamethylcyclopentadienyl) and the subsequent reactions with electrophiles are reported. The reaction of **1** and deprotonated ethynylbenzene or doubly deprotonated 1,4-diethynylbenzene gives the anionic complexes [(Cp*Fe(η^4-P_5≡-Ph)]$^-$ (**2a**) and [(Cp*Fe(η^4-P_5))$_2$(≡-C_6H_4-≡)]$^{2-}$ (**2b**), respectively. Compounds [(Cp*Fe(η^4-P_5CH_2Ph)]$^-$ (**3a**) and [(Cp*Fe(η^4-P_5CHPh_2)]$^-$ (**3b**) can be obtained by the reaction of **1** with KCH_2Ph or $KCHPh_2$, respectively. Further functionalization of **3a** was possible with the electrophile MeI to yield the neutral iron complex [(Cp*Fe(η^4-P_5(Me)CH_2Ph)] (**4**) with a distorted cyclo-P_5 ring. The anionic complex [(Cp*Fe(η^4-P_5Me)]$^-$ (**1**) was reacted with different electrophiles (^{n}BuBr, ^{i}PrI, $Br(CH_2)_3Br$ and $Br(CH_2)_3Br$) to yield the neutral iron complexes [Cp*Fe(η^4-P_5(R)Me)] (R = ^{i}Pr (**5a**), ^{n}Bu (**5b**), $(CH_2)_3Br$ (**5c**), $(CH_2)_4Br$ (**5d**)).*

White phosphorus is the starting material for numerous different reactions to yield organophosphorus derivatives.[1] Usually it is halogenated to PCl_3 and the chlorine substituents are further replaced by organic groups, which leads to stochiometric amount of waste (HCl, LiCl).[2] Another approach to organophosphorus derivatives is the coordination of polyphosphorus units to transition metals and the subsequent functionalization. One special compound for this purpose is pentaphosphaferrocene [Cp*Fe(η^5-P_5)] (**1**) (Cp* = pentamethylcyclopentadienyl) which was discovered in 1987 by Scherer *et al.*.[3] The reactivity of **1** was widely investigated. Especially, the coordination chemistry of **1** towards copper halides is remarkable which results in the formation of 1D, 2D polymers[4] or even larg spherical aggregates with fullerene-like structure.[5] The redox chemistry of pentaphosphaferrocene was investigated via cyclovoltammetry by Winter and Geiger.[6] Later, these predicted complexes *i.e.* the dication [(Cp*Fe)$_2$(μ,$\eta^{4:4}$-P_{10})]$^{2+}$ and the dianion [(Cp*Fe)$_2$(μ,$\eta^{4:4}$-P_{10})]$^{2-}$ as well as the monomeric dianion [(Cp*Fe(η^4-P_5)]$^{2-}$ were synthesized and characterized by our group.[7] In these complexes the P_5 ligand shows a distorted, envelope-like conformation. Furthermore, complexes containing envelope-like *cyclo*-P_5 rings can be synthesized via the reaction of **1** with main group nucleophiles, such as $LiCH_2SiMe_3$ and $LiNMe_2$.[8] Until now, only nucleophiles which do not contain any functional groups were reacted with **1**. However, nucleophiles that can be further functionalized, or possess a functional group would be of special interest for the functionalization of **1**. Our group already showed that complexes of the type [(Cp*Fe(η^4-P_5R)]$^-$ (R = organic residue) react towards the organic electrophile MeI.[9] The resulting neutral complexes [(Cp*Fe(η^4-P_5(R')R)] (R = nucleophile, R' = electrophile) exhibit a four times substituted phosphorus atom. Nevertheless, only methylated compounds were fully characterized and reactivity studies of electrophiles with a functional group are missing. Herein, we report the reactivity of pentaphosphaferrocene towards nucleophiles that can be further functionalized, such as phenylethyn-1-ide and 1,4-phenylenebis(ethyn-1-ide) and the subsequent reactions towards electrophiles.

5.2 Results and Discussion

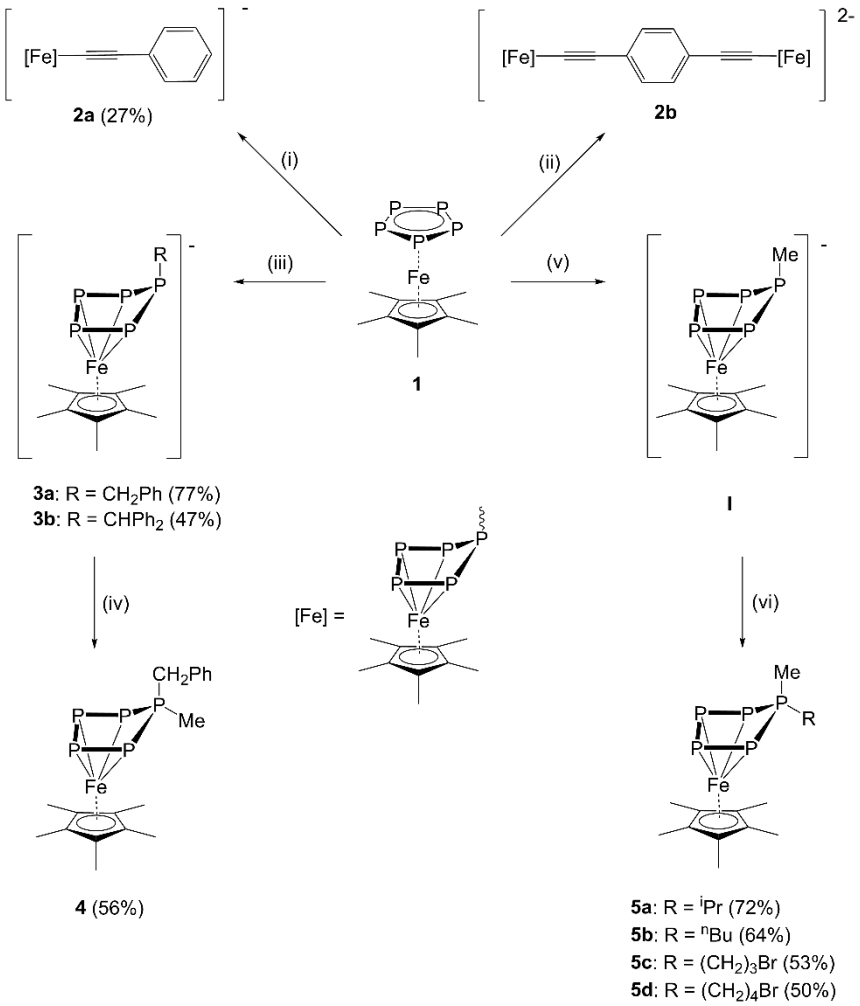

Scheme 1. Reaction of **1**: (i) ethynylbenzene, KCH_2Ph in thf, -78° C → r.t; (ii) 1,4-diethynylbenzene, KCH_2Ph in thf, -78°C → r.t; (iii) KCH_2Ph or $KCHPh_2$ in thf, -78°C → r.t; (v) LiMe in dme, -78°C → r.t.; reaction of **3a**: (iv) MeI in thf, r.t.; reaction of **I**: (vi) isopropyl iodide, 1-bromobutane, 1,3-dibromopropane or 1,4-dibromobutane in dme, r.t; yields are given in parenthesis.

When ethynylbenzene or 1,4-diethynylbenzene is deprotonated with benzyl potassium and added to a solution of **1** in thf a color change from green to brown is observed. The $^{31}P\{^1H\}$ NMR spectra of the reaction solutions of the resulting products **2a** and **2b** show an ABB'XX' spin system with resonances centered at 37.3, 27.9 and -58.4 ppm and at 35.8, 27.1 and -26.9 ppm, respectively (Scheme 1). Crystals of **2a**,**b** are obtained from a concentrated thf solution layered with *n*-hexane. Single crystal X-ray diffractions of **2a** and **2b** reveal their molecular structure in the solid state (Figure 1). The main feature of the structure of **2a** is a P_5 ring in an envelope conformation which coordinates η^4 to the Cp*Fe fragment and to which a phenylethinyl unit is bound. In the solid state structure of **2b** the two Cp^*FeP_5 units are bridged by a 1,4-phenylenebis(ethynyl) substituent (Figure 1). All P-P bonds are in the expected range and reveal double bond character with an average P-P bond length of 2.152 Å in **2a** and 2.148 Å in **2b**.[10]

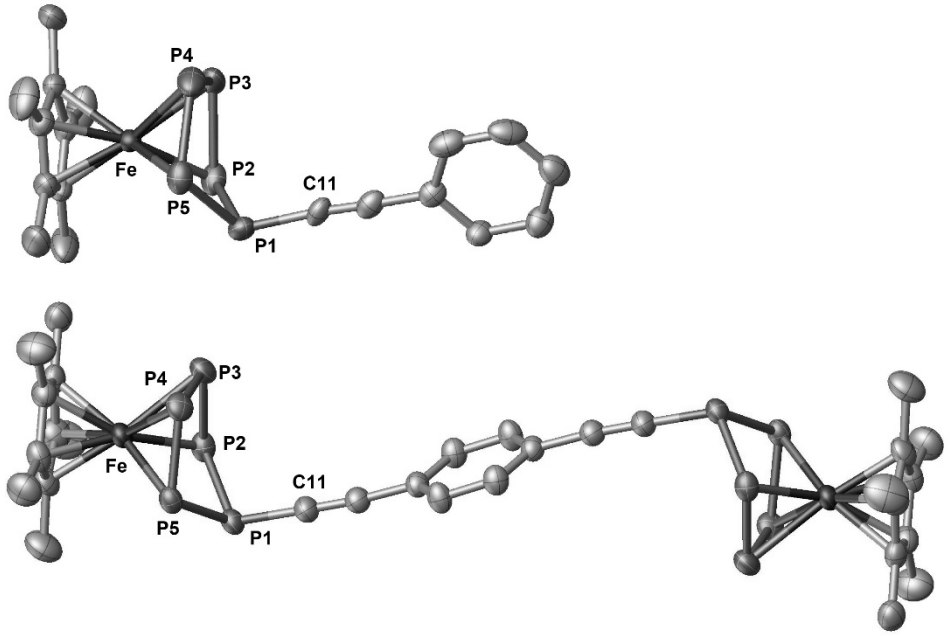

Figure 1. Molecular structure of **2a** (top) and **2b** (bottom). Hydrogen atoms, cations, 18c-6 and solvent molecules are omitted for clarity. Anisotropic displacement parameters are set to 50% probability. Selected bond lengths (Å) and angles (°): For **2a**: P1-P2 2.142(5), P1-P5 2.162(3), P2-P3 2.187(3), P3-P4 2.127(4), P4-P5 2.142(3), P1-C11 1.782(7), Fe1-P2 2.322(3), Fe1-P3 2.312(2), Fe1-P4 2.338(2), Fe1-P5 2.317(2); P5-P1-P2 93.56(16), P3-P2-P1 107.09(16), P4-P3-P2 103.14(13), P3-P4-P5 103.82(11), P4-P5-P1 107.18(14). For **2b**: P1-P2 2.170(2), P1-P5 2.1711(16), P2-P3 2.1341(14), P3-P4 2.1490(15), P4-P5 2.1410(19), P1-C11 1.775(3), Fe1-P2 2.2631(12), Fe1-P3 2.3383(8), Fe1-P4 2.3832(13), Fe1-P5 2.3616(11); P5-P1-P2 92.37(6), P3-P2-P1 106.96(7), P4-P3-P2 103.30(6), P3-P4-P5 103.28(8), P4-P5-P1 107.16(6).

The synthesis of analytically pure **2b** is very challenging. The deprotonation of 1,4-diethynylbenzene is in most cases not complete and mono-deprotonated 1,4-diethynylbenzene ((4-ethynyphenyl)ethyn-1-ide) still remains in the reaction mixture, and cannot be separated from the di-deprotonated species. In the $^{31}P\{^{1}H\}$ NMR spectra of the reaction mixture are two species with almost identical chemical shifts (Figure 2). For the simulation of the $^{31}P\{^{1}H\}$ NMR spectrum two fragments with each five phosphorus atoms was used in a ratio of 68:32. An unambiguous assignment of signals in the $^{31}P\{^{1}H\}$ NMR spectrum to the two complexes **2b** and $[Cp^*Fe(\eta^4\text{-}P_5\text{-}\equiv\text{-}C_6H_4\text{-}\equiv\text{-}H)]^-$ is not possible. Due to the pronounced instability of **2b**, it could not be isolated in manageable amounts and therefore it is only characterized in the reaction solution. After many attempts of crystallization, we obtained in one case few single crystals of **2b** which allowed its characterization by single crystal X-ray diffractions.

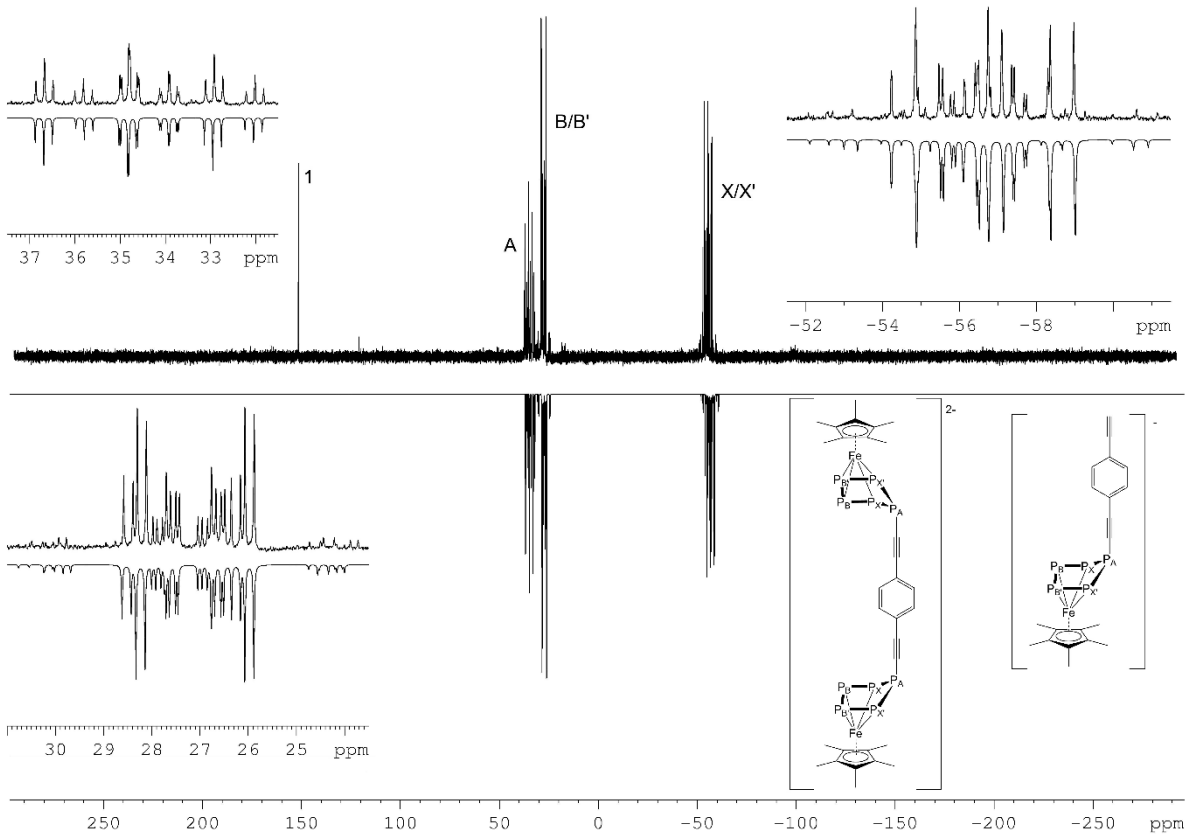

Figure 2. Experimental (top) and simulated (bottom) $^{31}P\{^{1}H\}$ NMR spectrum of **2b** and $[Cp^*Fe(\eta^4\text{-}P_5\equiv\text{-}C_6H_4\text{-}\equiv)]^-$ in thf with a C_6D_6 capillary at 300 K. The signal at 150 ppm corresponds to unreacted **1**.

An immediate color change from green to brown is observed when KCH_2Ph or $KCHPh_2$ is added to a solution of **1** in thf at -78°C, indicating the formation of **3a** and **3b**, respectively (Scheme 1). Compounds **3a** and **3b** can be isolated in good yields by layering a concentrated solution with *n*-hexane. The $^{31}P\{^{1}H\}$ NMR spectra of the isolated compounds **3a** and **3b** show an AMM'XX' spin-system with three distinct sets of signals centered at 89.7, 18.4 and -73.0 ppm and at 103.8, 17.6 and -63.3 ppm, respectively. The molecular structures of **3a**,**b** obtained by single crystal X-ray diffractions reveal an envelope-like P_5 ring, similar to compounds **2a**,**b** to which the nucleophiles are attached (Figure 3). The average P-P distances are 2.145 Å in **3a** and 2.153 Å in **3b**, respectively, indicating double bond character for all P-P bonds. The other geometrical parameters are unexceptional.

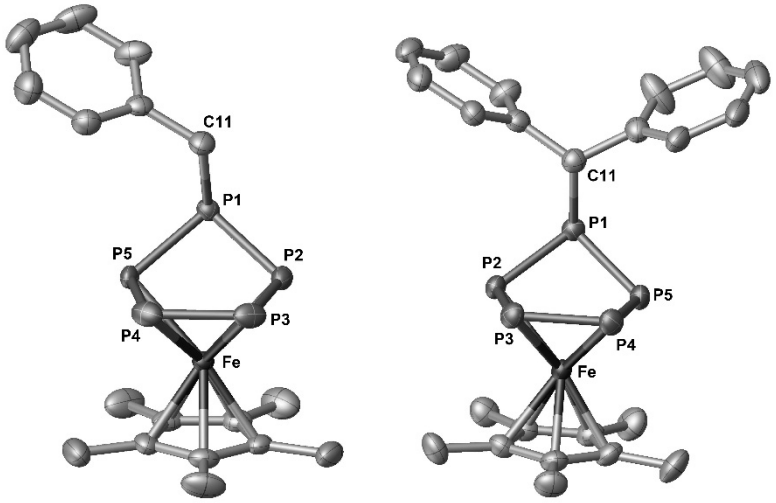

Figure 3. Molecular structure in the solid state of **3a** (left) and **3b** (right). Hydrogen atoms, cations, 18c-6 and solvent molecules are omitted for clarity. Anisotropic displacement parameters are set to 50% probability. Selected bond lengths (Å) and angles (°): For **3a**: P1-P2 2.145(8), P1-P5 2.162(7), P2-P3 2.176(7), P3-P4 2.111(7), P4-P5 2.130(7), P1-C11 1.844(7), Fe1-P2 2.349(6), Fe1-P3 2.319(5), Fe1-P4 2.307(6), Fe1-P5 2.306(5); P5-P1-P2 93.0(3), P3-P2-P1 105.8(3), P4-P3-P2 103.5(3), P3-P4-P5 103.7(3), P4-P5-P1 106.7(3). For **3b**: P1-P2 2.1657(8), P1-P5 2.1671(8), P2-P3 2.1514(8), P3-P4 2.1329(8), P4-P5 2.1502(8), P1-C11 1.900(2), Fe1-P2 2.3098(6), Fe1-P3 2.3333(6), Fe1-P4 2.3432(6), Fe1-P5 2.3180(6); P5-P1-P2 91.88(3), P3-P2-P1 106.37(3), P4-P3-P2 103.23(3), P3-P4-P5 103.12(3), P4-P5-P1 106.77(3).

As it was shown earlier by our group, complexes of the type $[Cp^*Fe(\eta^4\text{-}P_5R)]^-$ (R = CH_2SiMe_3, NMe_2, Me) possess nucleophilic character and are able to react with small electrophiles like MeI leading to the alkylated species.[9] The so formed neutral complexes contain an envelope-like P_5 ring and a double substituted phosphorus atom. The sterical demand of the nucleophile as well as of the electrophile plays a crucial role in these reactions, even preventing in some cases the reaction. Since only reactions of MeI as electrophile with $[Cp^*Fe(\eta^4\text{-}P_5R)]^-$ have been reported, the question arose, if also other electrophiles can be used and if these electrophiles can possess functional groups.

The reaction of **3a** in thf with MeI do not leads to a color change but the $^{31}P\{^1H\}$ NMR spectrum of the reaction solution show a complete conversion to the new product **4** with the three corresponding multiplets of an AMM'XX' spin system centered at 119.7, 36.0 and -123.4 ppm. Crystalline **4** could be obtained from a saturated solution in *n*-hexane at -30°C. The molecular structure of **4** could be determined by X-ray diffractions (Figure 4). It shows an envelope-like P_5 ring η^4 coordinated to the Cp*Fe fragment. To the phosphorus atom, which do not bound to iron, the CH_2Ph group is attached in *endo*-position and the methyl group in *exo*-position (Figure 4). The P-P bond lengths range between 2.1214(11) Å and 2.1437(11) Å and are in the range of P-P double bonds. The P-C distances are

1.815(3) Å to the C atom in *exo*-position and 1.840(3) Å to the C atom in *endo*-position and corresponds as single bonds.

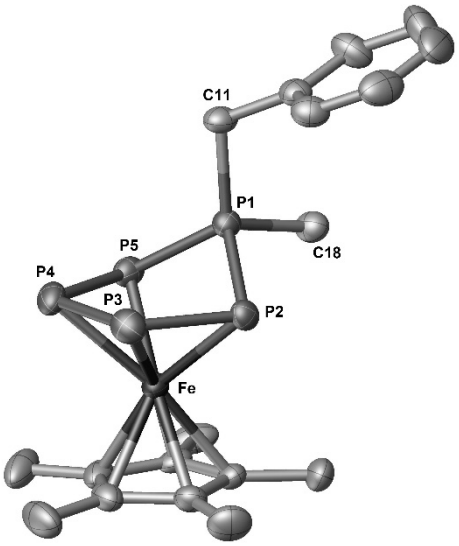

Figure 4. Molecular structure in the solid state of **4**. Hydrogen atoms are omitted are omitted for clarity. Anisotropic displacement parameters are set to 50% probability. Selected bond lengths (Å) and angles (°): P1-P2 2.1429(10), P1-P5 2.1307(10), P2-P3 2.1214(11), P3-P4 2.1437(11), P4-P5 2.1375(11), P1-C11 1.840(3), P1-C18 1.18158(3), Fe1-P2 2.3167(8), Fe1-P3 2.3391(8), Fe1-P4 2.3325(8), Fe1-P5 2.3290(8); P5-P1-P2 99.68(4), P3-P2-P1 100.35(4), P4-P3-P2 105.23(4), P3-P4-P5 105.33(4), P4-P5-P1 100.18(4).

The reactivity of the anionic complex $[Cp^*Fe(\eta^4\text{-}P_5Me)]^-$ (**I**) towards MeI leading to the neutral complex $[Cp^*Fe(\eta^4\text{-}P_5(Me)Me)]$ has been reported. To investigate the reactivity of **I** towards more bulky electrophiles or di-halogen-alkanes. We reacted **I** with isopropyl iodide, 1-bromobutane, 1,3-dibromopropane and 1,4-dibromobutane. To a solution of **1** in dme the corresponding RX was added and a slightly color change from dark greenish brown to dark reddish brown was observed. After work-up, compounds **5a-d** can be isolated in good crystalline yield from a saturated *n*-hexane solution (Scheme 1). The $^{31}P\{^1H\}$ NMR spectra of compounds **5a-d** show three distinct multiplets of an AMM'XX' spin system (Table 1). The chemical shift for the $P_M/P_{M'}$ atoms and the $P_X/P_{X'}$ atoms are almost identical. The biggest difference for the chemical shift of the P_A atoms is for complex **5a**, which could be explained by the strong +I effect of the isopropyl group and the therefore resulting in a downfield shift.

Table 1. $^{31}P\{^{1}H\}$ NMR shifts of complexes **5a-d**.

δ (ppm)	P_A	$P_M/P_{M'}$	$P_X/P_{X'}$
5a	152.0	33.3	-135.8
5b	132.3	32.2	-130.1
5c	128.9	32.0	-130.3
5d	130.7	32.0	-130.9

Single crystals X-ray structure determinations were carried out for all compounds **5a-d**. The molecular structures reveal an envelope-like P_5 ring, similar to their starting material **I**, with the electrophile attached to the phosphorus atom P1 (Figure 5). All P-P bonds are in the range of phosphorus double bonds with bond length between 2.119(9) Å and 2.155(3) Å (Table 2). The outstanding feature of **5c** and **5d** is the presence of the bromine in the side chain, which potentially allows the further functionalization and derivatization.

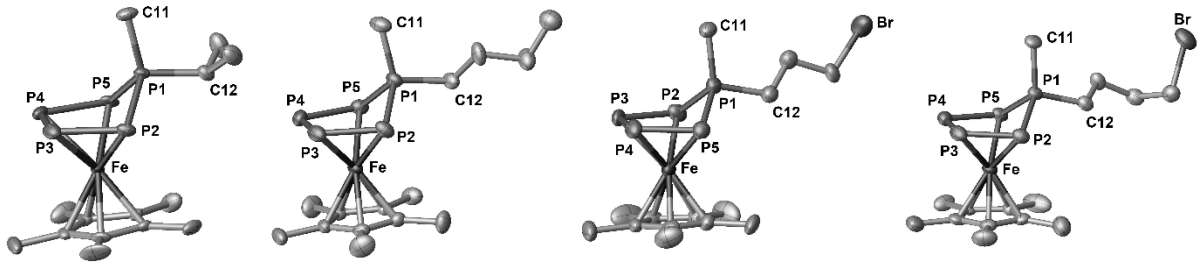

Figure 5. Molecular structure in the solid state of **5a** (left), **5b** (second from left), **5c** (second from right) and **5d** (right). Hydrogen atoms are omitted for clarity. Anisotropic displacement parameters are set to 50% probability. Selected bond lengths (Å) and angles (°): For **5a**: P1-P2 2.142(2), P1-P5 2.1472(19), P2-P3 2.132(2), P3-P4 2.155(3), P4-P5 2.145(2), P1-C11 1.821(6), P1-C12 1.843(6), Fe1-P2 2.3166(15), Fe1-P3 2.3342(17), Fe1-P4 2.3371(17), Fe1-P5 2.3168(16); P5-P1-P2 97.89(8), P3-P2-P1 98.79(9), P4-P3-P2 105.04(9), P3-P4-P5 104.20(8), P4-P5-P1 98.95(9). For **5b**: P1-P2 2.144(3), P1-P5 2.133(2), P2-P3 2.1341(14), P3-P4 2.134(3), P4-P5 2.141(3), P1-C11 1.829(6), P1-C12 1.833(6), Fe1-P2 2.304(3), Fe1-P3 2.3285(16), Fe1-P4 2.361(3), Fe1-P5 2.3359(17); P5-P1-P2 98.62(11), P3-P2-P1 99.53(13), P4-P3-P2 105.01(11), P3-P4-P5 104.80(13), P4-P5-P1 99.37(12). For **5c**: P1-P2 2.142(3), P1-P5 2.129(3), P2-P3 2.119(9), P3-P4 2.143(11), P4-P5 2.147(4), P1-C11 1.817(8), P1-C12 1.842(9), Fe1-P2 2.317(4), Fe1-P3 2.320(8), Fe1-P4 2.355(3), Fe1-P5 2.322(2); P5-P1-P2 98.89(14), P3-P2-P1 99.1(3), P4-P3-P2 106.0(3), P3-P4-P5 103.9(2), P4-P5-P1 99.49(14). For **5d**: P1-P2 2.1404(13), P1-P5 2.1419(13), P2-P3 2.1394(18), P3-P4 2.1511(16), P4-P5 2.1335(17), P1-C11 1.823(4), P1-C12 1.825(5), Fe1-P2 2.3319(11), Fe1-P3 2.3241(12), Fe1-P4 2.3406(14), Fe1-P5 2.3279(10); P5-P1-P2 99.10(5), P3-P2-P1 100.18(6), P4-P3-P2 105.16(6), P3-P4-P5 104.88(7), P4-P5-P1 100.19(6).

5.3 Conclusion and References

In summary, the nucleophiles KCH_2Ph and $KCHPh_2$ were used to create the anionic *cyclo*-P_5 iron complexes $[Cp^*Fe(\eta^4\text{-}P_5CH_2Ph)]^-$ (**3a**) and $[Cp^*Fe(\eta^4\text{-}P_5CHPh_2)]^-$ (**3b**), respectively. With the knowledge that these anionic iron complexes react with small organic halides like MeI $[Cp^*Fe(\eta^4\text{-}P_5(Me)CH_2Ph)]$ (**4**) was synthesized. The attempt to synthesize bigger molecules with more than one pentaphosphaferrocene unit was quite difficult. The reactions of deprotonated ethynylbenzene and doubly deprotonated 1,4-diethynylbenzene with $[Cp^*Fe(\eta^5\text{-}P_5)]$ (**1**) yield the novel compounds $[Cp^*Fe(\eta^4\text{-}P_5\text{-}C{\equiv}\text{-}Ph)]^-$ (**2a**) and $[(Cp^*Fe(\eta^4\text{-}P_5))_2(\equiv\text{-}C_4H_6\text{-}\equiv)]^{2-}$ (**2b**), respectively. A total deprotonation of 1,4-diethynylbenzene is very important to obtain the exclusive formation of the desired compound **2b**. However, complexes **2a**,**b** are interesting starting materials due to their carbon carbon triple bonds and can probably be used in organic synthesis. The knowledge of the reported reactivity of the anionic complex $[Cp^*Fe(\eta^4\text{-}P_5Me)]^-$ (**I**) towards organic nucleophiles gives access to novel functionalized compounds $[Cp^*Fe(\eta^4\text{-}P_5(R)Me)]$ (R = ^{i}Pr (**5a**), ^{n}Bu (**5b**), $(CH_2)_3Br$ (**5c**), $(CH_2)_4Br$ (**5d**)). One phosphorus atom of the *cyclo*-P_5 ligand is functionalized twice. Especially compound **5c** and **5d** with a bromine functionality are interesting starting materials for further reactions like Grignard reaction or nucleophilic attack, to produce longer organic chains, unusual ring systems or groups that can subsequent substituted. Nevertheless, a wide range of different nucleophiles and electrophiles where used to discover more and understand better the reactivity of **1** towards these ionic groups of compounds.

References:

[1] a) B. M. Cossairt, C. C. Cummins, *New J. Chem.* **2010**, *34*, 1533; b) A. R. Fox, R. J. Wright, E. Rivard, P. P. Power, *Angew. Chem. Int. Ed.* **2005**, *44*, 7729-7733; c) R. Riedel, H.-D. Hausen, E. Fluck, *Angew. Chem. Int. Ed.* **1985**, *24*, 1056-1057.

[2] D. E. C. Corbridge, *Phosphorus. Chemistry, Biochemistry and Technology*, Taylor & Francis Group, Boca Raton, FL, **2013**.

[3] O. J. Scherer, T. Brück, *Angew. Chem. Int. Ed.* **1987**, *26*, 59-59.

[4] a) M. Scheer, L. J. Gregoriades, A. V. Virovets, W. Kunz, R. Neueder, I. Krossing, *Angew. Chem. Int. Ed.* **2006**, *45*, 5689-5693; b) J. Bai, A. V. Virovets, M. Scheer, *Angew. Chem. Int. Ed.* **2002**, *41*, 1737-1740.

[5] a) S. Welsch, C. Groger, M. Sierka, M. Scheer, *Angew. Chem. Int. Ed.* **2011**, *50*, 1435-1438; b) T. Li, J. Wiecko, N. A. Pushkarevsky, M. T. Gamer, R. Köppe, S. N. Konchenko, M. Scheer, P. W. Roesky, *Angew. Chem. Int. Ed.* **2011**, *50*, 9491-9495; c) M. Scheer, A. Schindler, J. Bai, B. P. Johnson, R. Merkle, R. Winter, A. V. Virovets, E. V. Peresypkina, V. A. Blatov, M. Sierka, H. Eckert, *Chem. Eur. J.* **2010**, *16*, 2092-2107; d) M. Scheer, A. Schindler, C. Groger, A. V. Virovets, E. V. Peresypkina, *Angew. Chem. Int. Ed.* **2009**, *48*, 5046-5049; e) M. Scheer, A. Schindler, R. Merkle, B. P. Johnson, M. Linseis, R. Winter, C. E. Anson, A. V. Virovets, *J. Am. Chem. Soc.* **2007**, *129*, 13386-13387; f) M. Scheer, J. Bai, B. P. Johnson, R. Merkle, A. V. Virovets, C. E. Anson, *Eur. J. Inorg. Chem.* **2005**, *2005*, 4023-4026; g) J. Bai, A. V. Virovets, M. Scheer, *Science* **2003**, *300*, 781-783.

[6] R. F. Winter, W. E. Geiger, *Organometallics* **1999**, *18*, 1827-1833.

[7] M. V. Butovskiy, G. Balázs, M. Bodensteiner, E. V. Peresypkina, A. V. Virovets, J. Sutter, M. Scheer, *Angew. Chem. Int. Ed.* **2013**, *52*, 2972-2976.

[8] E. Mädl, M. V. Butovskii, G. Balázs, E. V. Peresypkina, A. V. Virovets, M. Seidl, M. Scheer, *Angew. Chem. Int. Ed.* **2014**, *53*, 7643-7646.
[9] E. Mädl, Investigations of the reactivity of selected Pn ligand complexes. *Dissertation*, Universität Regensburg, **2016**.
[10] P. Pyykkö, M. Atsumi, *Chem. Eur. J.* **2009**, *15*, 12770-12779.

5.4 Supporting Information

Experimental details: complex syntheses and characterization

General procedures: All manipulations were performed with rigorous exclusion of oxygen and moisture in Schlenk-type glassware on a dual manifold Schlenk line in Argon atmosphere or in Argon filled glove box with a high-capacity recirculator (<0.1 ppm O_2). Toluene thf, dme and *n*-hexane were dried using conventional techniques, degassed and saturated with Argon. Deuterated solvents were degassed, dried and distilled prior to use. The complexes [Cp*Fe(η^5-P_5)][1] (**1**) and [Cp*Fe(η^4-P_5Me)]$^-$[2] (**I**) and were prepared according to its published procedure. NMR spectra were recorded on a Bruker Avance 300 MHz and Bruker Avance 400 MHz spectrometers. Chemical shifts are given in ppm; they are referenced to TMS for ^{1}H and ^{13}C, and 85% H_3PO_4 for ^{31}P as external standard. Elemental analyses (CHN) were determined using in-house facility.[3]

Synthesis of [K(18c-6)(thf)][2a], [2a] = [Cp*Fe(η^4-P_5-≡-Ph)]$^-$: 0.18 mL of a stock solution of ethynylbenzene (c = 0.828 mol·L^{-1}) in thf was added to 18.9 mg (0.145 mmol) benzyl potassium in thf and the color was changed from red to colorless. Afterwards this solution was added to a solution of 50 mg (0.145 mmol) [Cp*Fe(η^5-P_5)] (**1**) at -78°C to obtain a color change from green to brown. The solution was slowly warmed up to ambient temperatures. All volatiles were removed in vacuum and the brown residue was washed three times with 10 mL *n*-hexane. 38 mg (144 mmol) 18c-6 was dissolved in thf 5 mL, added to the brown residue, layered with 20 mL *n*-hexane and stored at 4°C. After two weeks metallic dark green blocks of [K(18c-6)(thf)][Cp*Fe(η^4-P_5)-≡-Ph)] (32 mg, 0.0389 mmol, 27% yield) were formed.

^{1}H NMR (thf-d_8, 300 K): δ [ppm] = 6.97 (m, 5H, Ph), 1.49 (s, 15H, Cp*).

^{31}P{^{1}H} NMR (thf-d_8, 300 K): δ [ppm] = 37.3 (m, 1P), 27.9 (m, 2P), -58.4 (m, 2P). For coupling constants see Table S 1.

Synthesis of [K(18c-6)(thf)$_2$)]$_2$[2b], [2b] = [(Cp*Fe(η^4-P_5))$_2$(≡-C_6H_4-≡)]$^{2-}$: A solution of 75 mg (0.576 mmol) benzyl potassium in thf was added to 36.5 mg (0.289 mmol) 1,4-diethynylbenzene in thf. The red color of the benzyl potassium solution vanished and the resulting colorless, dreary solution was stirred for one hour. This solution was added to 200 mg (0.578 mmol) of [Cp*Fe(η^5-P_5)] (**1**) in thf at -78°C to obtain a color change from green to brown. The solution was slowly warmed up to ambient temperatures. All volatiles were removed in vacuum and the resulting brownish residue washed with 10 mL *n*-hexane three times. A solution of 152 mg (0.575 mmol) 18c-6 was dissolved in 3 mL thf, added to the brown residue and layered with 10 mL *n*-hexane. After three weeks at 4°C dark brown plates of [K(18c-6)(thf)$_2$][(Cp*Fe(η^4-P_5))$_2$(≡-C_6H_4-≡)] (a few crystals) could be isolated.

^{1}H NMR (thf-d_8, 300 K): δ [ppm] = 7.25 (m, 4H, Ph), 1.46 (s, 15H, Cp*).

^{31}P{^{1}H} NMR (thf/C_6D_6 capillary, 300 K): δ [ppm] = 34.8 (m, 1P), 27.1 (m, 2P), -56.9 (m, 2P). For coupling constants see Figure S 2.

Synthesis of [K(18c-6)][3a], [3a] = [Cp*Fe(η^4-P$_5$CH$_2$Ph)]$^-$: 100 mg (0.289 mmol) of **1** were dissolved in 5 mL thf and a solution of 37 mg (0.284 mmol) of benzyl potassium in thf was added at -78°C. After warming up to ambient temperature overnight, all volatiles were removed in vaccum and the brownish residue was washed with 10 mL *n*-hexane three times. A solution of 65 mg (0.245 mmol) 18c-6 was dissolved in 3 mL thf and was added to the brownish residue and layered with 10 mL *n*-hexane. After two weeks dark brown blocks of [K(18c-6)][Cp*Fe(η^4-P$_5$CH$_2$Ph)] (164 mg, 0.222 mmol, 77% yield) could be isolated.

^{1}H NMR (thf-d_8, 300 K): δ [ppm] = 6.84 (m, 5H, Ph), 3.64 (s, 24H, [K(18c-6)]), 1.48 (s, 15H, Cp*), 1.10 (s, 2H, CH_2).

^{31}P{^{1}H} NMR (thf-d_8, 300 K): δ [ppm] = 89.7 (m, 1P), 18.4 (m, 2P), -73.0 (m, 2P). For coupling constants see Table S 3.

EA calculated for $C_{17}H_{22}FeKP_5$ (476.17 g·mol^{-1}): C: 42.88, H: 4.66; found [%]: C: 42.30, H: 4.53.

Synthesis of [K(thf)$_2$][3b], [3b] = [Cp*Fe(η^4-P$_5$CHPh$_2$)]$^-$: At -78°C a solution of $KCHPh_2$ 59 mg (0.286 mmol) in 5 mL thf was added to a solution of 100 mg (0.289 mmol) **1** in 7 mL thf. The color of the solution turned from green to brown. After slowly warming up to ambient temperature all volatiles were removed, the resulting brownish residue was washed with 10 mL *n*-hexane, dissolved in 4 mL thf and layered with 15 mL *n*-hexane. After ten days dark brown blocks of [K(thf)$_2$][Cp*Fe(η^4-P$_5$CHPh$_2$)] (95 mg, 0.136 mmol, 47% yield) can be isolated.

^{1}H NMR (thf-d_8, 300 K): δ [ppm] = 6.99 (m, 10H, Ph), 1.78 (s, 1H, $CHPh_2$), 1.48 (s, 15H, Cp*).

^{31}P{^{1}H} NMR (thf-d_8, 300 K): δ [ppm] = 103.8 (m, 1P), 17.6 (m, 2P), -63.3 (m, 2P). For coupling constants see Table S 4.

EA calculated for $C_{27}H_{34}FeKOP_5$ (624.37 g·mol^{-1}): C: 51.93, H: 5.48; found [%]: C: 52.09, H: 5.08.

Synthesis of [4], [4] = [Cp*Fe(η^4-P$_5$(Me)CH$_2$Ph)]: 300 mg (0.513 mmol) [K(thf)$_{1.5}$][Cp*Fe(η^4-P$_5$CH$_2$Ph)] (**3a**) were dissolved in thf and 0.45 mL MeI in Et_2O (c = 1.11 mol·L^{-1}, 0.500 mmol) was added slowly. After stirring for 18 hours, the solvent was removed, the brown residue extracted with *n*-hexane and the solution filtered through a frit. The solvent was reduced to 3 mL and

after seven days at -30°C [Cp*Fe(η^4-P_5(Me)$CHPh_2$)] (130 mg, 0.288 mmol, 56% yield) could be isolated as dark brown blocks.

^{1}H NMR (C_6D_6, 300 K): δ [ppm] = 6.81 (m, 5H, Ph), 1.91 (d, 2H, CH_2), 1.63 (s, 15H, Cp*), 1.61 (s, 3H, P-Me).

^{31}P{^{1}H} NMR (C_6D_6, 300 K): δ [ppm] = 119.7 (tt, 1P), 36.0 (m, 2P), -123.4 (m, 2P). For coupling constants see Table S 5.

EA calculated for $C_{19,2}H_{27,8}FeP_5$ (469,34 g·mol^{-1}): C: 49.13, H: 5.97; found [%]: C: 49.08, H: 5.67.

General synthesis of [5a-d], [5a-d] = [Cp*Fe(η^4-P_5(R)Me)] (R = ^{i}Pr (5a), ^{n}Bu (5b), $(CH_2)_3Br$ (5c), $(CH_2)_4Br$ (5d)): To a solution of 85 mg (0.148 mmol) [Li(dme)$_{2.3}$][Cp*Fe(η^4-P_5Me)] in 10 mL dme an excess (0.04 mL) of isopropyl iodide (0.400 mmol), 1-bromobutane (0.370 mmol), 1,3-dibromopropane (0.394 mmol) or 1,4-dibromobutane (0.339 mmol) was added. The brownish solution was stirred overnight, all volatiles were removed in vacuum and the brown residue was dissolved in *n*-hexane and filtered through a frit. The resulting solution was concentrated to 3 mL and stored at -30°C.

Yields and analytical details of [5a-d]:

Dark red blocks of [Cp*Fe(η^4-P_5(^{i}Pr)Me)] (**5a**) (43 mg, 0.106 mmol, 72% yield) could be isolated after two days.

^{1}H NMR (C_6D_6, 300 K): δ [ppm] = 2.45 (sextet, 1H, ^{i}Pr-H), 1.63 (s, 15H, Cp*), 1.07 (d, 3H, ^{i}Pr-CH_3), 1.03 (d, 3H, ^{i}Pr-CH_3), 0.09 (d, 3H, P-Me).

^{31}P{^{1}H} NMR (C_6D_6, 300 K): δ [ppm] = 152.0 (tt, 1P), 33.3 (m, 2P), -135.8 (m, 2P). For coupling constants see Table S 6.

Dark red blocks of [Cp*Fe(η^4-P_5(^{n}Bu)Me)] (**5b**) (40 mg, 0.0957 mmol, 64% yield) could be isolated after two weeks.

^{1}H NMR (C_6D_6, 300 K): δ [ppm] = 2.05 (m, 2H, CH_2), 1.65 (s, 15H, Cp*), 1.44 (m, 2H, CH_2), 1.20 (m, 2H, CH_2), 0.80 (t, 3H, CH_3), 0.12 (d, 3H, P-Me).

^{31}P{^{1}H} NMR (C_6D_6, 300 K): δ [ppm] = 132.3 (tt, 1P), 32.2 (m, 2P), -130.1 (m, 2P). For coupling constants see Table S 7.

EA calculated for $C_{16.5}H_{30.5}FeP_5$ (439.63 g·mol^{-1}): C: 45.08, H: 6.99; found [%]: C: 45.10, H: 6.94.

Dark red plates of [Cp*Fe(η^4-P_5($(CH_2)_3$Br)Me)] (**5c**) (38 mg, 0.0787 mmol, 53% yield) could be isolated after four days.

^{1}H NMR (C_6D_6, 300 K): δ [ppm] = 2.86 (t, 2H, R-CH_2-Br), 2.03 (m, 2H, R-CH_2-R), 1.73 (m, 2H, R-CH_2-R), 1.60 (s, 15H, Cp*), 0.01 (d, 3H, P-Me).

^{31}P{^{1}H} NMR (C_6D_6, 300 K): δ [ppm] = 128.9 (tt, 1P), 32.0 (m, 2P), -130.3 (m, 2P). For coupling constants see Table S 8.

EA calculated for $C_{14}H_{24}FeP_5Br$ (482,96 g·mol^{-1}): C: 34.82, H: 5.01; found [%]: C: 35.61, H: 4.91.

Dark brown needles of [Cp*Fe(η^4-P_5($(CH_2)_4$Br)Me)] (**5d**) (37 mg, 0.0745 mmol, 50% yield) could be isolated after one day.

^{1}H NMR (C_6D_6, 300 K): δ [ppm] = 2.87 (t, 2H, R-CH_2-Br), 1.86 (m, 2H, P-CH_2-R), 1.64 (s, 15H, Cp*), 1.46 (m, 4H, R-CH_2-CH_2-R), 0.10 (d, 3H, P-Me).

^{31}P{^{1}H} NMR (C_6D_6, 300 K): δ [ppm] = 130.7 (tt, 1P), 32.0 (m, 2P), -130.9 (m, 2P). For coupling constants see Table S 9.

EA calculated for $C_{20.4}H_{38.6}BrFeP_5$ (574.54 g·mol^{-1}): C: 42.65, H: 6.77; found [%]: C: 42.64, H: 6.50.

Experimental and simulated NMR spectra

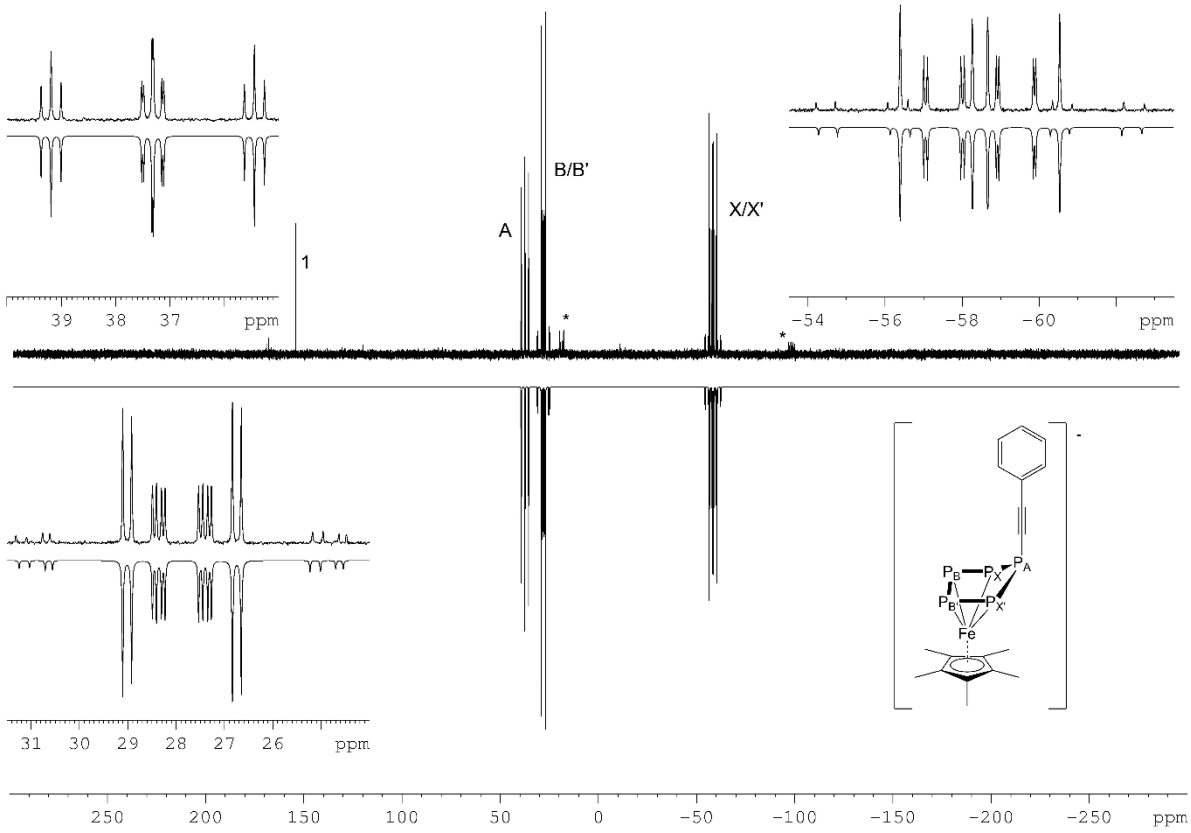

Figure S 1. ^{31}P NMR spectrum of compound **2a** at 298 K in THF-d_8. Impurities are marked with *.

Table S 1. ^{31}P NMR chemical shifts and coupling constants for **2a** obtained from the simulation.

***J* (Hz)**				***δ* (ppm)**	
$^{2}J_{P_A,P_B}$	-29.9	$^{1}J_{P_B,P_X}$	377.5	P_A	37.3
$^{2}J_{P_A,P_{B'}}$	-29.9	$^{2}J_{P_B,P_{X'}}$	-10.0	P_B, $P_{B'}$	27.9
$^{1}J_{P_A,P_X}$	303.0	$^{1}J_{P_{B'},P_{X'}}$	377.5	P_X, $P_{X'}$	-58.4
$^{1}J_{P_A,P_{X'}}$	303.0	$^{2}J_{P_{B'},P_X}$	-10.0		
$^{1}J_{P_B,P_{B'}}$	409.7	$^{2}J_{P_X,P_{X'}}$	-47.3		

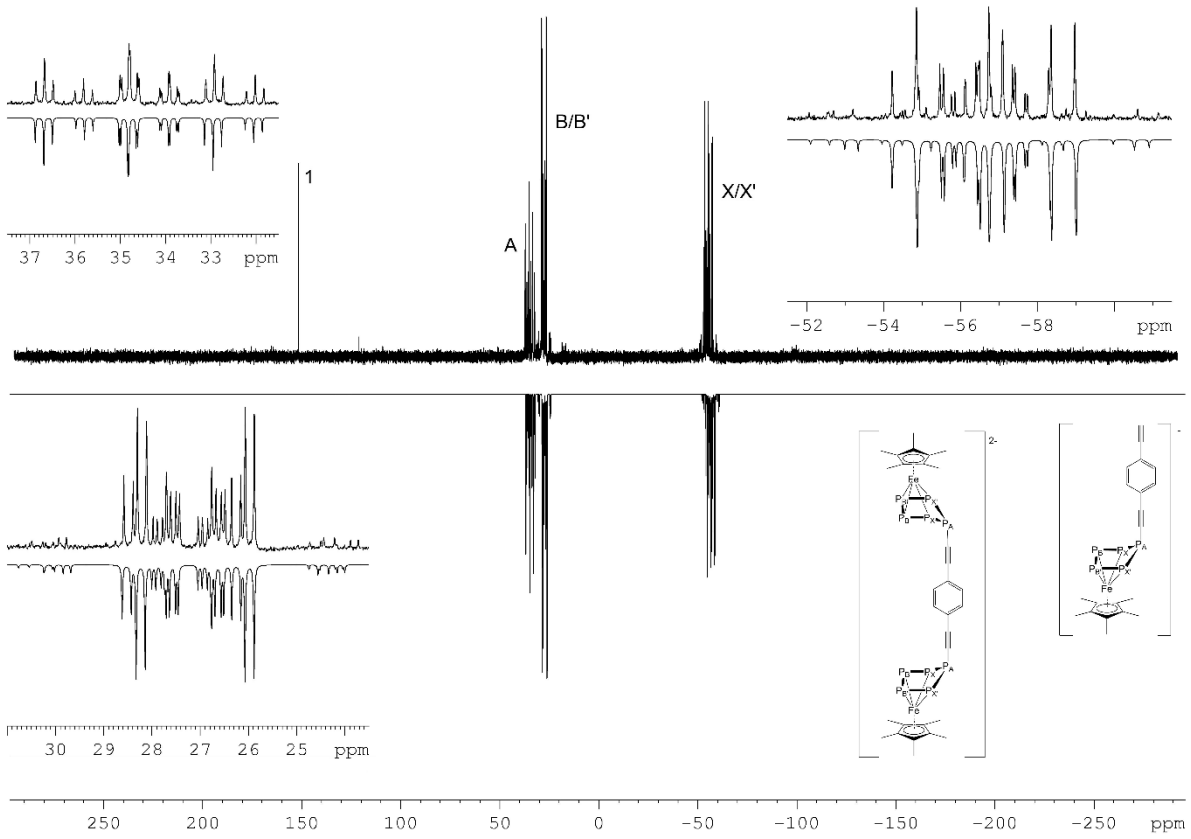

Figure S 2. ^{31}P NMR spectrum of compound **2b** at 298 K in thf with a C_6D_6 capillary.

Table S 2. ^{31}P NMR chemical shifts and coupling constants for **2b** obtained from the simulation.

***J* (Hz)**				***δ* (ppm)**	
$^{2}J_{P_A,P_M}$	-30.7	$^{1}J_{P_M,P_X}$	370.0	P_A	35.8
$^{2}J_{P_A,P_{M'}}$	-30.7	$^{2}J_{P_M,P_{X'}}$	-4.3	P_M, $P_{M'}$	27.1
$^{1}J_{P_A,P_X}$	303.0	$^{1}J_{P_{M'},P_{X'}}$	370.0	P_X, $P_{X'}$	-56.9
$^{1}J_{P_A,P_{X'}}$	303.0	$^{2}J_{P_{M'},P_X}$	-4.3		
$^{1}J_{P_M,P_{M'}}$	384.0	$^{2}J_{P_X,P_{X'}}$	-34.6		

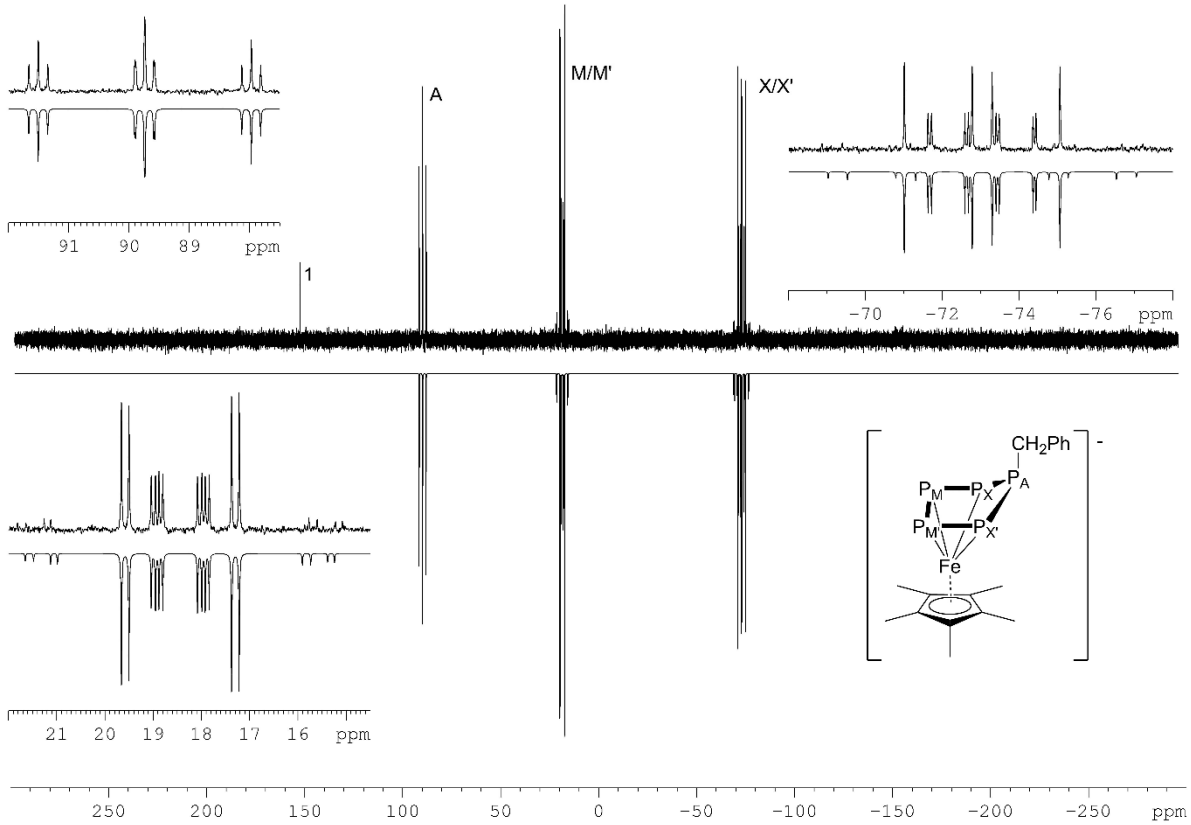

Figure S 3. ^{31}P NMR spectrum of compound **3a** at 298 K in THF-d_8.

Table S 3. ^{31}P NMR chemical shifts and coupling constants for **3a** obtained from the simulation.

***J* (Hz)**				***δ* (ppm)**	
$^2J_{P_A,P_M}$	-25.4	$^1J_{P_M,P_X}$	374.4	P_A	89.7
$^2J_{P_A,P_{M'}}$	-25.4	$^2J_{P_M,P_{X'}}$	-48.2	P_M, $P_{M'}$	18.4
$^1J_{P_A,P_X}$	286.2	$^1J_{P_{M'},P_{X'}}$	374.4	P_X, $P_{X'}$	-73.0
$^1J_{P_A,P_{X'}}$	286.2	$^2J_{P_{M'},P_X}$	-48.2		
$^1J_{P_M,P_{M'}}$	387.6	$^2J_{P_X,P_{X'}}$	-4.4		

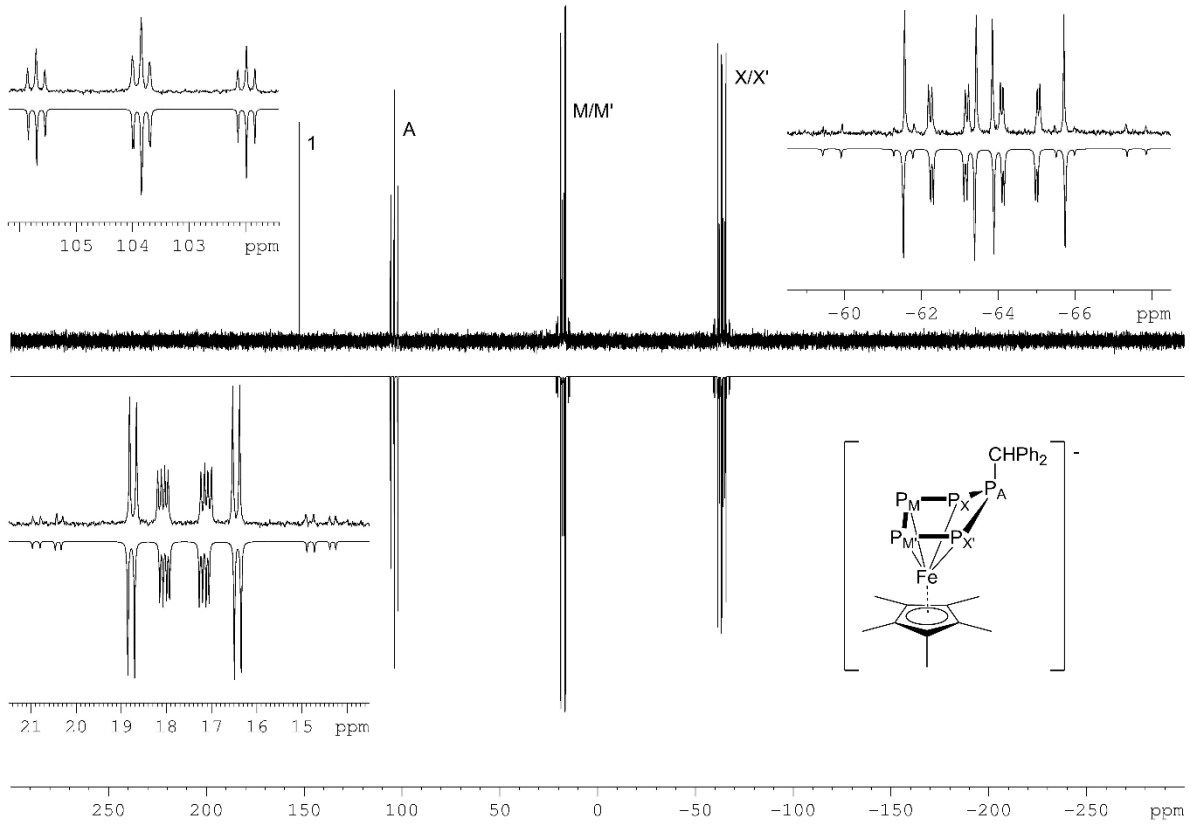

Figure S 4. ^{31}P NMR spectrum of compound **3b** at 298 K in THF-d_8.

Table S 4. ^{31}P NMR chemical shifts and coupling constants for **3b** obtained from the simulation.

***J* (Hz)**				***δ* (ppm)**	
$^{2}J_{P_A,P_M}$	-24.3	$^{1}J_{P_M,P_X}$	377.2	P_A	103.8
$^{2}J_{P_A,P_{M'}}$	-24.3	$^{2}J_{P_M,P_{X'}}$	-45.2	P_M, $P_{M'}$	17.6
$^{1}J_{P_A,P_X}$	301.0	$^{1}J_{P_{M'},P_{X'}}$	377.2	P_X, $P_{X'}$	-63.6
$^{1}J_{P_A,P_{X'}}$	301.0	$^{2}J_{P_{M'},P_X}$	-45.2		
$^{1}J_{P_M,P_{M'}}$	421.8	$^{2}J_{P_X,P_{X'}}$	-4.9		

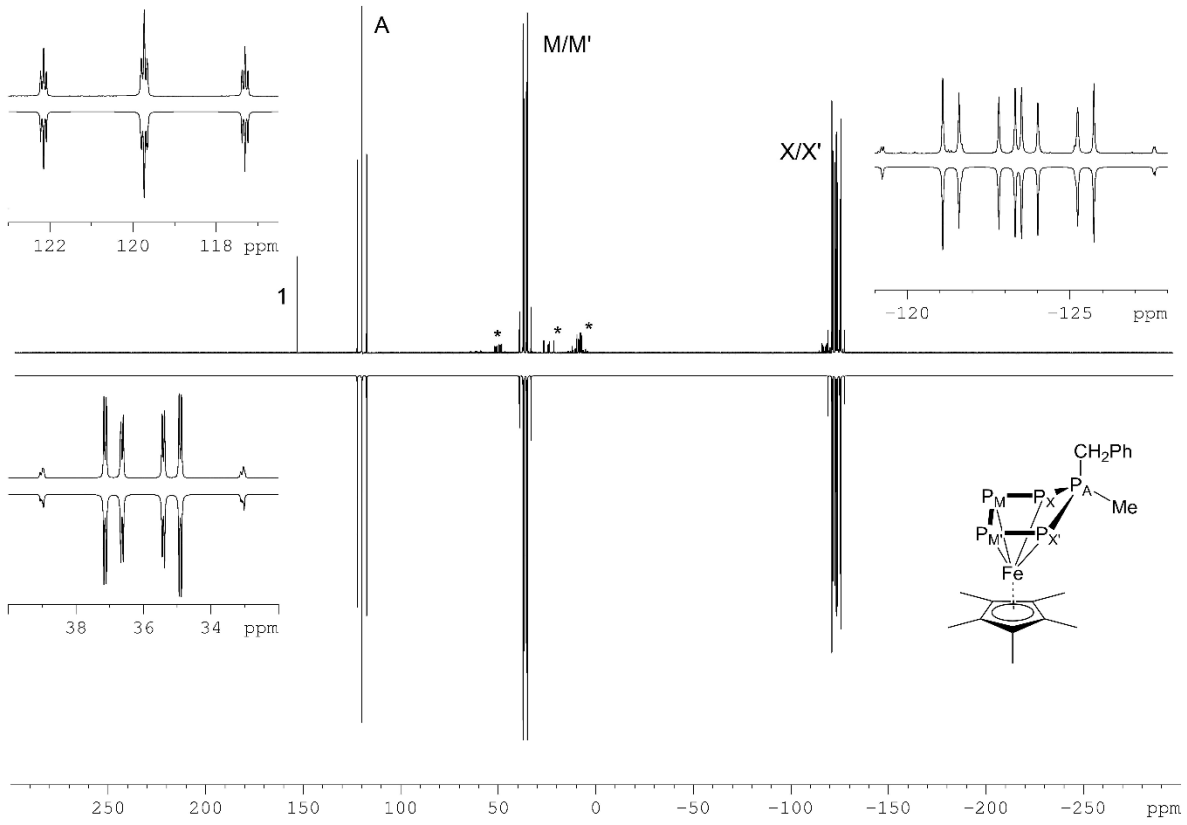

Figure S 5. Experimental (top) and simulated (bottom) $^{31}P\{^{1}H\}$ NMR (162 MHz, C_6D_6) spectrum of **4** at 298 K. Impurities are marked with *.

Table S 5. $^{31}P\{^{1}H\}$ NMR chemical shifts and coupling constants for **4** obtained from the simulation.

***J* (Hz)**				***δ* (ppm)**	
$^{2}J_{P_A,P_M}$	-10.9	$^{1}J_{P_M,P_X}$	388.3	P_A	119.7
$^{2}J_{P_A,P_{M'}}$	-11.8	$^{2}J_{P_M,P_{X'}}$	-48.3	P_M, $P_{M'}$	36.0
$^{1}J_{P_A,P_X}$	393.0	$^{1}J_{P_{M'},P_{X'}}$	409.3	P_X, $P_{X'}$	-123.4
$^{1}J_{P_A,P_{X'}}$	392.6	$^{2}J_{P_{M'},P_X}$	-28.1		
$^{1}J_{P_M,P_{M'}}$	381.6	$^{2}J_{P_X,P_{X'}}$	-3.1		

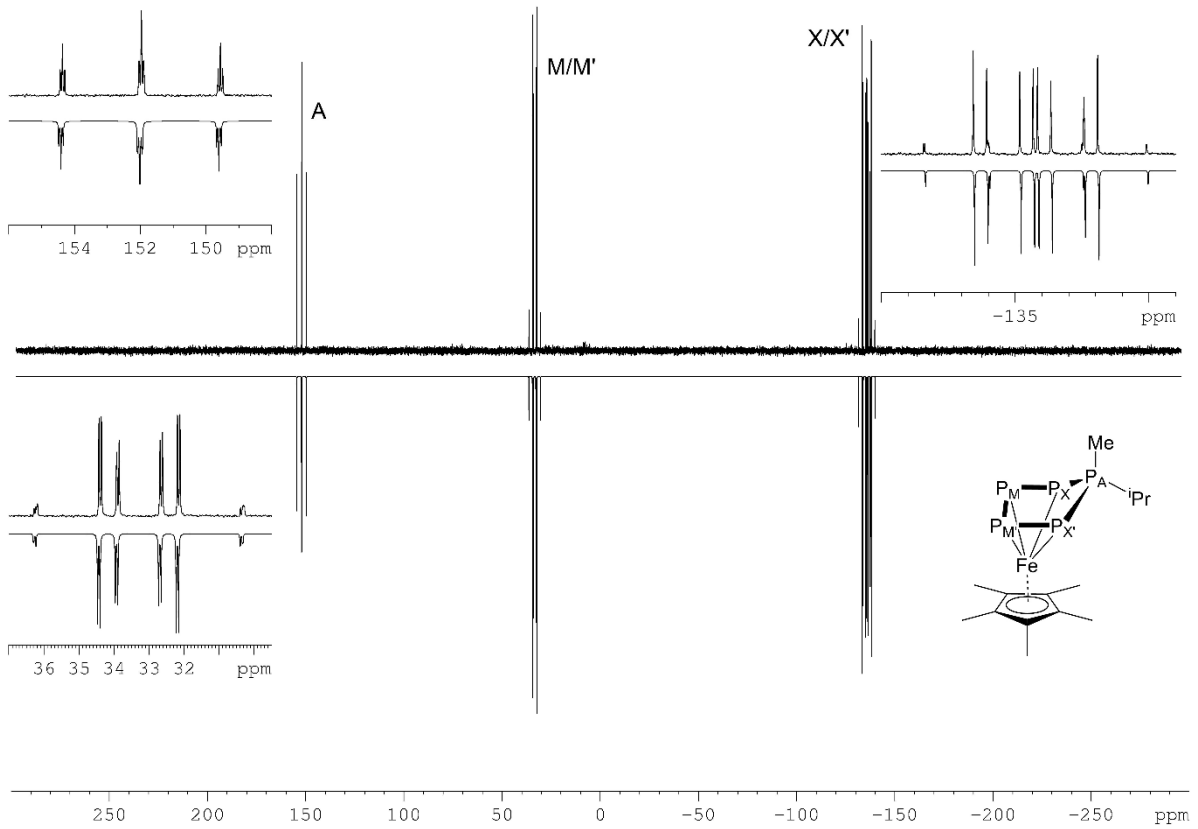

Figure S 6. Experimental (top) and simulated (bottom) $^{31}P\{^{1}H\}$ NMR (162 MHz, C_6D_6) spectrum of **5a** at 298 K.

Table S 6. $^{31}P\{^{1}H\}$ NMR chemical shifts and coupling constants for **5a** obtained from the simulation.

***J* (Hz)**				***δ* (ppm)**	
$^{2}J_{P_A,P_M}$	-12.6	$^{1}J_{P_M,P_X}$	403.2	P_A	152.0
$^{2}J_{P_A,P_{M'}}$	-9.9	$^{2}J_{P_M,P_{X'}}$	-34.9	P_M, $P_{M'}$	33.3
$^{1}J_{P_A,P_X}$	389.6	$^{1}J_{P_{M'},P_{X'}}$	397.0	P_X, $P_{X'}$	-135.8
$^{1}J_{P_A,P_{X'}}$	388.7	$^{2}J_{P_{M'},P_X}$	-40.0		
$^{1}J_{P_M,P_{M'}}$	377.7	$^{2}J_{P_X,P_{X'}}$	-0.1		

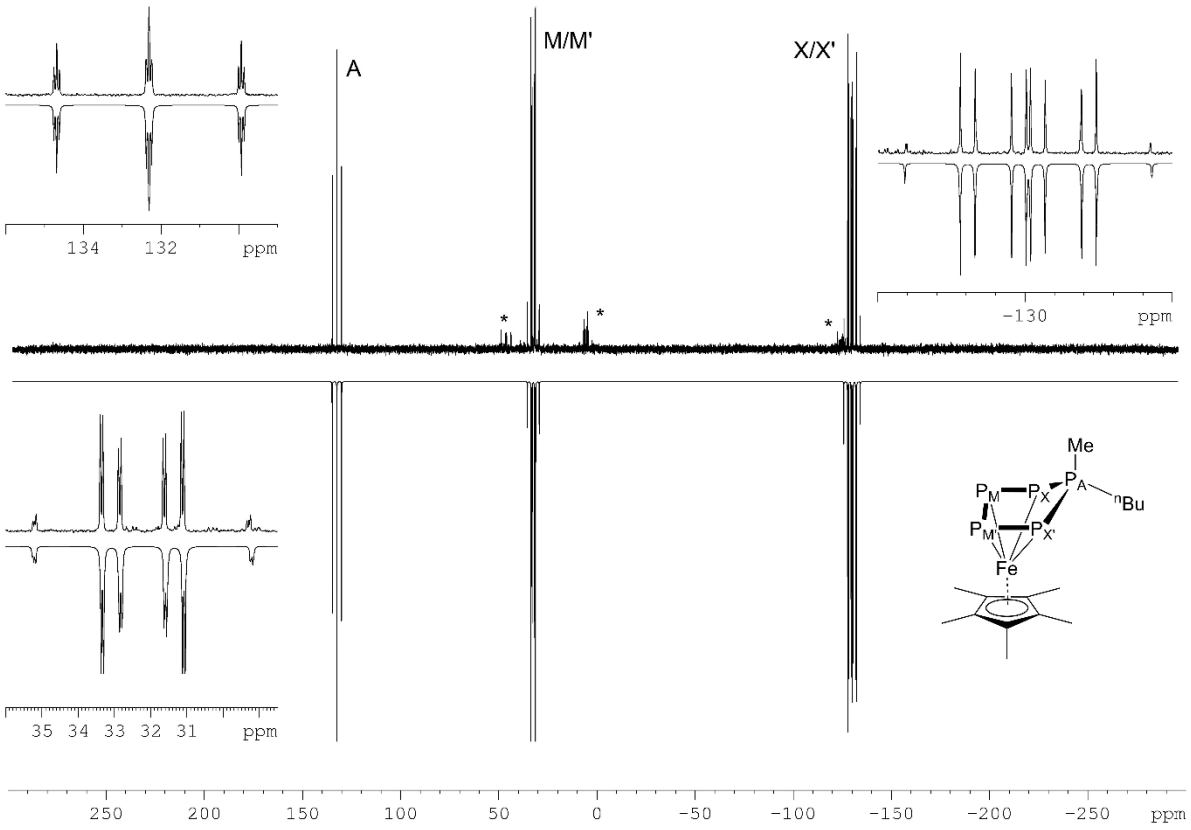

Figure S 7. Experimental (top) and simulated (bottom) $^{31}P\{^{1}H\}$ NMR (162 MHz, C_6D_6) spectrum of **5b** at 298 K. Impurities are marked with *.

Table S 7. $^{31}P\{^{1}H\}$ NMR chemical shifts and coupling constants for **5b** obtained from the simulation.

***J* (Hz)**				***δ* (ppm)**	
$^{2}J_{P_A,P_M}$	-11.2	$^{1}J_{P_M,P_X}$	410.0	P_A	132.3
$^{2}J_{P_A,P_{M'}}$	-11.2	$^{2}J_{P_M,P_{X'}}$	-37.0	P_M, $P_{M'}$	32.2
$^{1}J_{P_A,P_X}$	385.9	$^{1}J_{P_{M'},P_{X'}}$	397.2	P_X, $P_{X'}$	-130.1
$^{1}J_{P_A,P_{X'}}$	385.9	$^{2}J_{P_{M'},P_X}$	-41.8		
$^{1}J_{P_M,P_{M'}}$	385.7	$^{2}J_{P_X,P_{X'}}$	-0.7		

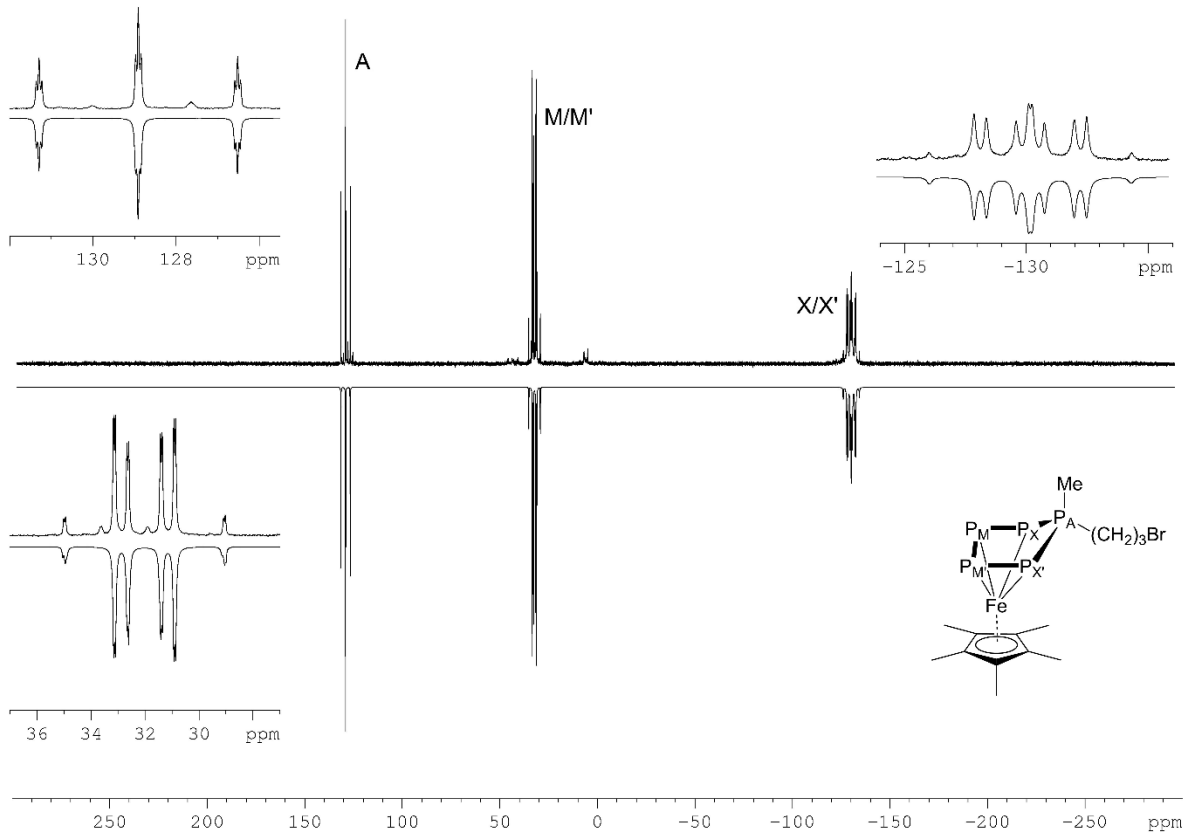

Figure S 8. Experimental (top) and simulated (bottom) $^{31}P\{^{1}H\}$ NMR (162 MHz, C_6D_6) spectrum of **5c** at 298 K.

Table S 8. $^{31}P\{^{1}H\}$ NMR chemical shifts and coupling constants for **5c** obtained from the simulation.

***J* (Hz)**				***δ* (ppm)**	
$^{2}J_{P_A,P_M}$	-10.7	$^{1}J_{P_M,P_X}$	390.1	P_A	128.9
$^{2}J_{P_A,P_{M'}}$	-10.7	$^{2}J_{P_M,P_{X'}}$	-49.4	P_M, $P_{M'}$	32.0
$^{1}J_{P_A,P_X}$	386.9	$^{1}J_{P_{M'},P_{X'}}$	404.0	P_X, $P_{X'}$	-130.3
$^{1}J_{P_A,P_{X'}}$	386.9	$^{2}J_{P_{M'},P_X}$	-24.2		
$^{1}J_{P_M,P_{M'}}$	377.9	$^{2}J_{P_X,P_{X'}}$	-7.8		

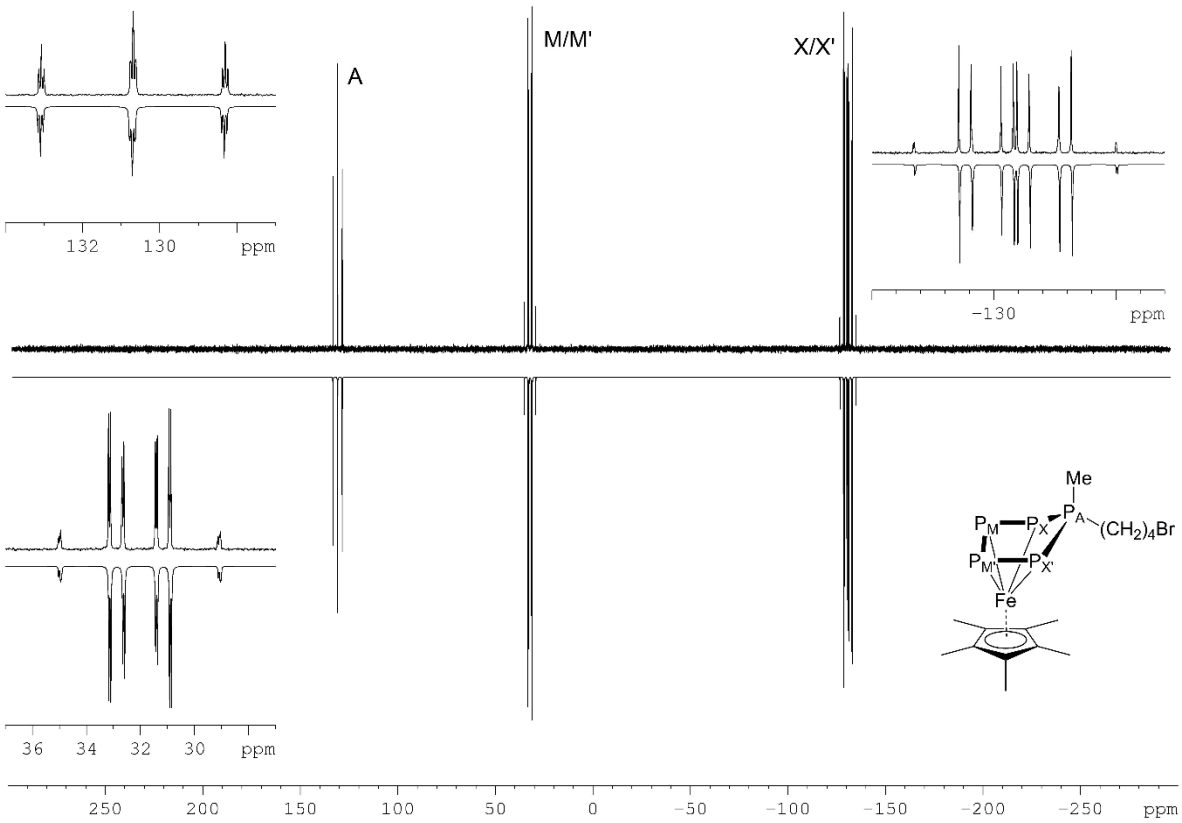

Figure S 9. Experimental (top) and simulated (bottom) $^{31}P\{^{1}H\}$ NMR (162 MHz, C_6D_6) spectrum of **5d** at 298 K.

Table S 9. $^{31}P\{^{1}H\}$ NMR chemical shifts and coupling constants for **5d** obtained from the simulation.

***J* (Hz)**				***δ* (ppm)**	
$^{2}J_{P_A,P_M}$	-12.6	$^{1}J_{P_M,P_X}$	398.1	P_A	130.7
$^{2}J_{P_A,P_{M'}}$	-9.8	$^{2}J_{P_M,P_{X'}}$	-35.0	P_M, $P_{M'}$	32.0
$^{1}J_{P_A,P_X}$	386.5	$^{1}J_{P_{M'},P_{X'}}$	397.2	P_X, $P_{X'}$	-130.9
$^{1}J_{P_A,P_{X'}}$	384.5	$^{2}J_{P_{M'},P_X}$	-35.1		
$^{1}J_{P_M,P_{M'}}$	380.3	$^{2}J_{P_X,P_{X'}}$	-4.4		

Details on X-ray structure determinations

All single crystal structure analyses were performed using Agilent Technologies diffractometer (GV50, TitanS2 detector) with $Cu_{K\alpha}$ radiation. Frames integration and data reduction were performed with the CrysAlisPro ver. 1.171.41.54a[4] software package. Using **Olex2**,[5] all structures were solved by **ShelXT**[6] and a least-square refinement on F^2 was carried out with **ShelXL**.[7] All non-hydrogen atoms were refined anisotropically. Hydrogen atoms at the carbon atoms were located in idealized positions and refined isotropically according to the riding model.

The images showing the compounds were generated using **Olex2**.[5]

Compound 2a: The P atoms are disordered over two positions (92:08) and one thf molecule is disordered over two positions (50:50). The restraints SADI and SIMU were applied to describe these disorders.

Compound 2b: The P atoms are disordered over two positions (73:27). The restraints SADI and SIMU were applied to describe these disorders.

Compound 3a: The P atoms are disordered over two positions (66:34). The restraint SIMU was applied to describe these disorders.

Compound 3b: One thf molecule is disordered over two positions (72:28). The restraint SIMU was applied to describe these disorders.

Compound 4: There is one single molecule of **4** in the asymmetric unit.

Compound 5a: There is one single molecule of **5a** in the asymmetric unit.

Compound 5b: There is one single molecule of **5b** in the asymmetric unit.

Compound 5c: There is one single molecule of **5a** in the asymmetric unit.

Compound 5d: The Cp* ligand is disordered over two positions (50:50). The restraint SIMU was applied to describe these disorders

Table S 10. Crystallographic data and detail of the compounds [K(18c-6)(thf)][**2a**], [K(18c-6)(thf)$_2$][**2b**], [K(18c-6)][**3a**], [K(thf)$_2$][**3b**] and **4**.

Compound	[K(18c-6)(thf)][**2a**]	[K(18c-6)(thf)$_2$][**2b**]	[K(18c-6)][**3a**]	[K(thf)$_2$][**3b**]	**4**
File Name	FR200	FR230	FR252	FR295	FR340
CCDC	xxx	xxx	xxx	xxx	xxx
Formula	$C_{68}H_{104}Fe_2K_2O_{14}P_{10}$	$C_{35}H_{57}FeKO_8P_5$	$C_{29}H_{46}FeKO_6P_5$	$C_{31}H_{42}FeKO_2P_5$	$C_{18}H_{25}FeP_5$
$D_{calc.}$/ g cm^{-3}	1.364	1.338	1.363	1.353	1.395
μ/mm^{-1}	6.192	5.877	6.791	7.045	9.111
Formula Weight	1645.11	855.60	740.46	696.44	452.08
Color	metallic dark green	dark brown	dark brown	dark brown	dark brown
Shape	block	plate	block	block	block
Max size/mm	0.37	0.76	0.57	0.83	0.23
Mid size/mm	0.15	0.31	0.18	0.60	0.17
Min size/mm	0.11	0.07	0.14	0.37	0.16
T/K	123.00(10)	123.00(10)	122.99(11)	123.00(13)	123.01(10)
Crystal System	monoclinic	triclinic	monoclinic	monoclinic	orthorhombic
Space Group	$P2_1/c$	P-1	$P2_1/c$	$P2_1/c$	$Pbca$
a/Å	20.3442(5)	9.1295(4)	15.1860(3)	17.1655(2)	10.5451(2)
b/Å	26.2921(5)	15.2051(5)	13.4831(2)	17.8974(2)	16.8844(3)
c/Å	15.0828(3)	15.8988(6)	17.6986(3)	22.2624(3)	24.1818(4)
α/°	90	81.173(3)	90	90	90
β/°	96.721(2)	78.651(3)	95.339(2)	90.7420(10)	90
γ/°	90	81.847(3)	90	90	90
V/Å^3	8012.2(3)	2123.97(14)	3608.14(11)	6838.83(14)	4305.51(13)
Z	4	2	4	8	8
Z'	1	1	1	2	1
Q_{min}/°	3.362	2.859	2.923	2.574	3.656
Q_{max}/°	66.600	73.813	74.884	74.529	73.671
Measured Reflexes	41460	22718	33923	45789	17042
Independent Reflexes	14019	8375	7209	13605	4299
Reflections with I > 2(I)	10664	7215	6544	12970	4007
R_{int}	0.0652	0.0549	0.0426	0.0574	0.0526
Parameters	1010	493	433	777	314
Restraints	279	0	150	18	136
Largest Peak	0.659	0.993	0.357	0.451	0.917
Deepest Hole	-0.535	-0.736	-0.445	-0.893	-0.368
GooF	1.085	1.029	1.041	1.031	1.141
wR2 (all data)	0.1963	0.1529	0.0872	0.1210	0.1136
wR2	0.1829	0.1450	0.0839	0.1191	0.1110
R1 (all data)	0.0981	0.0629	0.0368	0.0466	0.0469
R1	0.0754	0.0553	0.0324	0.0450	0.0438

Table S 11. Crystallographic data and detail of the compounds **5a**, **5b**, **5c** and **5d**.

Compound	**5a**	**5b**	**5c**	**5d**
File Name	FR340	FR350	FR352	FR353
CCDC	xxx	xxx	xxx	xxx
Formula	$C_{14}H_{25}FeP_5$	$C_{15}H_{27}FeP_5$	$C_{14}H_{24}BrFeP_5$	$C_{18}H_{32}BrFeP_5$
$D_{calc.}$/ g cm^{-3}	1.401	1.400	1.595	1.493
μ/mm^{-1}	10.167	9.837	12.027	10.146
Formula Weight	404.04	418.06	482.94	539.04
Color	dark red	dark red	dark red	dark brown
Shape	block	block	plate	needle
Max size/mm	0.20	0.15	0.21	0.89
Mid size/mm	0.08	0.14	0.12	0.12
Min size/mm	0.07	0.13	0.03	0.10
T/K	123.01(11)	123.00(10)	122.9(2)	122.9(2)
Crystal System	monoclinic	orthorhombic	orthorhombic	monoclinic
Space Group	$P2_1/n$	$P2_12_12_1$	$P2_12_12_1$	$P2_1/n$
a/Å	7.8144(3)	8.0201(2)	8.1330(2)	14.6139(4)
b/Å	9.1949(4)	9.5556(3)	9.6956(2)	8.2362(3)
c/Å	26.6544(9)	25.8761(6)	25.5069(6)	20.3049(5)
α/°	90	90	90	90
β/°	90.623(3)	90	90	101.048(2)
γ/°	90	90	90	90
V/Å^3	1915.08(13)	1983.06(9)	2011.33(8)	2398.66(13)
Z	4	4	4	4
Z'	1	1	1	1
Q_{min}/°	5.088	3.416	3.466	3.434
Q_{max}/°	73.618	73.607	74.916	75.053
Measured Reflexes	3743	11777	6543	18008
Independent Reflexes	3743	3760	3431	4840
Reflections with I > 2(I)	3405	3544	3190	4136
R_{int}	.	0.0554	0.0322	0.1140
Parameters	190	252	259	289
Restraints	0	13	69	84
Largest Peak	0.902	0.686	0.888	1.772
Deepest Hole	-0.655	-0.410	-1.150	-0.758
GooF	1.117	1.074	1.071	1.055
wR2 (all data)	0.2053	0.1064	0.1397	0.1862
wR2	0.1999	0.1049	0.1360	0.1764
R1 (all data)	0.0842	0.0483	0.0551	0.0761
R1	0.0764	0.0455	0.0510	0.0678
Flack Parameter	-	0.010(5)	-0.008(7)	-
Hooft Parameter	-	0.006(4)	-0.003(5)	-

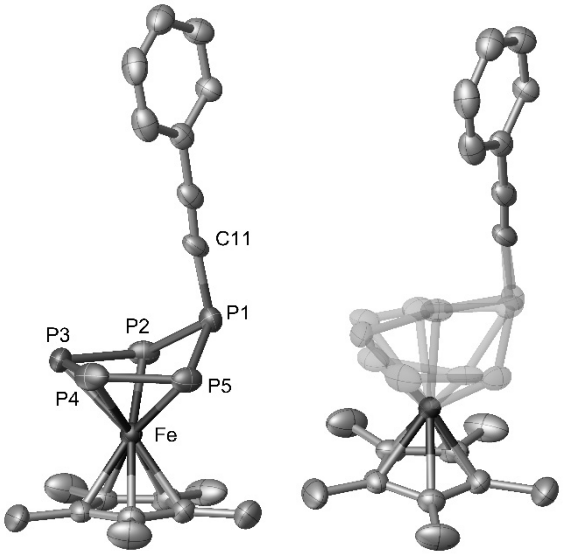

Figure S 10. Molecular structure of **2a** in the solid state. Hydrogen atoms, cations, 18c-6 and solvent molecules are omitted for clarity. Anisotropic displacement parameters are set to 50% probability. Selected bond lengths (Å) and angles (°) of Part 1: P1-P2 2.142(5), P1-P5 2.162(3), P2-P3 2.187(3), P3-P4 2.127(4), P4-P5 2.142(3), P1-C11 1.782(7), Fe1-P2 2.322(3), Fe1-P3 2.312(2), Fe1-P4 2.338(2), Fe1-P5 2.317(2); P5-P1-P2 93.56(16), P3-P2-P1 107.09(16), P4-P3-P2 103.14(13), P3-P4-P5 103.82(11), P4-P5-P1 107.18(14).

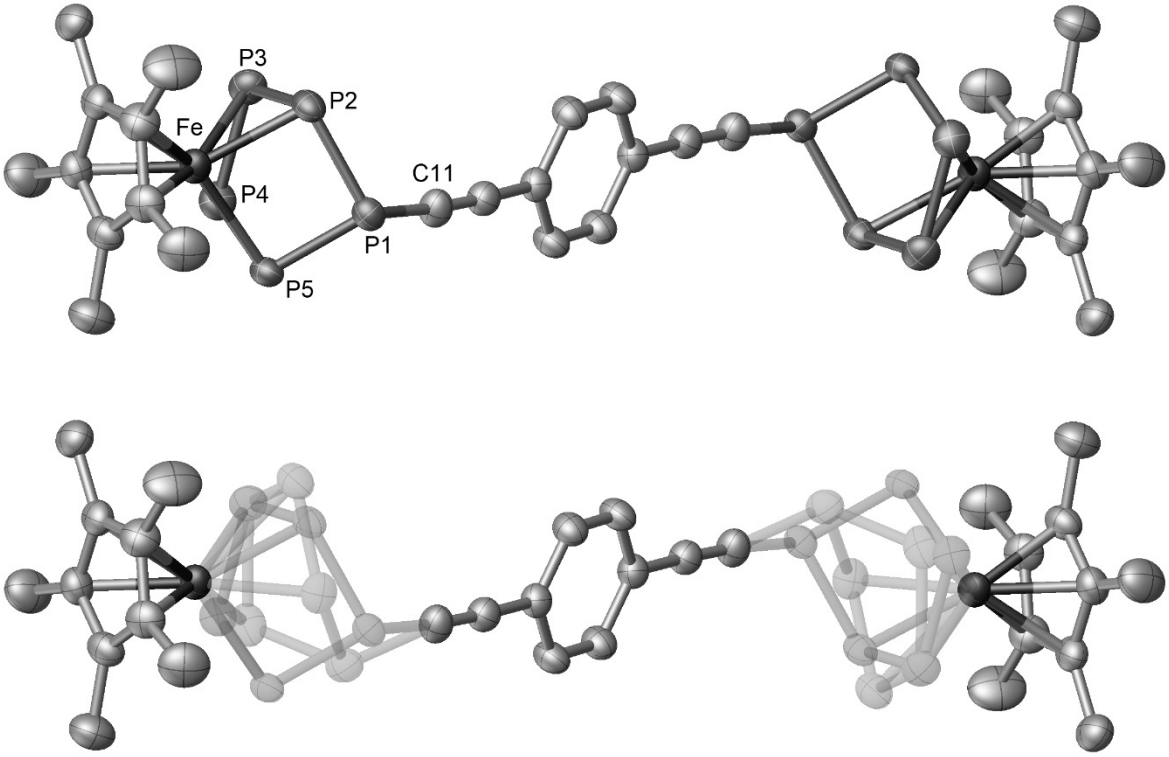

Figure S 11. Molecular structure of **2b** in the solid state. Hydrogen atoms, cations, 18c-6 and solvent molecules are omitted for clarity. Anisotropic displacement parameters are set to 50% probability. Selected bond lengths (Å) and angles (°) of Part 1: P1-P2 2.170(2), P1-P5 2.1711(16), P2-P3 2.1341(14),

P3-P4 2.1490(15), P4-P5 2.1410(19), P1-C11 1.775(3), Fe1-P2 2.2631(12), Fe1-P3 2.3383(8), Fe1-P4 2.3832(13), Fe1-P5 2.3616(11); P5-P1-P2 92.37(6), P3-P2-P1 106.96(7), P4-P3-P2 103.30(6), P3-P4-P5 103.28(8), P4-P5-P1 107.16(6).

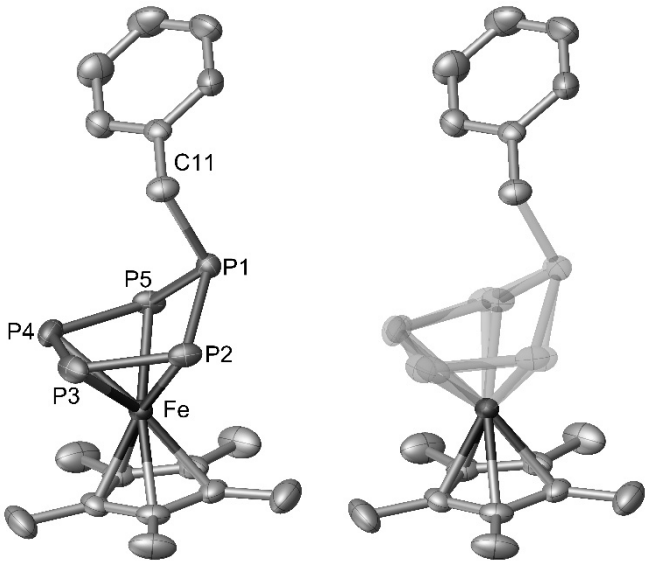

Figure S 12. Molecular structure of **3a** in the solid state. Hydrogen atoms, cations and 18c-6 molecules are omitted for clarity. Anisotropic displacement parameters are set to 50% probability. Selected bond lengths (Å) and angles (°) of Part 1: P1-P2 2.145(8), P1-P5 2.162(7), P2-P3 2.176(7), P3-P4 2.111(7), P4-P5 2.130(7), P1-C11 1.844(7), Fe1-P2 2.349(6), Fe1-P3 2.319(5), Fe1-P4 2.307(6), Fe1-P5 2.306(5); P5-P1-P2 93.0(3), P3-P2-P1 105.8(3), P4-P3-P2 103.5(3), P3-P4-P5 103.7(3), P4-P5-P1 106.7(3).

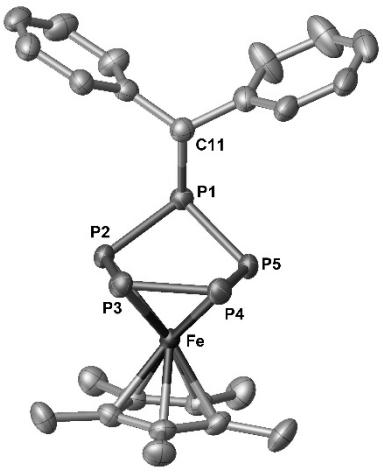

Figure S 13. Molecular structure in the solid state of **3b**. Hydrogen atoms, cations and solvent molecules are omitted for clarity. Anisotropic displacement parameters are set to 50% probability. Selected bond

lengths (Å) and angles (°): P1-P2 2.1657(8), P1-P5 2.1671(8), P2-P3 2.1514(8), P3-P4 2.1329(8), P4-P5 2.1502(8), P1-C11 1.900(2), Fe1-P2 2.3098(6), Fe1-P3 2.3333(6), Fe1-P4 2.3432(6), Fe1-P5 2.3180(6); P5-P1-P2 91.88(3), P3-P2-P1 106.37(3), P4-P3-P2 103.23(3), P3-P4-P5 103.12(3), P4-P5-P1 106.77(3).

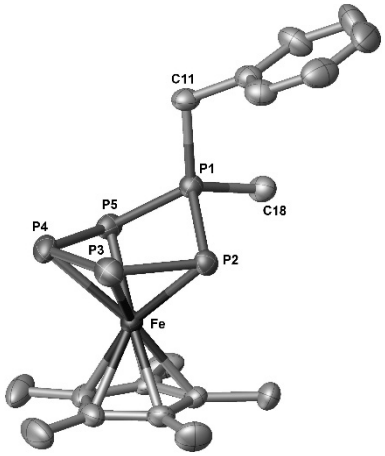

Figure S 14. Molecular structure in the solid state of **4**. Hydrogen atoms are omitted are omitted for clarity. Anisotropic displacement parameters are set to 50% probability. Selected bond lengths (Å) and angles (°): P1-P2 2.1429(10), P1-P5 2.1307(10), P2-P3 2.1214(11), P3-P4 2.1437(11), P4-P5 2.1375(11), P1-C11 1.840(3), P1-C18 1.18158(3), Fe1-P2 2.3167(8), Fe1-P3 2.3391(8), Fe1-P4 2.3325(8), Fe1-P5 2.3290(8); P5-P1-P2 99.68(4), P3-P2-P1 100.35(4), P4-P3-P2 105.23(4), P3-P4-P5 105.33(4), P4-P5-P1 100.18(4).

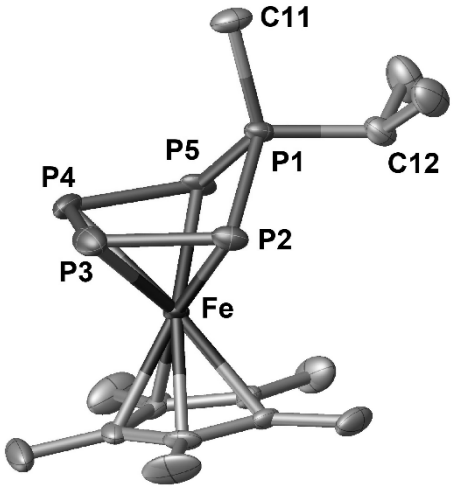

Figure S 15. Molecular structure in the solid state of **5a**. Hydrogen atoms are omitted for clarity. Anisotropic displacement parameters are set to 50% probability. Selected bond lengths (Å) and angles (°): P1-P2 2.142(2), P1-P5 2.1472(19), P2-P3 2.132(2), P3-P4 2.155(3), P4-P5 2.145(2), P1-C11 1.821(6), P1-C12 1.843(6), Fe1-P2 2.3166(15), Fe1-P3 2.3342(17), Fe1-P4 2.3371(17), Fe1-P5 2.3168(16); P5-P1-P2 97.89(8), P3-P2-P1 98.79(9), P4-P3-P2 105.04(9), P3-P4-P5 104.20(8), P4-P5-P1 98.95(9).

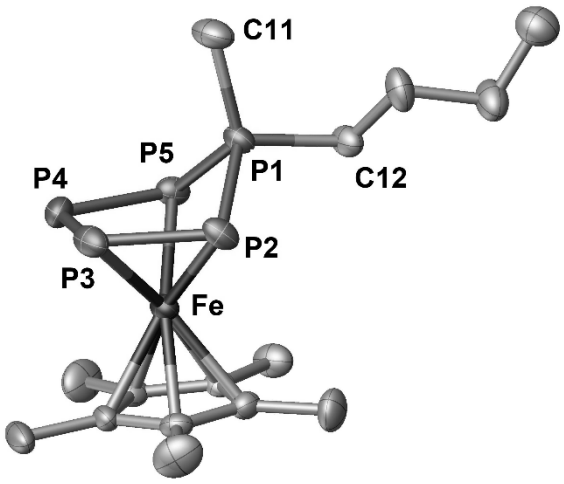

Figure S 16. Molecular structure in the solid state of **5b**. Hydrogen atoms are omitted for clarity. Anisotropic displacement parameters are set to 50% probability. Selected bond lengths (Å) and angles (°): P1-P2 2.144(3), P1-P5 2.133(2), P2-P3 2.1341(14), P3-P4 2.134(3), P4-P5 2.141(3), P1-C11 1.829(6), P1-C12 1.833(6), Fe1-P2 2.304(3), Fe1-P3 2.3285(16), Fe1-P4 2.361(3), Fe1-P5 2.3359(17); P5-P1-P2 98.62(11), P3-P2-P1 99.53(13), P4-P3-P2 105.01(11), P3-P4-P5 104.80(13), P4-P5-P1 99.37(12).

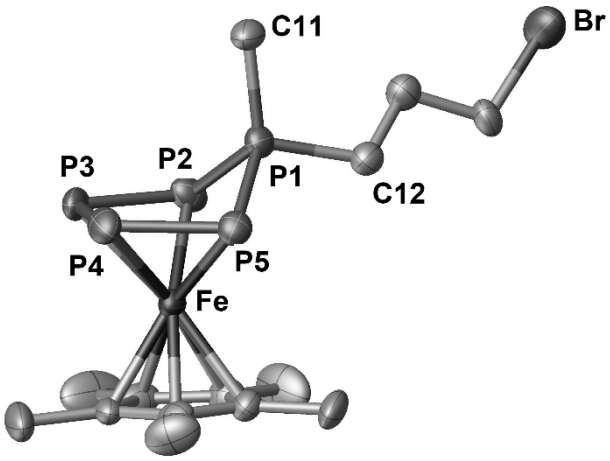

Figure S 17. Molecular structure in the solid state of **5c**. Hydrogen atoms are omitted for clarity. Anisotropic displacement parameters are set to 50% probability. Selected bond lengths (Å) and angles (°): P1-P2 2.142(3), P1-P5 2.129(3), P2-P3 2.119(9), P3-P4 2.143(11), P4-P5 2.147(4), P1-C11 1.817(8), P1-C12 1.842(9), Fe1-P2 2.317(4), Fe1-P3 2.320(8), Fe1-P4 2.355(3), Fe1-P5 2.322(2); P5-P1-P2 98.89(14), P3-P2-P1 99.1(3), P4-P3-P2 106.0(3), P3-P4-P5 103.9(2), P4-P5-P1 99.49(14).

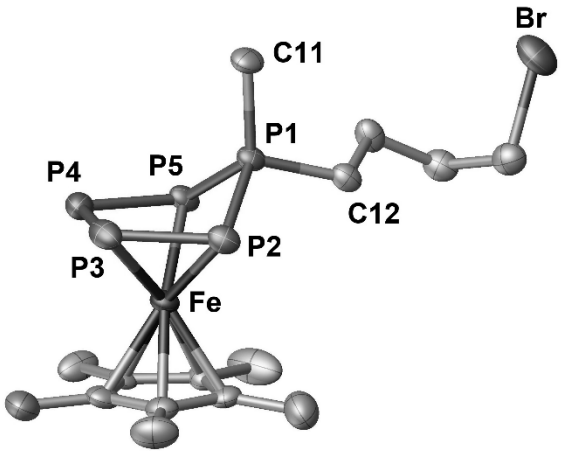

Figure S 18. Molecular structure in the solid state of **5d**. Hydrogen atoms are omitted for clarity. Anisotropic displacement parameters are set to 50% probability. Selected bond lengths (Å) and angles (°): P1-P2 2.1404(13), P1-P5 2.1419(13), P2-P3 2.1394(18), P3-P4 2.1511(16), P4-P5 2.1335(17), P1-C11 1.823(4), P1-C12 1.825(5), Fe1-P2 2.3319(11), Fe1-P3 2.3241(12), Fe1-P4 2.3406(14), Fe1-P5 2.3279(10); P5-P1-P2 99.10(5), P3-P2-P1 100.18(6), P4-P3-P2 105.16(6), P3-P4-P5 104.88(7), P4-P5-P1 100.19(6).

References:

[1] O. J. Scherer, T. Brück, *Angew. Chem. Int. Ed.* **1987**, *26*, 59-59.
[2] E. Mädl, Investigations of the reactivity of selected Pn ligand complexes. *Dissertation*, Universität Regensburg, **2016**.
[3] some MS experiments were not yet completed by the end of this thesis.
[4] CrysAlisPro Software System, Rigaku Oxford Diffraction, (**2018**).
[5] a) L. J. Bourhis, O. V. Dolomanov, R. J. Gildea, J. A. K. Howard, H. Puschmann, The Anatomy of a Comprehensive Constrained, Restrained, Refinement Program for the Modern Computing Environment - **Olex2** Disected, *Acta Cryst. A* **2015**, A71, 59–71; b) O. V. Dolomanov, L. J. Bourhis, R. J. Gildea, J. A. K. Howard, H. Puschmann, Olex2: A complete structure solution, refinement and analysis program, *J. Appl. Cryst.* **2009**, 42, 339–341.
[6] G. M. Sheldrick, ShelXT-Integrated space-group and crystal-structure determination, *Acta Cryst.* **2015**, A71, 3–8.
[7] G. M. Sheldrick, Crystal structure refinement with ShelXL, *Acta Cryst.* **2015**, C71, 3–8.

6. Summary

6.1 NHCs as Neutral Donors towards Polyphosphorus Complexes

The reactivity of [Cp*Fe(η^5-P_5)] (**1**) towards main group nucleophiles has been studied in our group. Only ionic nucleophiles have been used in these studies and the question arose, how **1** reacts towards neutral nucleophiles like NHCs (= *N*-heterocyclic carbenes). Therefore, the reactivity of **1** towards the NHCs IMe (= 1,3,4,5-tetramethylimidazolin-2-ylidene), IMes (= 1,3-bis(2,4,6-trimethylphenyl)-imidazolin-2-ylidene) and IDipp (= 1,3-bis(2,6-diisopropylphenyl)-imidazolin-2-ylidene) was investigated. Furthermore, the reactivity of IMe towards the *cyclo*-P_4 complex [Cp''Ta$(CO)_2(\eta^4$-$P_4)$] (**2**) was investigated (Scheme 1).

Reaction mixtures of [Cp*Fe(η^5-P_5)] with IMe, IMes or IDipp show broad signals in the corresponding $^{31}P\{^1H\}$ NMR spectra. At lower temperatures, these $^{31}P\{^1H\}$ NMR spectra show distinct signal groups corresponding to the formation of complexes in which one NHC molecule is attached to a folded *cyclo*-P_5 ring. Despite this highly dynamical system in solution, the adducts as neutral complexes in form of [Cp*Fe(η^4-P_5(NHC)] could be crystallized and isolated as solids. For a better understanding of this highly dynamical behavior, EXSY and MAS NMR studies were performed, which clearly shows that in solutions of [Cp*Fe(η^4-P_5(NHC)] a bond breaking and bond formation process takes place. All experimental results have been substantiated by DFT calculations. However, the reaction product of [Cp''Ta$(CO)_2(\eta^4$-$P_4)$] and IMe is no adduct but a phosphorus abstraction of the P_4 unit leading to the anionic *cyclo*-P_3 complex [Cp''Ta$(CO)_2(\eta^3$-$P_3)]^-$ and the cation $[(IMe)_2P]^+$. If less than two equivalents are used, the conversion is not complete and the $^{31}P\{^1H\}$ NMR spectrum shows unreacted **2** and [Cp''Ta$(CO)_2(\eta^3$-$P_3)]^-$.

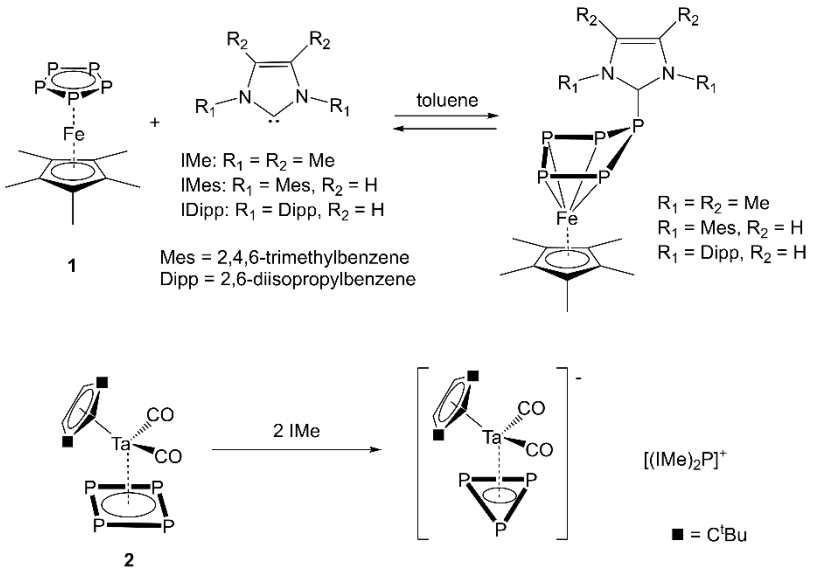

Scheme 1. Reactivity of **1** and **2** towards NHCs.

6.2 The reactivity of $[Cp_2Mo_2(CO)_4(\mu,\eta^{2:2}\text{-}P_2)]$ and $[Cp''Ta(CO)_2(\eta^4\text{-}P_4)]$ towards Hydroxide and *tert*-Butyl nucleophiles

The reactions of main group nucleophiles with $[Cp^*Fe(\eta^5\text{-}P_5)]$ result into anionic complexes with a distorted *cyclo*-P_5 unit in an envelope conformation. Our group showed that even neutral nucleophiles like NHCs can be used to obtain complexes containing this envelope-like P_5 ring. The question arose, if other P_n ligand complexes can be activated with main group nucleophiles. Therefore, the reactivity of the complexes $[Cp_2Mo_2(CO)_4(\mu,\eta^{2:2}\text{-}P_2)]$ (**1**) and $[Cp''Ta(CO)_2(\eta^4\text{-}P_4)]$ (**2**) towards the anions OH^- and $^tBu^-$ was investigated.

Reaction of OH^- or $^tBu^-$ with **2** yields the anionic complexes $[Cp''Ta(CO)_2(\eta^3\text{-}P_4OH)]^-$ and $[Cp''Ta(CO)_2(\eta^3\text{-}P_4{}^tBu)]^-$, respectively (Scheme 2). The solid state structure of these complexes shows a distorted *cyclo*-P_4 ring with three phosphorus atoms coordinating to the tantalum atom. The fourth phosphorus atom is not coordinating anymore to the tantalum but is substituted by the ^tBu unit in *endo*-position or the oxygen atom in *endo*-position and the hydrogen atom in *exo*-position. Similarly, the reaction of complex **1** with $^tBu^-$ yields to the anionic complex $[Cp_2Mo_2(CO)_4(\mu,\eta^{2:1}\text{-}PP^tBu)]^-$. X-ray structure investigations show that one Mo-P bond of the previous tetrahedron is broken and a new C-P bond was formed. When **1** is reacted with KOH, a phosphorus atom can be abstracted leading to the formation of $[Cp_2Mo_2(CO)_4(\mu\text{-}PH_2)]^-$, containing a bridging PH_2 unit. The abstracted P atom cannot be detected by ^{31}P NMR spectroscopic investigations or with other conventional analytical methods.

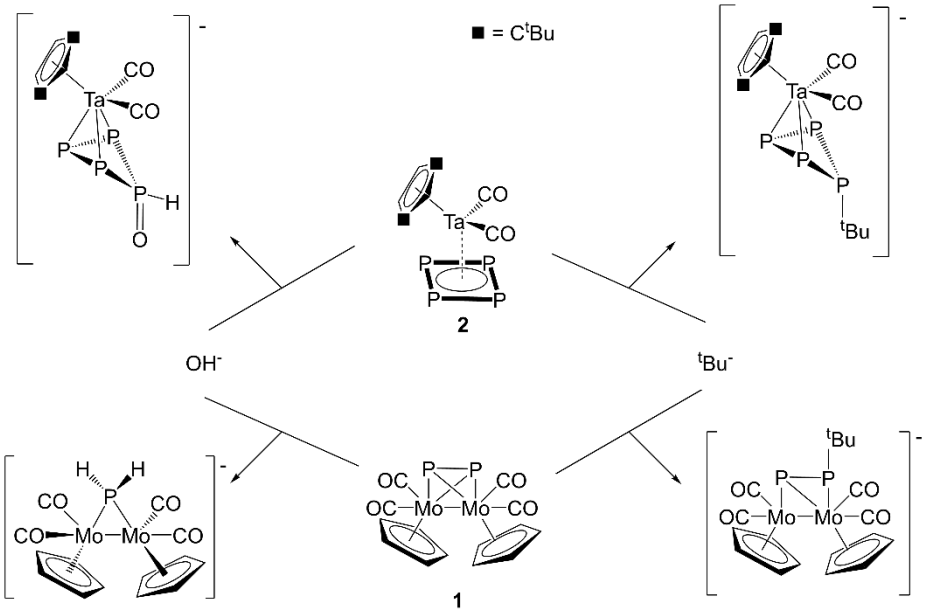

Scheme 2. Reactivity of **1** and **2** towards the anions OH^- and $^tBu^-$.

6.3 Functionalization of [Cp*Fe(η^5-P_5)] by successive reactions with main group nucleophiles and electrophiles containing functional groups

The reactions of [Cp*Fe(η^5-P_5)] with nucleophiles yield anionic complexes and subsequent reactions with electrophiles leads to the formation of neutral complexes. The nucleophiles as well as the electrophiles attack the same phosphorus atom of the *cyclo*-P_5 ring leading to the formation of a distorted P_5 unit containing two substituents and coordinating to the iron leading to complexes of the type [Cp*Fe(η^4-P_5R)]$^-$ and [Cp*Fe(η^4-P_5(R')R)] (R = nucleophile, R' = electrophile). In this reactivity studies no substituents which can be further functionalized were used. Therefore, the question arose if **1** can be reacted with nucleophiles that contain functional groups i.e. halides which might show further reactivity for example towards Grignard reagents or compounds like $LiPH_2$.

The reaction of deprotonated ethynylbenzene and deprotonated 1,4-diethynylbenzene with **1** yield the anionic complex [Cp*Fe(η^4-P_5-≡-Ph)]$^-$ (**2a**) and [(Cp*Fe(η^4-P_5))$_2$(≡-C_6H_4-≡)]$^{2-}$ (**2b**), respectively (Scheme 3). To obtain the desired product **2b** a complete deprotonation of 1,4-diethynylbenzene is required. This was quite difficult and the byproduct [Cp*Fe(η^4-P_5-≡-C_4H_6-≡-H)]$^-$ was obtained as well. The reactions of KCH_2Ph or $KCHPh_2$ with **1** gives the anionic complexes [Cp*Fe(η^4-P_5CH_2Ph)]$^-$ (**3a**) and [Cp*Fe(η^4-P_5CHPh_2)]$^-$ (**3b**), respectively. Compound **3a** was reacted with the electrophile MeI to obtain the neutral complex [Cp*Fe(η^4-P_5(Me)$CHPh_2$)] (**4**). Compound **I** (= [Cp*Fe(η^4-P_5Me)]$^-$) can be obtained by reaction of **1** with LiMe. Subsequent reactions with different electrophiles yield [Cp*Fe(η^4-P_5(R)Me)] (R = ^{i}Pr (**5a**), ^{n}Bu (**5b**), $(CH_2)_3Br$ (**5c**), $(CH_2)_4Br$ (**5d**)). Especially compounds **5c** and **5d** with their bromine functionality are interesting starting materials for further substitution reactions.

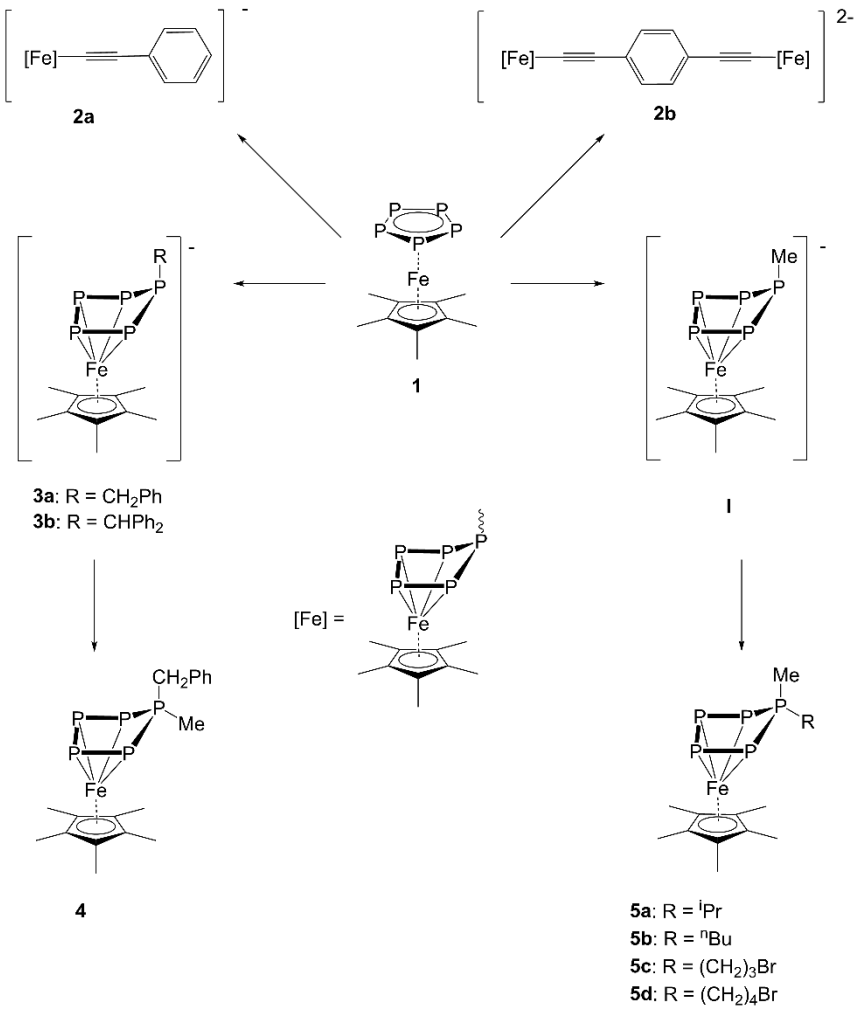

Scheme 3. Reactivity of **1** towards different nucleophiles and reactivity of **I** towards different electrophiles.

7. Appendix

7.1 List of used abbreviations

Cp	cyclopentadienyl, C_5H_5
Cp*	pentamethylcyclopentadienyl, C_5Me_5
Cp''	1,3-di-*tert*-butylcyclopentadienyl, $C_5H_3(CMe_3)_2$
Cp'''	1,2,4-tri-*tert*-butylcyclopentadienyl, $C_5H_2(CMe_3)_3$
NMR	nuclear magnetic resonance
δ	chemical shift (ppm)
ppm	parts per million
s (NMR)	singlet
d (NMR)	dublet
t (NMR)	triplet
m (NMR)	multiplet
J	coupling constant (Hz)
Hz	Hertz
°C	degree celsius
K	degree kelvin
Å	Angström (1 Å = 10^{-10} m)
EI	electron ionization
ESI	electronspray ionization
r.t.	room temperature
thf	tetrahydrofuran
dme	dimethoxyethane
tol	toluene
MeCN	acetonitrile
Et_2O	diethyl ether

EA	elemental analysis
DFT	density functional theory
WBI	Wiberg bond indixes
CV	cyclic voltammetry
HOMO	highest occupied molecular orbital
LUMO	lowest unoccupied molecular orbital
Me	methyl, -CH_3
Et	ethyl, -C_2H_5
^{t}Bu	*tert*-butyl, -CMe_3
18c-6	18-crown-6, 1,4,7,10,13,16-hexaoxacyclooctadecane

7.2 Acknowledgement

At this point I want to express my gratitude to:

- Prof. Dr. Manfred Scheer for giving me the opportunity to create this work under such excellent working conditions.
- Dr. Gábor Balázs for his ideas, proof-reading, “you got something there” and answering all questions, chemical or other nature.
- The entire ZA for NMR, MS, EA and X-ray experiments.
- Dr. Michael Seidl for checking all my crystal structures.
- Dr. Alexey Y. Timoshkin for performing DFT calculations.
- Prof. Dr. Piero Mastrorilli and Dr. Stefano Todisco for the interesting research stay in Bari and making it not only a chemical experience.
- All former and present members of the working group Scheer (listing is totally random): Julian (die ewige Tabelle), Maria, Dominik, Fabi, Moritz (Putenbrust), Sebi, Claudia, Anna (teaching me Italian), Martin W., Moni (Karamöll), Matthias L., Mehdi, Susanne, Helena (BEEEER), Barbara K., Claudia, Daniela, Lena, Jana (nice talks), Rebecca, Billi (for trying), Kevin, Walter, Eva, Andi, Matthias H., Michi, Tobi, Christian, Eric (wie soll ein Mensch das ertragen?), Rudi, Reinhard, Luigi, Jens, Boi, Hias, Olli, Felix L., Martin F., Martin P., Vroni, Gábor, Bianca, Christoph (for the best compliment I got in months), Luis, David, Julian L., Mia, Barbara, Petra, Nadja, Schotti und Karin & Barbara B.
- Special thanks to Mr. Nose, who made my time in the lab funnier and more bearable. Thanks for helping and adopting Margareta. Thanks for the roasted almonds to the duck. Thanks for reviving my passion for little trees. And especially that you believed in me all the time.
- Jana, for answering all my questions, no matter how stupid they were.
- Arndti. Thanks!
- My roommates: thanks for taking me as I am.
- My friends in and out of chemistry. You made it better.
- Sonne: thanks for everything! Proof-reading, fun, festivals, talk, standing always by my side.
- My family for their endless and enduring support and love.
- Steffi: thank you so much for making me believe in myself again and for your love.